

MEASURING THE ENERGY BUDGET OF A
PLANT IN A CLOSED SYSTEM


Pierre Brassard

A Thesis
in
The Department
of
Biology

Presented in Partial Fulfillment of the Requirements
for the degree of Master of Science at
Concordia University
Montréal, Québec, Canada

October, 1979

© Pierre Brassard, 1979



To the memory of Professor J. A. Lenoir, Chemist
and Biologist extraordinaire, who devoted a great
deal of time and energy to this project. His
total involvement to teaching and research was
only equalled by his great sense of humour. He
brought confidence and support to all the students
who learned from him.

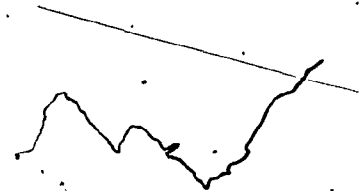
MEASURING THE ENERGY BUDGET OF A PLANT IN A CLOSED SYSTEM

Pierre Brassard

ABSTRACT

The interaction of a plant with its immediate environment implies that the physiological processes occur while the balance between incoming and outgoing energy must be maintained. For a given amount of radiation entering the plant, an equivalent amount is dissipated in the form of transpiration, convection, and reradiation, while a small amount is used for photosynthesis. The relationship between these different terms and environmental conditions required the precise control and measurements of plant and environmental parameters such that the investigations had to be restricted mainly to the laboratory, with only cautious projections into the field conditions, where such control was not possible or became impractical.

This study proposes a mathematical solution to the energy budget using only environmental parameters. The solution is based on



the theory that the simultaneous exchange of heat, mass (water vapour) and radiation in a leaf is intermediate in performance between the properties of an equivalent water saturated body and a dry one.

The resulting calculations yielded values for the water vapour diffusion resistance of both stomatal and boundary layer pathways of the leaf which compared favorably with the ones found in the literature. A linear relation was found between net photosynthesis, diffusion resistance and light intensity. Results from this study and from the literature indicate that the relation appears stable for a wide range of both environment and plant parameters, as long as the light intensity is not saturating net photosynthesis. The combination of the proposed mathematical solution and this relation is believed to provide a practical approach in a field situation, by solving the energy budget without the need for a direct measurement of the leaf temperature, thus permitting the use of remote sensing methodology to a greater extent in evaluating the productivity of larger systems.

ACKNOWLEDGMENTS

The author wishes to thank the following people and societies for contributing their expertise and material support. The completion of this project would not have been possible without their help.

Atlas Asbestos Ltd.

Mr. Kevin Callaghan

Mr. Melvin Cox

Mr. Thanassios Cristodouloupoulos

Mr. Ken Cunningham

Fiberglass Canada (Eastern division)

Prof. Jacques A. Lenoir

Mr. Jacques Lousteau

Dr. Sui Lin

Miss Diane Ludlow

Mr. Cristos Melas

Mr. Rainier Poshubay

TABLE OF CONTENTS

	Page
ACKNOWLEDGMENT	vi
LIST OF TABLES	x
LIST OF FIGURES	xii
LIST OF SYMBOLS	xiv
 Chapter	
1. INTRODUCTION	1
1.1 Properties of the Air	3
1.2 Properties of the Plant: the Energy Budget	6
1.3 Measuring the Energy Budget	9
2. MATERIALS AND METHODS	14
2.1 General Description of the System	14
2.2 Construction	16
2.2.1 Air Conditioning of the Enclosure	16
2.2.2 The Enclosure	19
2.2.3 The Lighting Assembly	19
2.2.4 Reference and Analytical Boxes	21
2.2.5 Psychrometers and Pumping Stations	23
2.3 Experimental Protocol	23
2.3.1 Growing the Plants in the Greenhouse	23
2.3.2 Adjustment Period in the Enclosure	25
2.3.3 Stabilization Period in the Box	25
2.3.4 The Experiment in a Closed System	26
2.3.5 Treatments	28

Chapter	Page
2.4 Measurements	30
2.4.1 Temperature	30
2.4.2 Flowrate	31
2.4.3 Leaf Area	32
2.4.4 Visible Light	34
2.4.5 Rate of CO ₂ Exchange and Concentration	34
2.5 Psychrometric Calculations	35
2.6 Energy Exchange Calculations	41
2.6.1 Sensible Heat	42
2.6.2 Latent Heat	45
2.6.3 Error in the Estimation of Individual Terms	48
2.7 Data Processing	49
3. RESULTS AND DISCUSSION	52
3.1 Transpiration, Humidity and Light Intensity	52
3.2 Net Photosynthesis and Transpiration	58
3.3 Effect of CO ₂ Concentration	62
3.4 Diffusion Resistance and CO ₂ Exchange	69
3.5 Solving the Energy Budget	73
3.6 Values of Diffusion Resistances	82
3.7 Effect of Chemicals on Diffusion Resistance	89
3.8 Diffusion Resistance, Net Photosynthesis and Yield	93
4. CONCLUSION	99

	Page
BIBLIOGRAPHY	103
APPENDIXES	
I. DIAGRAMS	108
II. PROGRAMS	111

LIST OF TABLES

Table	Page
1. Classification of Variables	10
2. Experimental Treatments	29
3. Description and Location of Temperature Probes	30
4. Moist Air Properties	37
5. Calculation of Moist Air Properties	40
6. Sensible Heat Loss Calculation	44
7. Experimental Verification of Energy Conservation	47
8. Regression of Latent Energy with Visible Absorbed Radiation and Absolute Humidity	52
9. Variability of Diffusion Resistance	56
10. Net Photosynthesis, Light Intensity and Transpiration	57
11. Net Photosynthesis Yield	58
12. Trend for Transpiration and Assimilation: Light Variations	60
13. Effect of CO ₂ Concentration on Net Photosynthesis and Transpiration in Tobacco	64
14. Trend for Transpiration and Assimilation: CO ₂ Variations	65
15. Regression of Sensible Heat on Visible Absorbed Radiation and Wet Bulb Depression	77
16. Regression of Plant Parameters with Absolute Humidity and Visible Absorbed Radiation: Tobacco	84
17. Regression of Plant Parameters with Absolute Humidity and Visible Absorbed Radiation: Tomato	86

Table

Page

18. Regression of Plant Parameters with Absolute Humidity and Visible Absorbed Radiation: Bean	89
19. Diffusion Resistance and Net Photosynthesis	96

LIST OF FIGURES

Figure	Page
1. Psychrometric Chart	4
2. General System	15
3. Air Conditioning of the Enclosure	18
4. Enclosure Assembly	20
5. Analytical Box Assembly	22
6. Psychrometer Assembly.....	24
7. Experimental Protocol	27
8. Leaf Area Measurement	33
9. Location of Temperature Probes	36
10. Heat Losses in the Boxes	43
11. Data Processing	50
12. Effect of Light and Humidity on Transpiration in Tobacco	53
13. Effect of Light and Humidity on Transpiration in Tomato	54
14. Effect of Light and Humidity on Transpiration in Bean	55
15. Net Photosynthesis and Visible Absorbed Radiation for Tomato, Tobacco and Bean	59
16. Trend for Transpiration and Assimilation: Light Variations	61
17. Transpiration and Humidity for Tobacco at Decreasing CO ₂ Treatments	63

Figure.	Page
18. Trend for Net Assimilation and Transpiration in Tobacco: CO ₂ Variations	66
19. Effect of CO ₂ Concentration on Net Photosynthesis and Transpiration in Tobacco	67
20. Resistance Network for Photosynthesis and Respiration	69
21. Resistance Network for Diffusion and Convection	74
22. Parameter Grid for the Tobacco Experiments	81
23. Effect of Visible Absorbed Radiation on Plant Parameters: Tobacco	83
24. Effects of Visible Absorbed Radiation on Plant Parameters : Tomato	85
25. Effects of Visible Absorbed Radiation on Plant Parameters: Bean	88
26. Leaf Resistance and SO ₂ Doses in Tobacco	90
27. Leaf Resistance and 10 ⁻³ M Amitrole in Bean	92
28. Relation between Net Photosynthesis and Total Diffusion Conductance	95

LIST OF SYMBOLS

Main Symbol	Description	Units
A	Effective leaf area	cm ²
a, b, c, f	Proportionality constants	—
C _a	CO ₂ concentration	vpm
d	Dilution value	—
E	Transpiration	nMH ₂ O/cm ² /sec
E _T	Transpiration rate at CO ₂ compensation*	nMH ₂ O/cm ² /sec
F	Flowrate	cm ³ /sec
F _i	Empirical constant	—
G	Specific heat of dry air	j/gr/°C
H _S	Sensible heat	btu/lb dry air
H _L	Latent heat	btu/lb dry air
H _T	Total heat	btu/lb dry air
HLOSS	Heat loss	btu/lb dry air
I _{CO₂}	Transpiration-Assimilation rate: CO ₂ variation.	MH ₂ O/MCO ₂
I _L	Transpiration-Assimilation rate: Light variation.	MH ₂ O/MCO ₂
I _p	Photosynthetic yield	MCO ₂ /Einstein
I _v	Variability of diffusion resistance	—
K	Regression constant for heat loss calculations	—
K _a	Convection transfer coefficient	j/cm ² /sec/°C
K _n	Rate of net Photosynthesis to conductance	nMCO ₂ /cm ³

Main Symbol	Description	Units
K_r	Reradiation transfer coefficient	$\text{j/cm}^2/\text{sec}/^\circ\text{C}$
L	Heat of vaporization for water	$\text{j/nMH}_2\text{O}$
M	Elapsed time	sec
n	Power of a number	—
N_{rv}	Normalized Coefficient: Visible light	—
N_{wa}	Normalized Coefficient: Absolute Humidity	—
O	Psychrometer offset	$\text{j/cm}^2/\text{sec}$
P_{DS}	Saturation pressure of water, dry bulb	atm
P_n	Net Photosynthesis (assimilation)	$\text{nMCO}_2/\text{cm}^2/\text{sec}$
P_{ws}	Saturation pressure of water, wet bulb	atm
P_o	Assimilation at closure of stomates	$\text{nMCO}_2/\text{cm}^2/\text{sec}$
Q_{ABS}	Total absorbed Radiation	$\text{j/cm}^2/\text{sec}$
Q_N	Net Absorbed Radiation	$\text{j/cm}^2/\text{sec}$
Q_p	Photosynthetic yield	nMCO_2/j
RAD	Thermal reradiation	$\text{j/cm}^2/\text{sec}$
R_a	Gas constant for dry air	$\text{ft lb}_f/\text{lb}_m/^\circ\text{R}$
R_v	Visible absorbed radiation	$\text{j/cm}^2/\text{sec}$
R_T	Thermal absorbed radiation	$\text{j/cm}^2/\text{sec}$
$r_s, r_a, r_p,$ r_c, r_m, r_{tw}	Resistance to diffusion	sec/cm
S	Sensible heat rate	$\text{j/cm}^2/\text{sec}$
t	Temperature	$^\circ\text{C}$
T	Temperature	$^\circ\text{K}$
V	Infrared analyser cell volume	ml

Main Symbol	Description	Units
v	Volume density of dry air	ft ³ /lb dry air
W	Humidity ratio	lb water/lb dry air
W_{SD}	Saturation humidity ratio: dry bulb	lb water/lb dry air
W_{SW}	Saturation humidity ratio: wet bulb	lb water/lb dry air
x	Degree of saturation	—
α, β, γ	Error in evaluation of Energy terms	j/cm ² /sec
ϵ	Emissivity	—
σ	Stephan-Boltzman constant	j/cm ² /sec/°K ⁴
θ	Leaf temperature minus air temperature	°C
θ^*	Wet bulb minus dry bulb	°C
ϕ	Relative humidity	—
Γ	CO ₂ compensation point	vpm
ψ	Psychrometer transition bias	—

Symbol Subscript

a

e

i

l

n

o

p

r

s

w

Meaning

Analytical Box

Enclosure

Inlet

Leaf

Nutrient pan

Outlet

Psychrometer

Reference Box

at Saturation

Wet Bulb

Chapter 1

INTRODUCTION

The importance of plant life on this planet resides in the ability of plants to convert the sun's energy into usable chemical energy through the process of photosynthesis. The resulting growth serves as the primary food to be grazed upon by all the other forms of life with man being the very last consumer of this long and intricate food chain. Being the primary producer confers to the plant the advantage of self sufficiency and the disadvantage of being the most exposed of all forms of life to environmental excess of temperature, humidity and radiation. In harvesting the sun's radiation the plant must constantly solve the dilemma of exposing the necessary leaf surface to the sun while minimizing the ensuing exposure to the environmental stress. The resulting adaptation in growth, leaf shape and orientation is a feat in itself since only 3% of the total solar radiation is actually converted into the energy that maintains life in the whole biosphere. The remaining 97% is absorbed by the atmosphere, the clouds and the surrounding objects and is released mainly in the form of thermal (infrared) radiation. The available radiation that actually strikes this leaf ranges from 50% of the total solar radiation, when directly exposed, to lower values when indirectly exposed. The leaf absorbs 50% of this available radiation and almost all (97%) of the

thermal radiation coming from the surroundings. The leaf reradiates part of this energy in the form of thermal and visible reradiation, owing its green color to the latter. The remaining energy is dissipated in the form of convection and in the transpiration of water. Convection occurs when the leaf warms or cools the surrounding air and thus allows heat to escape or enter depending on whether the leaf temperature is above or below that of the air. Transpiration requires energy in order to vaporize the water into the air. The evaporating water has a cooling effect on the leaf and provides the means by which the leaf maintains its temperature close to that of the air in spite of high incoming radiation. An equilibrium is maintained between incoming radiation, convection and transpiration where the optimum leaf temperature for best physiological performance can be achieved by the control of transpiration. This control is made possible by regulating the stomatal opening, acting as a valve to check the outward flow of water vapour. Transpiration and convection are also influenced by environmental conditions of wind, temperature, and humidity. The ability of the leaf to maintain physiological stability in a range of radiation, temperature, humidity and wind conditions defines the scope of operation of that leaf in that environment. By extension, the evaluation of the energy budget of whole plant communities gives the ecologist a valuable tool in estimating the performances of ecosystem. The purpose of this research is to define this tool by measuring the energy budget of whole plants in a controlled environment. The understanding of properties of both the air and plant leaves are

essential in order to design and execute a proper experimental procedure.

1.1 Properties of the Air

The aerial parts of a plant are subjected to the properties of air itself. These properties are well established and used in refrigeration and air conditioning engineering as exemplified in ASHRAE (1972) and Gaffney et al (1978). The psychrometric chart shown in figure 1 is a graphic display of the air properties and permits fast and accurate calculations. The term moist air refers to the binary mixture of dry air and water vapour. The chart shows the moisture content on a vertical axis and air temperature on the horizontal axis. The moisture content is expressed in the form of a humidity ratio (W) in pounds of water per pound of dry air and the temperature in $^{\circ}\text{F}$. Any combination of humidity ratio and temperature brought on the chart fixes the values of all the other properties represented by the other lines on the chart and described as follows:

- a) Relative humidity Expresses the ratio of actual moisture at a given temperature to the maximum possible moisture at that temperature.
- b) Enthalpy in (Btu/lba) Expresses the total amount of energy contained in the mixture and is the summation of Latent and Sensible heat.
- c) Volume ratio in (ft^3/lba) Expresses the volume occupied by one pound of dry air at that point.

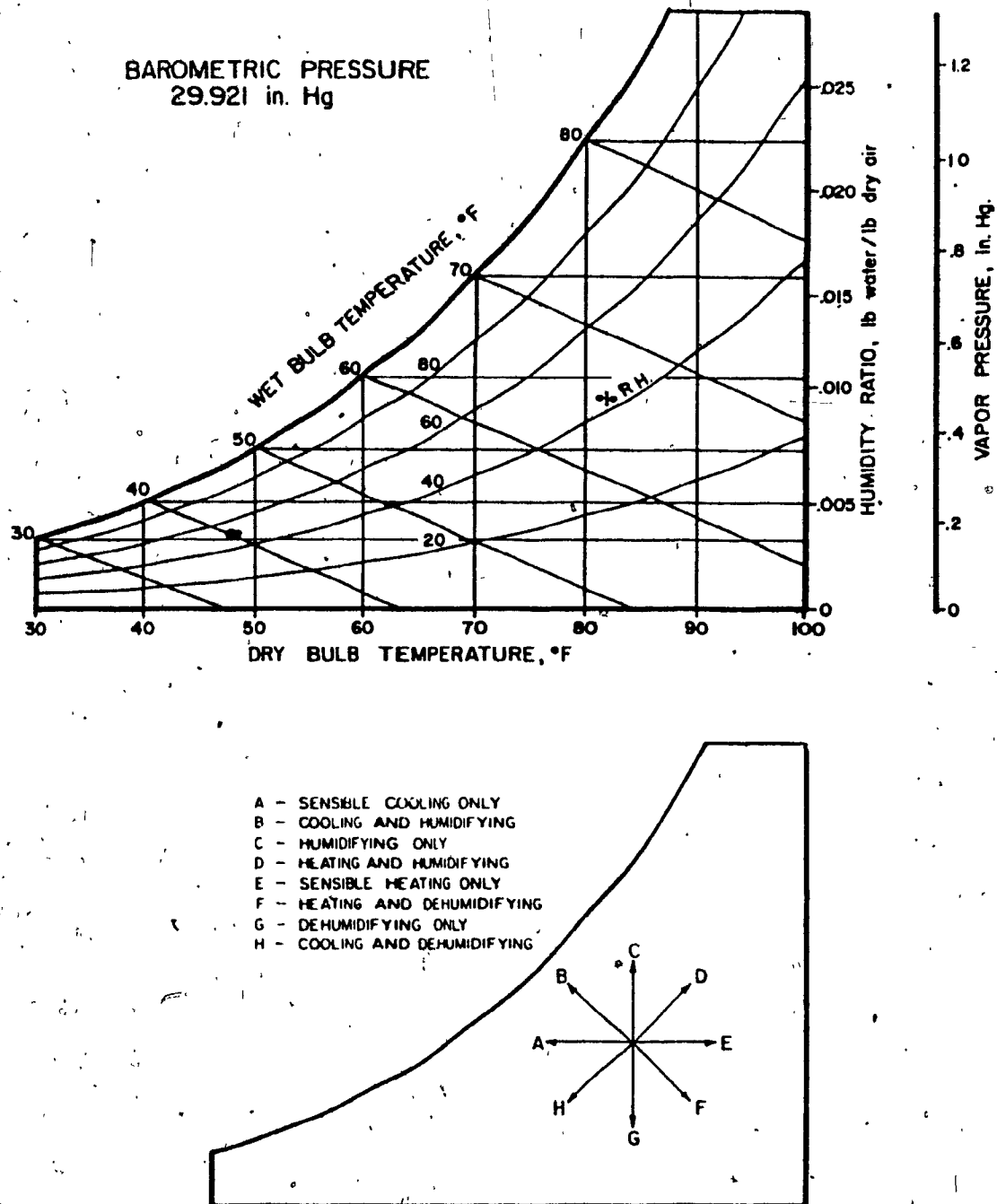


Fig. 17 Psychrometric Chart

The various moist air properties explained in the text are shown in the top drawing. The lower figure indicates all the possible ways in which energy is added or subtracted from moist air, along with the corresponding displacements on the chart. The above figures were taken from Gaffney (1978).

d) Wet bulb temperature The lowest temperature reached by a mixture of air and water if allowed to cool without any net expenditure of heat. The wet bulb lines are very close to the enthalpy lines.

The wet bulb temperature is achieved whenever a thermometer bulb is surrounded by a wet evaporating surface and allowed to achieve equilibrium with the surrounding air. The sling psychrometer uses the above principle of operation. Looking at the chart and starting at any point corresponding to a specific temperature and humidity it is possible to add energy into the mixture either by increasing the moisture, raising the temperature, or both. The displacement of the point on the chart will follow a direction that is the resultant combination of sensible heat, which is produced by a temperature change, and latent heat, produced by a moisture change. An upward motion of the point will be produced by a gain of moisture only while an horizontal displacement to the right signifies a gain of sensible energy (temperature gain). The converse is true for negative gains of either Sensible or Latent heat. A displacement of the point along an Enthalpy line signifies that no net gain or loss has occurred, and that the sum of Latent plus Sensible gains is zero. In that case, the energy required to evaporate the water is taken from the air itself which is cooled as a result. The line on the chart corresponding to the 100% humidity line represents moisture saturation at the given

temperature. The saturation humidity ratio for a given temperature is the saturation point, while the temperature at which saturation humidity occurs is the dew point.

Most of the natural processes occurring in air involve the simultaneous transfer of mass (water) and heat. The displacement produced on the chart is a measure of this transfer. A plant put in air at a known humidity and temperature will change the air condition from an original state point to a final state point according to the amounts of water and sensible heat released into that air by that plant.

1.2 Properties of the Plant: The Energy Budget

The exchange of energy between a plant and its environment was expressed in a mathematical form by Rashke (1960) following the work of Brown and Escombe (1905). It was known that the leaf temperature was the result of a dynamic balance between the various energy exchanges. Improved experimental methods permitted a more precise evaluation of the energy budget. Rabideau (1946) studied the absorption and reflection of visible light from intact leaves and the effect of thermal radiation on leaf temperature was investigated by Curtis (1936a, b) and Gates (1963a). Gates (1965, 1963b) discussed the convection phenomena and improved on measurement techniques for the water vapour boundary layer. A different approach was used when dummy metal leaves were compared to that of real ones in order to study the effect of wind and leaf shape on convection (Vogel 1970). The effect of transpiration, energy exchange and leaf temperature was reviewed by

Gates (1968) followed by the work of Lommen et al (1971) who further expanded the energy budget so as to include photosynthesis and respiration. The model of Gates (1968) is used in this paper and is described as follows:

The total energy budget of a plant consists in balancing the absorption of radiation with convection, transpiration and reradiation. The budget equation is written as follows:

$$Q_{ABS} = RAD + C + LE \quad \dots(1)$$

where

Q_{ABS} = All thermal and Visible radiation absorbed by the leaf.

RAD = Thermal reradiation released to environment.

C = Convection (Sensible heat) ($j/cm^2/sec$)

E = Transpiration ($nM/cm^2/sec$)

L = Latent heat of vaporization, a constant required to convert transpiration into latent heat. (J/nM)

Some explanation is required to develop each term. When transpiration occurs, water vapour diffuses from the inside of the leaf to the outside air along a gradient of humidity according to Ficks law. In doing so the diffusing vapour passes through the stomatal resistance (r_s) and through the air boundary layer resistance (r_a). The transpiration is written

$$E = \frac{1}{(r_s + r_a)} (W_{sl} - W_a) \quad (nM/cm^2/sec) \quad \dots(2)$$

The water vapour inside the leaf is assumed saturated at the leaf temperature (W_{sl}) and W_a represents the outside air humidity. For a

constant gradient, the closing of the stomata results in an increased resistance and therefore a diminished transpiration.

The heat Exchange description follows the same analogy. Heat flows along a temperature gradient between the leaf and the outside air ($t_l - t_a$) and according to a convection transfer coefficient (K_a)

$$C = K_a(t_l - t_a) \quad (\text{j/cm}^2/\text{sec}) \quad \dots(3)$$

The thermal reradiation is solely dependent upon leaf temperature. The Stephan - Boltzman law states that the thermal radiation of a black body is proportional to the fourth power of the body temperature in °K. then:

$$\text{RAD} = \epsilon \sigma (T_l)^4 \quad \dots(4)$$

where

$$T_l = 273 + t_l$$

ϵ = emissivity (0.95 for plant leaves)

σ = Stephan - Boltzman constant

Combining all the above terms in the energy budget gives:

$$Q_{\text{ABS}} = \text{RAD} + C + LE \quad \dots(5)$$

$$Q_{\text{ABS}} = \epsilon \sigma (273 + t_l)^4 + K_a(t_l - t_a) + \frac{L}{(r_s + r_a)} (W_{sl} - W_a) \quad \dots(6)$$

where

σ = Stephan - Boltzman constant = $5.665 \times 10^{-12} (\text{j sec}^{-1} \text{cm}^{-2} \text{°K}^{-4})$

ϵ = emissivity = 0.95

L = specific heat of vaporization = $4.5 \times 10^5 (\text{j nM}^{-1})$

r_s = stomatal resistance (sec cm^{-1})

r_a = boundary layer resistance to water vapour (sec cm^{-1})

K_a = convection transfer coefficient ($\text{j sec}^{-1} \text{cm}^{-2} \text{ } ^\circ \text{C}^{-1}$)

W_{sl} = saturation humidity at leaf temperature (nM/cm^3)

W_a = humidity of the surrounding air (nM/cm^3)

Q_{ABS} = total absorbed radiation ($\text{j/cm}^2/\text{sec}$)

Although photosynthesis and respiration are part of the energy budget, their energy contribution is small enough to be neglected without inducing measurable errors (Rashke 1960). These are considered independently as in the work of Lommen (1971). Graphical representations of the above equations are well covered in the literature mainly with Gates and Pipran (1971), who generated a family of curves for various values of Q_{ABS} , air temperature (t_a), humidity (W_a), and leaf temperature (t_l). Although the theoretical concept of the energy budget is well established, its present use in a practical situation is limited by the technical difficulties encountered in the actual measurement of the budget's individual terms.

1.3 Measuring the Energy Budget

The experimental verification of such a model is a complex task. For each value of total absorbed radiation (Q_{ABS}), there exists a hypothetical infinity of solutions to balance the budget. Hence, at this stage, one can only generate by calculation alone a family of equally possible mixtures of the transpiration, convection and

reradiation terms. Since the object of the energy budget model is to predict the plant's behavior in a given set of environmental conditions, it is desirable to present the model variables as controlled by the environment, by the plant leaf, and by both. Table 1 shows such a classification.

Table 1
Classification of Variables

Under Environmental Control	
Air Temperature Air humidity Wind speed and direction	(t_a) (w_a) Gates (1965)
Under Leaf Control	
Leaf shape and orientation Leaf stomatal resistance	(r_s) Gates (1965)
Controlled by Both	
Boundary layer resistance to water vapour Convection transfer coefficient Total absorbed radiation Leaf temperature and saturation humidity	(r_l) (K_a) (Q_{ABS}) (t_l) (w_{sl})

Several methods were used to measure transpiration and are based on the increase in air humidity produced by a plant leaf when inside a small chamber built for that purpose. The air humidity was measured either by psychrometry (Slayter, 1967) by IR analysis (Catsky, 1975) or by the condensation of humid air on a cool surface (Bazzaz, 1972). The net photosynthesis measurements were all done with IR analysers as in Nilsen (1975) Forrester (1966) and Ludwig (1971). The total absorbed

radiation term was measured, using thermopiles or calibrated photocells, by delimiting a precise area on the leaf and shining a precise amount of light on its surface (Brogardt, 1975). Bazzaz (1972) measured the residual radiation of his chamber after introducing the plant, and obtained the total absorbed radiation by reference to the empty chamber. The convection energy was determined by subtracting the transpiration from the net absorbed radiation (Bazzaz, 1972) (Decker, 1965). Boundary layer resistance to water vapour was obtained either by measuring the transpiration of wet paper analogues of leaves (Gastreaa 1959), or by calculations using the convection energy and the temperature difference between the leaf and the air (Slatyer 1967). Gates (1965b) has related the convection transfer coefficient to wind speed and the shape of leaves. The measurement of stomatal resistance using porometers was reviewed by Meidner and Mansfield (1968). Stomatal resistance was also obtained by calculations using transpiration, leaf temperature and air humidity (Slatyer 1967) (Bazzaz 1972) (Gastreaa 1963). Inserting fine temperature sensors directly into the leaf was the only method found in the literature to measure the leaf temperature.

The field applications of these methods passes some serious problems. Most of the above methods were done on single leaves allowing for a rigid control of fixed parameters such as leaf temperature or total absorbed radiation. Such a practice cannot be reproduced in the field and conclusions derived from laboratory work cannot be simply extended to actual field conditions owing to the changing nature

of field parameters. The work of Hari et al (1975), however, showed that transpiration of plants in the field was linear with the potential evapotranspiration and proposed that plant transpiration was a function of environmental parameters viz radiation, temperature and humidity. If a similar trend exists for convection and reradiation, it would then be possible to also relate leaf temperature to environmental parameters and thus propose a practical method as measuring the energy budget that would be applicable to the field. It is in order to fulfill this goal that the following procedure was used.

- a) Construction of a system to provide an environment to the plant.
- b) Construction of measuring devices to monitor:
 - 1) Physiological activity (Photosynthesis)
 - 2) Exposure of the plant to the environment (leaf area)
 - 3) Changes in air properties due to the transfer of heat, mass and radiation from the plant to the air.
- c) Verify the credibility of the above by comparing directly obtainable results (transpiration, photosynthesis) with the literature.
- d) Propose a solution to the energy budget using measurable environmental parameters (Radiation, air temperature and humidity, transpiration).
- e) Derive, from the above, numerical values for the plant parameters (diffusion resistances, leaf temperature) and compare with literature.

- f) Extend the above solution so as to include the net photosynthesis term and discuss the field application of proposed method.

Chapter 2

MATERIALS AND METHODS

2.1 General Description

The apparatus was designed to accomodate a maximum of 10 small plants; figure 2 shows the general layout. The areal part of the plants were housed in an analytical box, the top of which was then sealed with a glass cover. A reference box of identical shape and properties was left empty and permanently sealed with a glass cover. Each box was seated over a pan containing a nutrient solution to provide an adequate medium for the roots. The nutrient solution was recirculated to avoid stagnation. Both boxes and their respective pans were then placed in a larger enclosure in which temperature and light intensity were controlled. The circulating air was carried to and from the boxes by pipes which transported the gases across the enclosure to the monitoring and pumping stations. The monitoring station included one psychrometer for each box, a common infrared gas analyser, and a septum to inject small amount of gas in the sytem. The whole network could be operated in a closed or open circuit by setting the two three way valves accordingly. The open circuit configuration was used mainly for purging the system with a selected mixture of air which was provided by the regulated gas cylinders. During an experiment, the open circuit option was used

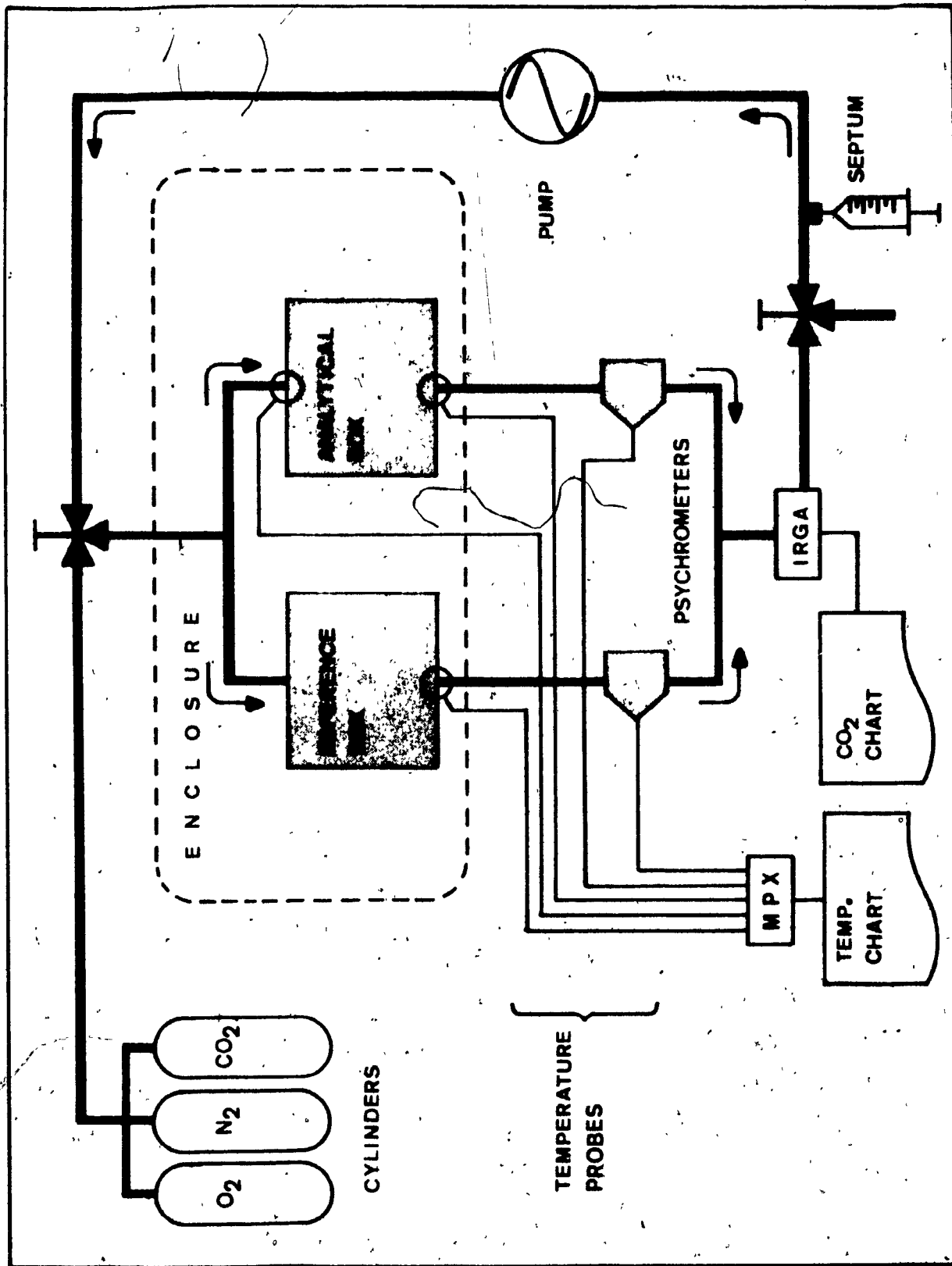


Fig. 2 General System.

MPX; Multiplexor. IRGA; Infrared Gas Analyser.

when humidity was to be kept constant and the closed circuit option used when a constant temperature was required. Each box was fitted with thermometer probes (t_r , t_a) at the respective outlets, while a common probe (t_i) measured the temperature of the incoming flux of air. All probes coming from the boxes were wired through the enclosure along with those coming from the psychrometers (t_{wr} , t_{wa}). The resulting cable was then fed to a multiplexor and the results displayed on a recorder. The output from the infrared gas analyser provided a measure of the CO_2 concentration. The raw data obtained from the experiments was then punched on computer cards and processed.

Psychrometric tables and equations were used in a sequence of programs to calculate the resulting temperatures, humidity, transpiration and heat exchanges that occurred. All temperature data was subjected to calibration and reference to known standards. CO_2 exchange was processed and standardized independently by injecting a precise amount of CO_2 in the system through the septum (Fig. 2). The total leaf area was determined with a calibrated photocell and the air flow rate through the boxes was obtained by the dilution method (Hammarstrand, 1976). All the above methods are detailed in the text (see measurements).

2.2 Construction

2.2.1 Air Conditioning

The function of the enclosure was to provide light and to control the temperature of the air surrounding the boxes. The measuring devices and controls were located on the side of the

enclosure itself while the lighting bank, forming a complete and self contained unit, rested on the top of the enclosure. Referring to figure 3 the air from the enclosure was circulated successively through a cooling and a heating coil before it was returned to the enclosure. The pump was made with a 120 cfm "squirrel cage" fan housed in the inlet unit. The pumped air was then carried by 3-inch diameter ABS drainpipes and fed to the bottom of the cooling coil assembly. Copper tubing was used to manufacture the cooling coil housed inside a 6-inch ABS sewer pipe. Two reducers at each end of the 6 inch pipe allowed the connections to the 3-inch pipe (bottom) and the heating coil/outlet unit (top) respectively. The heating coil assembly was seated in the outlet unit and consisted of a 3 foot heating strip loosely wound around a chicane of glass tubings. A maximum of 450 Watts of heat could thus be generated. The cooling coil was connected with a 1/4 H. P. compressor. A draining pan was installed below the cooling coil assembly, as shown, to collect water resulting from the deicing cycle. The controlling unit provided a centralized control and power distribution function to all air conditioning devices. The air conditioning inside the enclosure was sensed by a wet and a dry bulb thermometer probe, located at the inlet unit, and was referenced to wet and dry bulbs temperature settings on the control unit. The control unit accordingly activated the required cooling and heating devices and also a spray humidifier located inside the enclosure (not shown). Alternate settings were switched in or out by a timer switch so as to provide separate day/night conditions in the

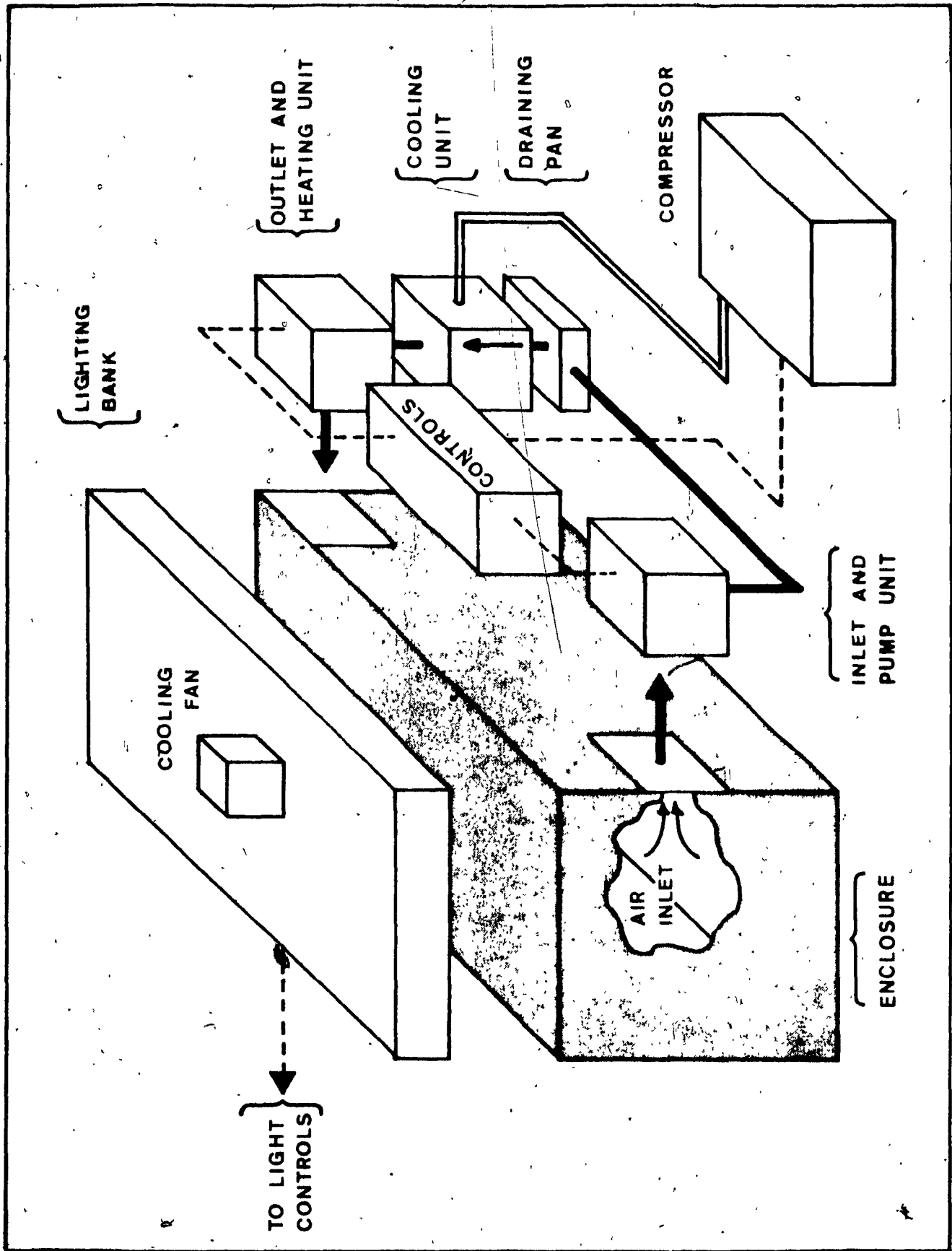


Fig. 3 Air Conditioning of the Enclosure.

enclosure. The timer was also used to program a deicing cycle. The whole system controlled temperature to 0.5°C and humidity to 5% R. H.; operation ranges were from 10 to 45°C and from 30% to 85% R. H.

2.2.2 The Enclosure

Sheets of translucent vision/asbestos (Filon, Reg TM Atlas Asbestos) were fixed to a window frame and formed an 8x4x4 feet enclosure (Fig. 4). The door was made from two layers of glass separated by a frame to provide insulation. All sides of the enclosure were covered by 1-inch fiberglass insulation. The lighting assembly was separated from the top of the enclosure by a glass window resting upon a frame. This construction permitted light to go through the top and provided an insulating layer as well. All tubing and wiring going across the walls were passed through rubber stoppers permanently mounted at the appropriate places. All joints were sealed with silicon glue and a rubber gasket was fitted on the door to ensure an airtight enclosure.

2.2.3 Lighting Assembly

The lighting assembly was put in the rectangular housing shown on figures 3 and 4, and consisted of 16 fluorescent tubes and 32 incandescent bulbs (40 W). The housing also included the ballasts and a ventilation fan of 400 cfm capacity resting upon the top to avoid overheating. The fluorescent tubes were controlled by a panel of 4 switches controlling 2, 2, 4, and 8 tubes respectively. This arrangement permitted a partial illumination from 0 to 16 tubes in increments

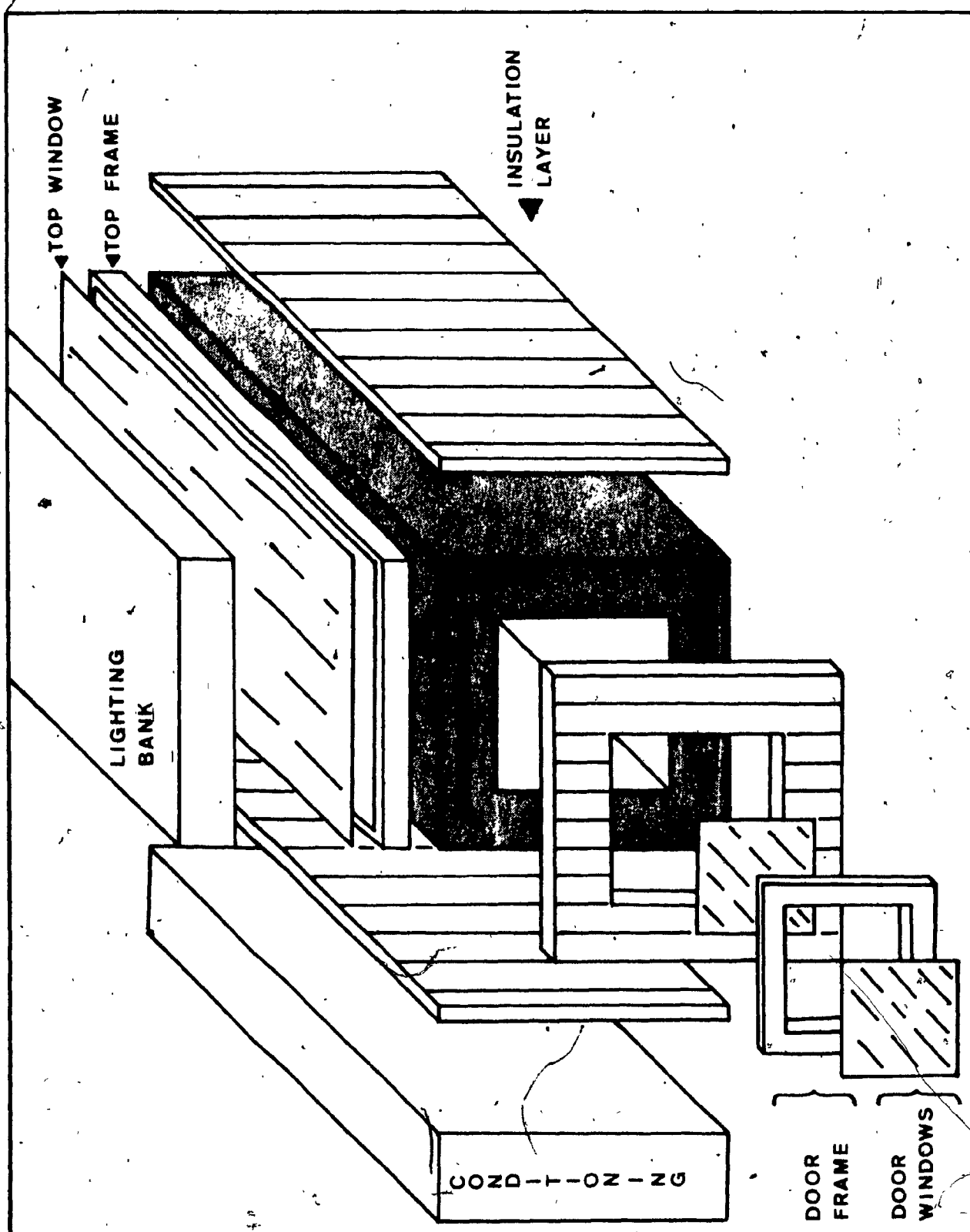


Fig. 4 Enclosure Assembly

of two at a time. The incandescent bulbs provided for the lower red portion of the spectrum and were controlled by a 15 Amp. thyristor light dimmer.

2.2.4 Reference and Analytical Boxes

Two identical polystyrene boxes were modified as shown in figure 5. The inner surface of each box was coated with flat white latex paint. The inlet and outlet parts were bored on the opposite walls and were fitted with a T coupling in order to accommodate a temperature probe and the tube carrying the recirculated air. An identical set of holes was bored in the floor of each box. Each hole could accept one plant which was held in place by a foam plug that had been previously slit to the center, as shown. The floor holes were always plugged, with or without a plant. A glass cover was laid on top of a sealing gasket coated with petroleum jelly which allowed for a tight fit and easy removal of the cover. Each box rested upon its individual nutrient pan: the nutrient medium was introduced by the side of the pan and drained over an overflow ring positioned over the drain. A constant level of recirculated nutrient medium could thus be maintained. A water pump lifted the solution from a holding tank located outside the enclosure (not shown). The solution was carried by flexible plastic tubing through the walls of the main enclosure. The plant material was always introduced in the same box which was named *Analytical Box*, while the *Reference box* was devoid of plants. Every other aspects of the boxes were identical.

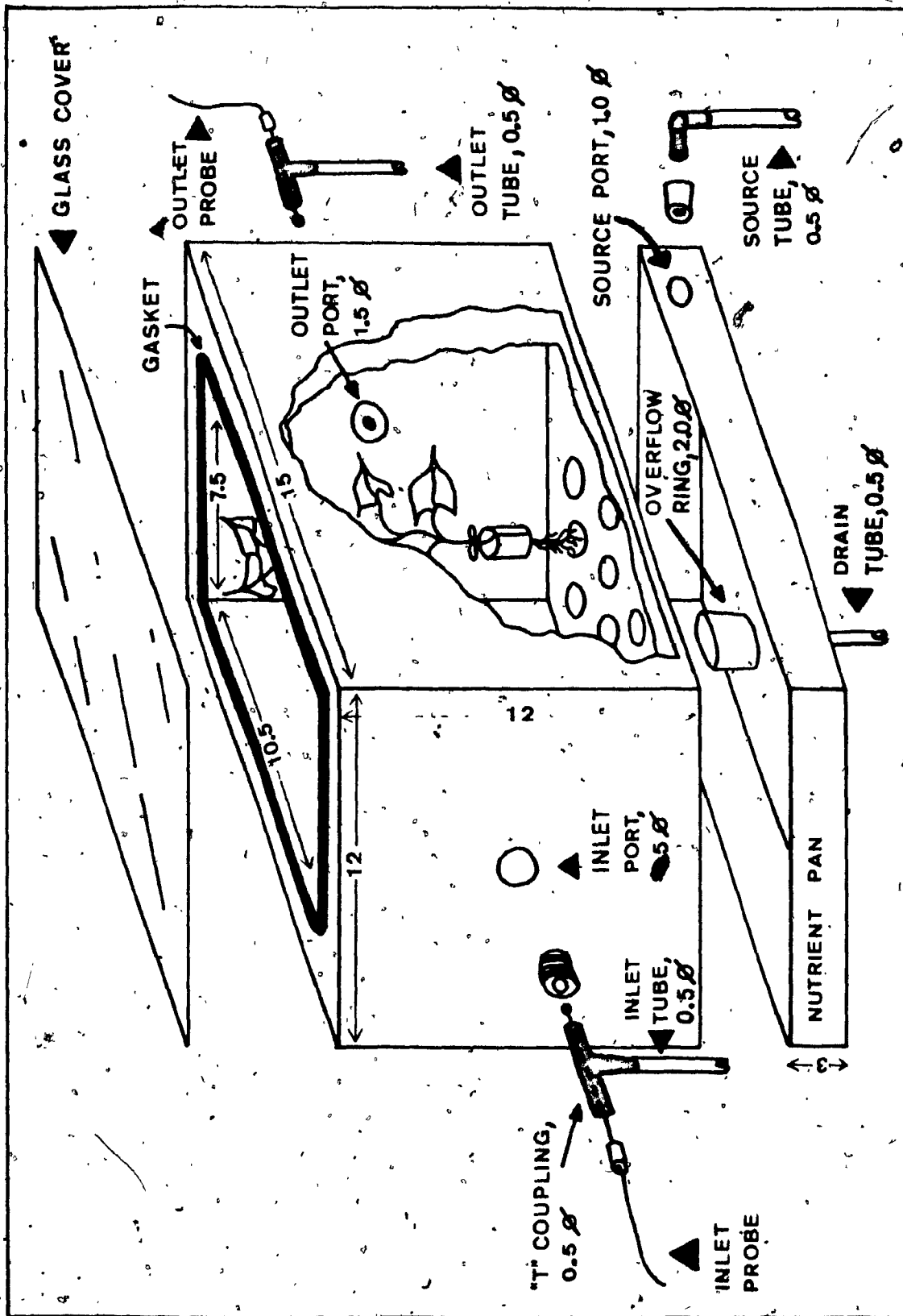


Fig. 5 Analytical Box Assembly.

All values shown are in inches. ϕ , cross section diameter.

2.2.5 Psychrometer and Pumping Stations

The psychrometers provided a continuous measurement of humidity in each box. The temperature of the gas coming from each box was elevated in a water bath. For this purpose, a copper pipe exchanger was manufactured as shown in figure 6. The exchanger rested on beads at the bottom of a water bath that was thermostatically controlled. The exchanger then allowed the air into the psychrometer proper which measured the dry and wet bulb. Thermistor probes were used to record the measurement. The wet wick surrounding the wet bulb probe dipped in a small vial which could be removed and filled. The support was made of acrylic plastic and allowed for a rapid visual inspection of the apparatus. The device was a slight modification of the one described by Slatyer and Bierhuizen (1964). A vacuum cleaner motor was glued in a 6-inch sewer pipe fitted at both ends with reducers, the half-inch tubes coming from the psychrometer were connected to the reducer.

2.3 Experimental Protocol

2.3.1 Growing the Plants

A uniform procedure was followed for growing the plant material. The seeds were started in shallow trays filled either with vermiculite (Dwarf bean, Soya) or fine black earth (tomato, tobacco) and left to grow until the seedlings reached a height of about 5 cm. Similar seedlings were then selected from the center of the tray and transplanted for the remainder of the growth period which varied

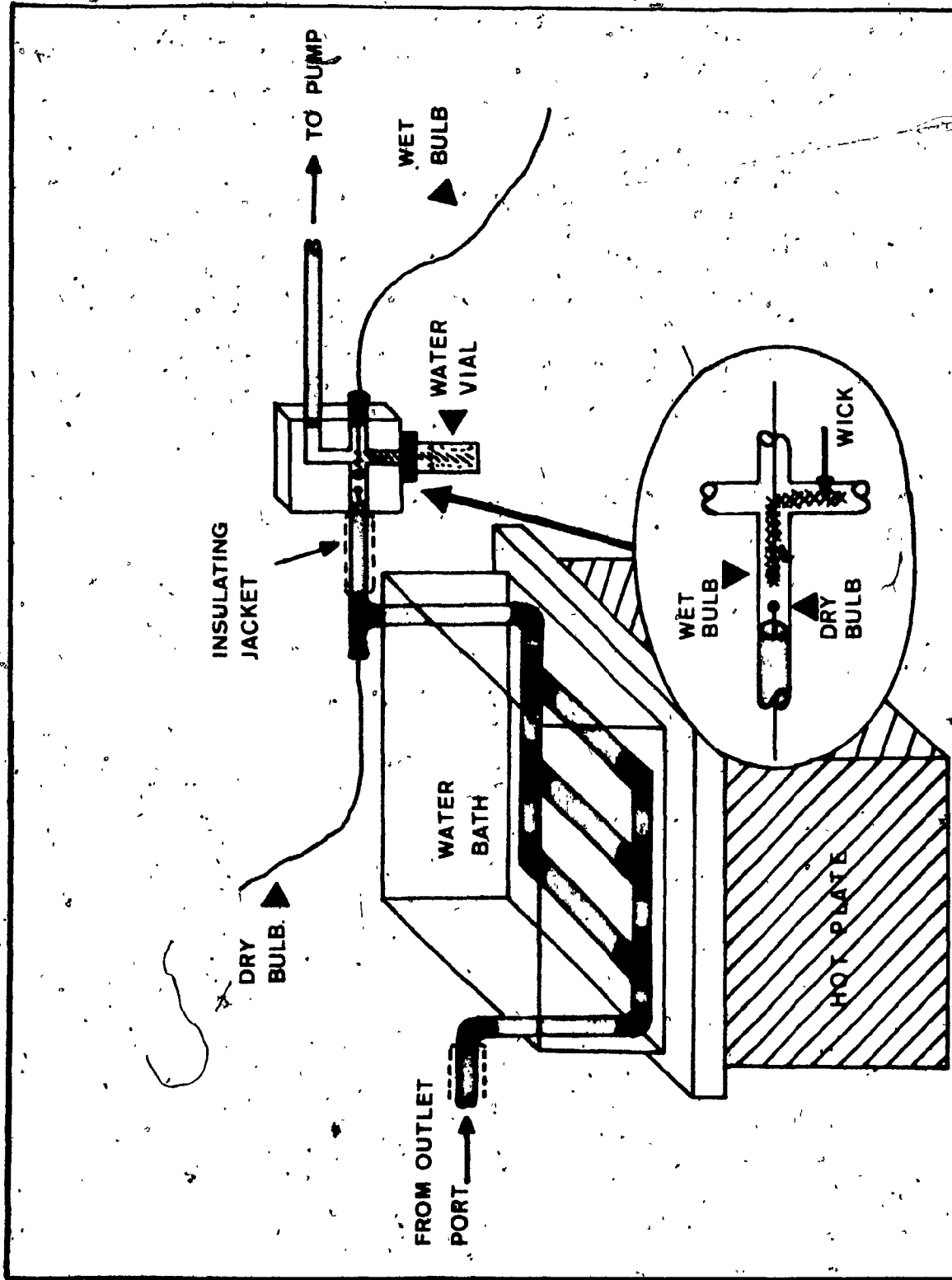


Fig. 6 Psychrometer Assembly.

according to plant species. This procedure was performed in a greenhouse equipped with automatic sprinklers and light banks set for a 14 hours diurnal cycle.

2.3.2 Adjustment Period

A second selection was made when plants reached a stem height of 20 cm. These plants were then fitted with foam plugs and inserted in the holes of a plastic support. The support maintained the plants over a hydroponic pan such that the roots dipped in a complete nutrient solution. The whole apparatus was transferred from the greenhouse to the enclosure where it remained not less than two days in order to allow the plants to adjust to the hydroponic medium and the new conditions of the enclosure. During this period, the enclosure maintained a relative humidity of 50% at a day temperature of 30°C and a night temperature of 25°C. The enclosure's light bank was set for the same 14 hours diurnal cycle as the one provided by the greenhouse.

2.3.3 Stabilization Period

This period was provided in order to allow the plant to adjust to new parameters of air, light and temperature that were to remain constant during the course of the ensuing experiment. The light intensity and either temperature or humidity were adjusted and stabilized. One or several plants were then transferred to the analytical box and the glass cover closed. A period of at least 20 minutes was allowed to

pass while both the analytical and reference boxes (see Fig. 2) were continuously flushed with air from enclosure or with a selected gas mixture provided by the battery of N_2 , O_2 , CO_2 cylinders located outside the enclosure. The system's 3-way valves were set such that the flow of air passed through the boxes, the psychrometers, and the pumping station, before being discharged outside. This open circuit configuration allowed a complete clean up of the residual air in the system. During that period, instruments were checked for stability and calibration data recorded. All recording devices were then activated and monitored to ensure a stable output free from electrical interferences.

2.3.4 The Experiment

The experiment itself was started as soon as the configuration was changed from open to closed circuit, thereby isolating the plants with a limited and recirculating supply of air. For this purpose, the valves were switched to close the circuit and the pump was simultaneously activated. From then on, the humidity of the recirculated air kept on rising while the transpiration was continuously measured by the psychrometers. The CO_2 concentration was kept constant by injecting small amounts in the circuit in order to make up for photosynthetic activity. Such a control was not possible in the dark. At the end of the experiment, the valves were switched back to open circuit and the pump was stopped.

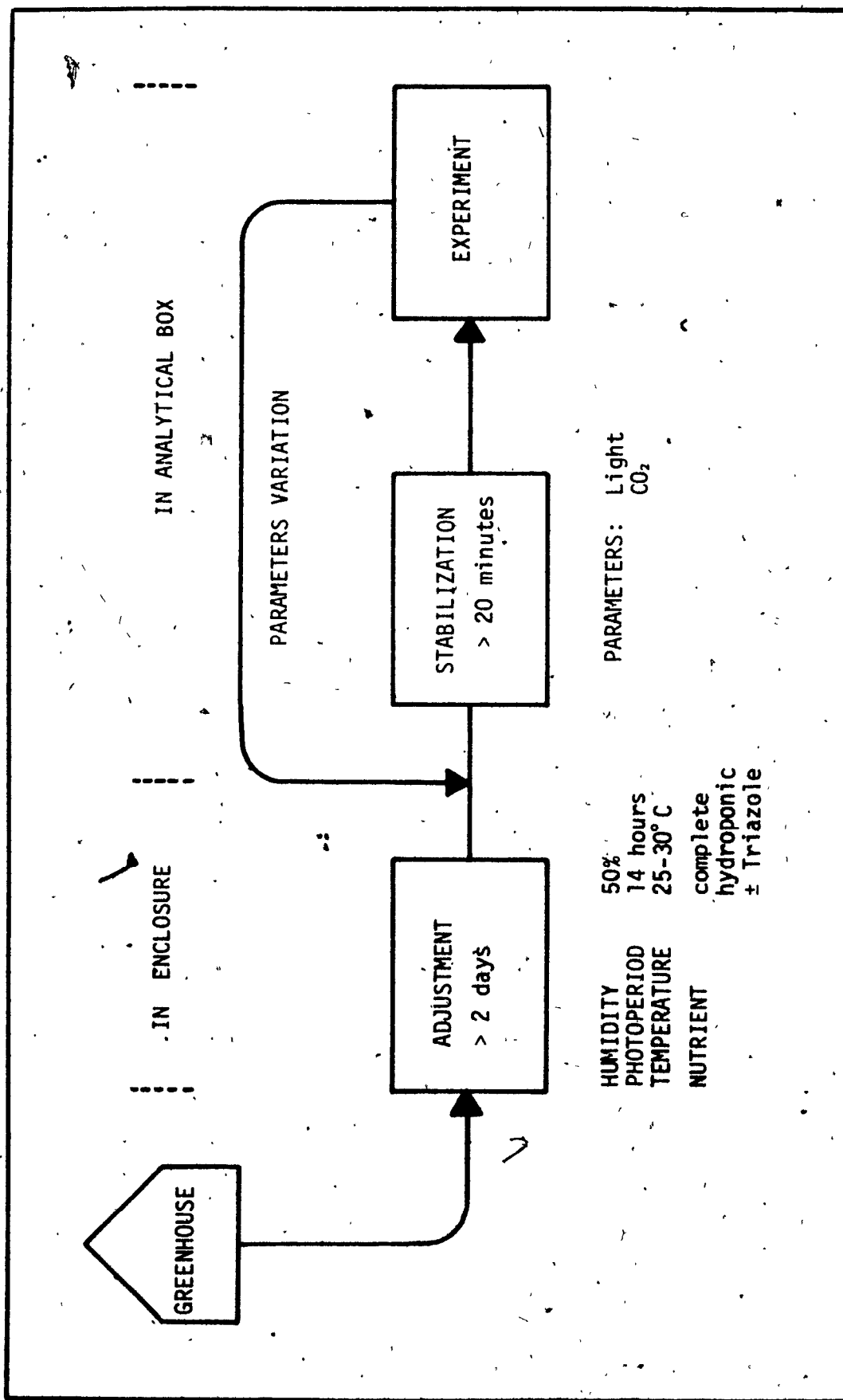


Fig. 7 Experimental Protocol

2.3.5 Treatments

Variation in light, temperature and CO_2 parameters were studied by performing a sequence of experiment on the same plant material, each time changing the value of a single parameter (Table 1). Light and CO_2 variations were performed more often than others because of their predominant effect on the energy budget of plants. Alternately, studies of the effects produced by contaminants were attempted: SO_2 gas was injected at the start of an experiment directly into the closed circuit using a gas syringe. The dose was increased in following experiment. The effects of Amitrole (3 amino -1 -2, 4 triazdo) on the energy budget were obtained by dissolving this herbicide to 10^{-3}M in the nutrient solution. Daily experiments were made during the 5 days that followed the treatments. The following table resumes the extent of treatments. Figure 7 shows the overall operation.

Table 2

Experimental Treatments

Exp	Date Month/Day	Subject	Treatment Light (J/sec/cm ²) × 10 ³	CO ₂ vpm	SO ₂ vpm	Amitrole days of exposure at 10 ⁻³ M
20	08/25	D. Bean	3.306	air	none	none
21	08/25	"	1.945	"	"	"
22	08/25	"	0.972	"	"	"
23	08/25	"	0.778	"	"	"
24	08/25	"	0.000	"	"	"
34	09/15	Tomato	3.306	air	none	none
35	09/15	"	1.556	"	"	"
36	09/15	"	0.778	"	"	"
37	09/16	"	0.389	"	"	"
38	09/16	"	0.000	"	"	"
50	10/22	Tobacco	3.306	air	none	none
51	10/22	"	1.945	"	"	"
52	10/22	"	0.972	"	"	"
53	10/22	"	0.000	"	"	"
50	10/22	Tobacco	3.306	326.2	none	none
54	10/22	"	"	133.4	"	"
55	10/22	"	"	78.3	"	"
56	10/22	"	"	28.8	"	"
57	10/23	Tobacco	3.306	air	none	0
58	10/23	"	"	"	"	0
59	10/24	"	"	"	"	1
60	10/25	"	"	"	"	2
61	10/27	"	"	"	"	4
62	10/28	"	"	"	"	5
84	01/06	Bean	3.306	air	0	none
85	01/06	"	"	"	0	"
86	01/06	"	"	"	22	"
87	01/06	"	"	"	33	"
88	01/06	"	"	"	55	"

2.4 Measurements

2.4.1 Temperature

All temperature measurements were made with 10 flexible thermistor probes. Five probes were used to record the air condition pertaining to the boxes and the psychrometers and were fed to a calibrated multiplexor/transducer unit. The unit produced a voltage proportional to the temperature of each probe. Each probe temperature was sequentially read for about 15 seconds, and the output displayed on a chart recorder. Three other probes were directly connected to a YSI *Telethermometer* and were manually recorded from time to time as their temperature variations were always small during the course of an experiment. These included the temperature of the nutrient pan and the inlet temperature. The last two probes were directly connected to the air conditioning control unit and were used to control the enclosure status as already mentioned. The following table resumes the total arrangement.

Table 3
Description and Location of Temperature Probes

Probe	Description	Location	Precision	Recording time
t_r	Dry Bulb	Outlet Ref. box	0.1 °C	sequenced on chart recorder
t_a	Dry Bulb	Outlet Anal box		
t_{wr}	Wet Bulb	Ref. Psychro		
t_{wa}	Wet Bulb	Anal Psychro		
t_p	Dry Bulb	Anal Psychro		
t_i	Dry Bulb	Inlet Analytical box	0.5 °C	Manual Recording
t_n	Dry	Nutrient pan		
t_{de}	Dry	Enclosure	0.1 °C	Air conditioning control of enclosure
t_{we}	Wet	Enclosure		

Measurements on the chart recorder were calibrated with a network of resistances against a primary standard as follows. The boiling point and melting point of distilled water were used to correct the readings of 0.1 °C precision thermometer. This thermometer was then used as secondary standard to establish the thermistor calibration curve. The electrical resistance of a probe was recorded at temperature intervals of 5 °C between 10 °C and 40 °C. Standard resistances were adjusted and permanently mounted in the transducer/multiplexor unit. It was thus possible to obtain a calibration curve directly on the recorder immediately before or after an experiment by replacing the probe with these standards. Actual temperature values were then calculated from a regression of the calibration curve.

2.4.2 Flowrate

The flowrate in the boxes was determined by the dilution method (Hammarstrand, 1976). For this purpose, a certain amount of CO₂ was injected in the IRGA cell and allowed to be diluted by the incoming air. The time required to dilute the cell volume was recorded and used in the dilution equation to yield the flowrate. Thus

$$F = \frac{V}{M} \ln\left(\frac{1}{d}\right)$$

where

F = flowrate in mL/sec

V = IRGA cell volume (5600 mL)

d = dilution achieved after M seconds (%)

M = elapsed time (sec)

The IRGA was put in the circuits of both boxes in actual running conditions to ascertain that the flowrates were identical. The Analytical box flowrate was then taken as representative. Flow was expressed as cubic centimeters per second (cm³/sec).

2.4.3 Leaf Area

The problem of estimating the total leaf-area of several plants presented a problem since not all leaves received an identical amount of light and also ran good chances of being in the shadow of others. A uniform method of leaf area measurement was adopted as follows: a photoconductive cell was mounted through the center of a translucent plastic sheet. This assembly was lowered on the glass cover of the analytical box. The light entered the box through the plastic sheet and was reflected back to the cell after being partially absorbed by the plant material and the sides of the box. The principle was that the amount of light absorbed by the leaves would not be reflected back to the photocell and that a linear relation existed between leaf area and the photocell readings. The calibration curve shown in figure 8 was produced by introducing known surfaces of flat black paper into the analytical box.

A red filter was put in front of the photocell in order to limit the detection to the absorption spectrum of the leaf. In this case, very little difference was found between the absorbance of the leaves and the black area standards (less than 1%). The method thus measured the total effective leaf area of the canopy as viewed from the top.

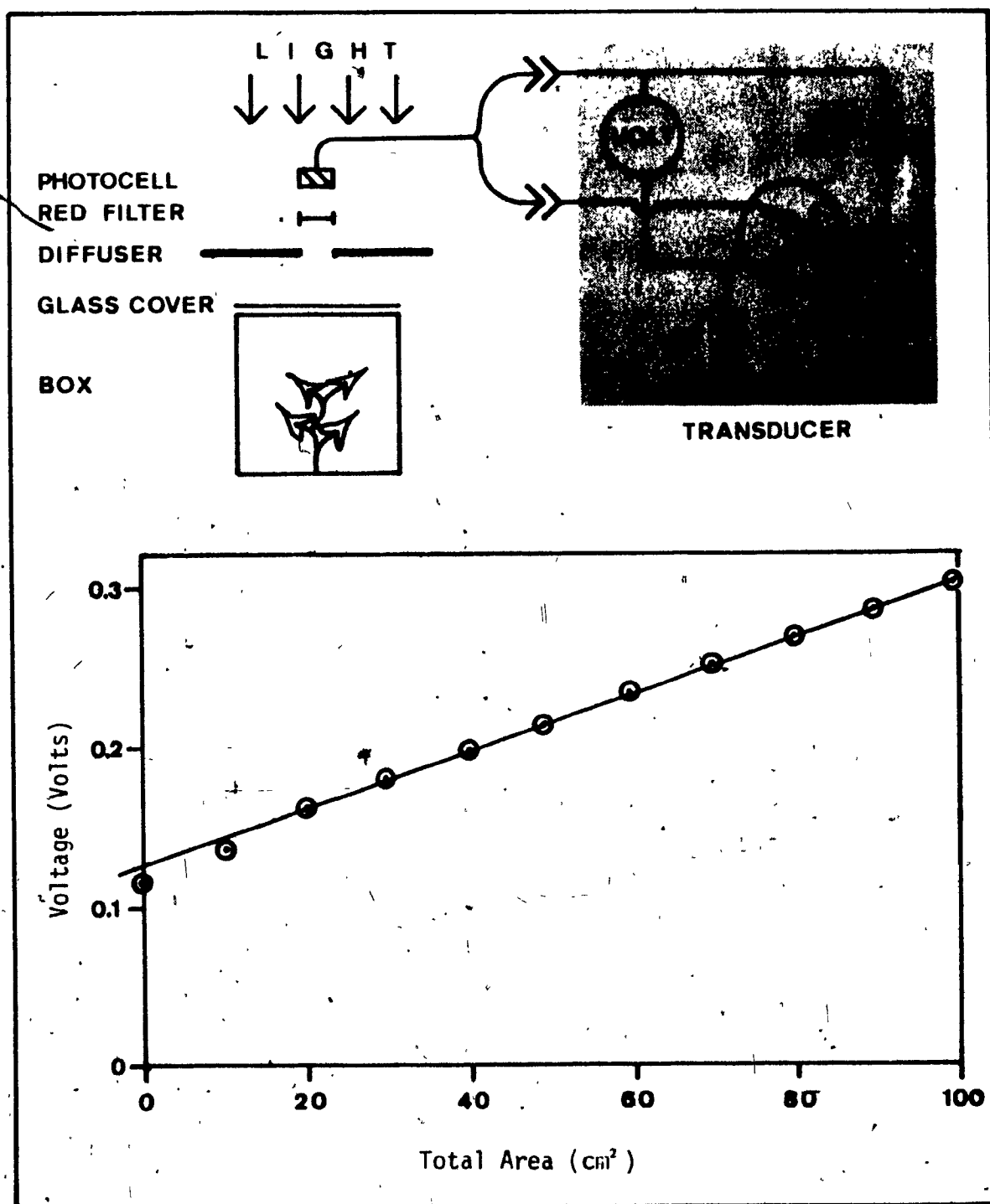


Fig. 8 Leaf Area Measurement

The role of the transducer is to convert the current flowing in the photocell into a voltage reading, since current and not voltage was linear with light flux. A calibration curve was generated for each area determination, the curve shown is typical of the results obtained.

All parameters of the plant were expressed according to this effective area. No attempt was made to discriminate the area into transpiration, infrared and visible parts. In other words the effective leaf area was considered as a flat horizontal plane of uniform response to all energy exchanges. Thus this assumption did not differentiate the orientation of individual leaves and their stomatal pore distribution on the top and bottom of the leaf blade, and therefore reflected the average response of the whole plant canopy in the analytical box.

2.4.4 Visible Light

The visible light component between 400 and 700 nanometers was measured with a photocell connected to a transducer similar to the previous one. No red filter was used. A calibration curve was generated using a standard visible light photometer (spectra physics number 404) held at the top of the analytical box and looking upward. The visible light intensity thus measured corresponded to the light absorbed by a perfect black body having an absorbance of 1. The true absorbed visible radiation (R_v) was calculated as 50% of the total available visible light radiation between 400 and 700 nanometers, this corresponding to an absorbance factor of 0.5 for green leaves (Gates, 1965b).

2.4.5 Rate of CO₂ Exchange and Concentration

A Wilk's model II *Miran* Analyser equipped with a 5.6 liter reading cell was used and calibrated according to the

manufacturer's protocol (Wilks, 1976). The IRGA was put in the closed loop circuitry after the psychrometers, and was connected to a recorder. The amount of CO_2 liberated or absorbed by the plant material was given by the slope of the changing concentration displayed on the recorder. An exact calibration of CO_2 exchange was obtained by injecting a precise amount of CO_2 in the system and observing the resulting deflection on the recorder. The IRGA was very stable and calibration could be kept up to a month. Concentrations of the gas were expressed as parts per million and exchange rates as nanomole CO_2 per second. The IRGA suffered no bias from the absorption spectrum of water vapour.

2.5 Psychrometric Calculations

The wet and dry bulbs temperatures readings were used to calculate the transpiration and sensible heat gains produced by the plant material located in the analytical box. The standard psychrometric tables and equation were found in the *ASHRAE Handbook of Fundamentals*. Although the results were expressed in SI units, psychrometric calculations were first computed with American Standard units and were then converted to SI. In this manner, it was easier to verify the calculations directly on the psychrometric chart and tables which were based on the American Standard units. This treatment was performed by computer programs to be described later. The moist air properties were calculated for each box using their respective temperature readings, (Fig. 9) namely: inlet (t_i), outlet (t_a), dry bulb psychrometer (t_p) and wet bulb psychrometer (t_{wa}) for the analytical box, and t_i , t_r , t_p

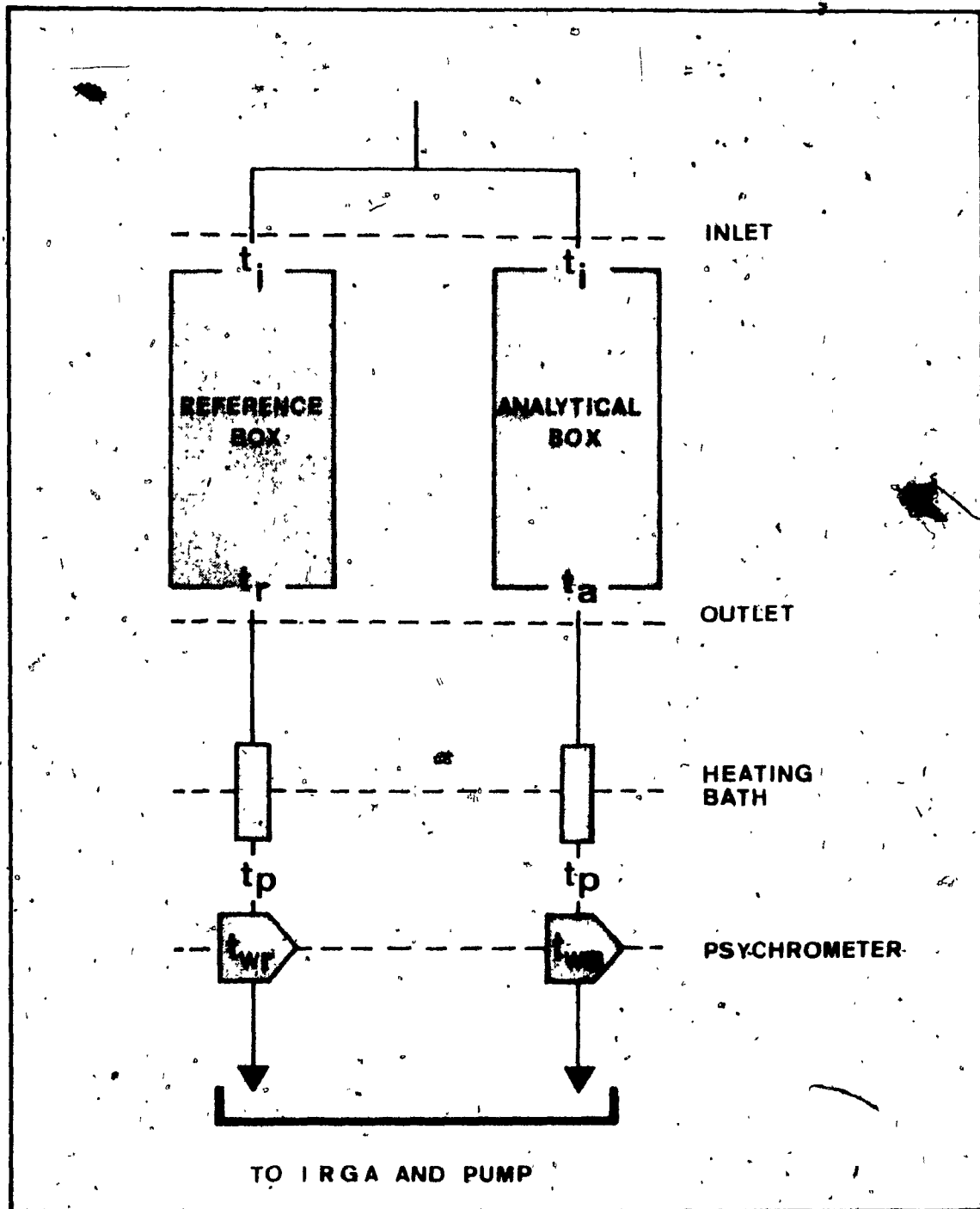


Fig. 9 Location of Temperature Probes

The heating bath elevated and equalized the outlet temperature (t_a , t_r) to a uniform psychrometer dry bulb temperature (t_p) thus preventing a condensation of water vapour in the tubing. t_r , Reference dry bulb; t_a , Analytical dry bulb; t_p , psychrometer dry bulb; t_{wr} Reference wet bulb; t_{wa} , Analytical wet bulb; inlet temperature, t_i .

t_{wr} for the reference box. These properties are listed below (Table 4).

Table 4

Moist Air Properties

Common Inlet W_i	Analytical Box W_a	Reference Box W_r	Properties Humidity ratio	Units lb water/ lb air
ϕ_i	ϕ_a	ϕ_r	Relative humidity	dimensionless
v_i	v_a	v_r	Volume density	(ft ³ /lb dry air)
H_{Ti}	H_{Ta}	H_{Tr}	Moist air Enthalpy	(Btu/lb dry air)
H_{Si}	H_{Sa}	H_{Sr}	Dry air Enthalpy	btu (lb dry air)
H_{Li}	H_{La}	H_{Lr}	Water vapour Enthalpy	btu (lb dry air)

- The humidity ratio (W) was calculated by the following procedure: In a first step, the saturation pressure of water vapour (P_{ws}) was calculated for the psychrometer wet bulb reading (t_w) according to the Keenan, Keyes, Hill and Moore formula (ASHRAE, 1972):

$$\ln \left(\frac{P_{ws}}{217.99} \right) = \frac{0.01}{T_w} (374.136 - t_w) \sum_{i=1}^5 F_i (0.65 - 0.01 t_w)^{i-1} \quad \dots (8)$$

where

P_{ws} = saturation pressure (atm) at T_w

T_w = Absolute temperature (Kelvin) = $t_w + 273.15$

t_w = wet bulb temperature ($^{\circ}\text{C}$) of psychrometer

F_i = empirical constant having the following values:

$F_1 = -741.9242$ $F_5 = 0.1094098$

$F_2 = -29.721$ $F_6 = 0.439993$

$F_3 = -11.55286$ $F_7 = 0.2520658$

$F_4 = -0.8685635$ $F_8 = 0.05218684$

the humidity ratio of saturated air was then obtained by the following:

$$W_{sw} = 0.62198 P_{ws} / (1 - P_{ws}); \text{ (lb water/lb dry air) } \dots(9)$$

where the atmospheric pressure was assumed constant and equal to unity.

Finally, the humidity ratio was calculated by:

$$W = \frac{(1093 - 0.556 t_w) W_{sw} - 0.24(t_p - t_w)}{(1093 + 0.444 t_p - t_w)} \dots(10)$$

where

W = humidity ratio (lb water/lb dry air)

t_p = Psychrometer dry bulb temperature ($^{\circ}\text{F}$)

t_w = wet bulb temperature ($^{\circ}\text{F}$) of psychrometer

W_{sw} = humidity ratio of saturated air (lb water/lb dry air)

the dry bulb temperature of the boxes (t_a , t_r , t_i) were always lower than that of the psychrometers (t_p) due to the heating bath. This elevation in temperature does not alter the humidity ratio calculations (W_a , W_r), which are the same whether taken at the box outlet or at the

psychrometer. This, however, is not true for the properties of relative humidity (ϕ_a, ϕ_r, ϕ_i) and volume density (v_a, v_r, v_i) which are dependent upon the dry bulb temperature of the boxes (t_a, t_r, t_i). Consequently the relative humidity was calculated as follows:

$$W_{SD} = \frac{0.62198 P_{DS}}{(1 - P_{DS})} \quad (\text{lb water/lb dry air}) \dots(11)$$

$$x = \frac{W}{W_{SD}} \quad (\text{dimensionless}) \dots(12)$$

$$\phi = \frac{x}{1 - P_{DS}(1 - x)} \quad (\text{dimensionless}) \dots(13)$$

where

P_{DS} = saturation pressure of water vapour AT the respective dry bulb temperatures of the boxes (using Keenan, Keyes, Hill and Moore formula)

W_{SD} = humidity ratio at saturation

W = Respective humidity ratio of the boxes (lb water/lb dry air)

x = degree of saturation

ϕ = Relative humidity

the volume density of dry air at the three location (v_i, v_a, v_r) was obtained by:

$$v = \frac{R_a T}{p} (1 + 1.6078 W) \quad (\text{ft}^3/\text{lb dry air}) \dots(14)$$

where

v = volume density of dry air

R_a = 53.352 (ft lb force/lb mass/F deg Abs), gas constant for dry air.

p = 2116.1986 (lb force/ft²), total atmospheric pressure

T = Respective dry bulb temperature of the boxes ($^{\circ}\text{F}$ absolute)

W = Respective humidity ratio of the boxes (lb water/lb dry air)

The dry air Enthalpy (H_{si} , H_{sa} , H_{sr}) involved the following

$$H_s = 0.240 t \quad \dots(15)$$

where

H_s = dry air enthalpy (Btu/lb dry air)

t = dry bulb temperature of the boxes ($^{\circ}\text{F}$)

and for the water vapour enthalpy (H_{Li} , H_{La} , H_{Lr}):

$$H_L = W(1061 + 0.444)t \quad (\text{Btu/lb dry air}) \quad \dots(16)$$

Finally, the total enthalpy was expressed:

$$H_T = H_s + H_L \quad (\text{btu/lb dry air}) \quad \dots(17)$$

The table that follows resumes the whole operation

Table 5

Calculation of Moist Air Properties

Description	Formula used	Property	Variable used
humidity ratio (lb water/lba)	2, 3, 4	W_i W_a W_r	t_p, T t_p, T_{wr} t_p, T_{wa} t_p, T_{wr}
Relative humidity (dimensionless)	5, 6, 7	ϕ_i ϕ_a ϕ_r	t_i, W_i t_a, W_a t_r, W_r
Volume density (ft ³ /lba)	8	v_i v_a v_r	t_i, W_i t_a, W_a t_r, W_r
dry air Enthalpy (btu.lba)	9	H_{si} H_{sa} H_{sr}	t_i t_a t_r

Table 5 (continued)

Description	Formula used	Property	Variable used
Water vapour Enthalpy (btu/lba)	10	H_{Li} H_{La} H_{Lr}	t_i, W_i t_a, W_a t_r, W_r
Moist air Enthalpy (btu/lba)	11	H_{Ti} H_{Ta} H_{Tr}	H_{Si}, H_{Li} H_{Sa}, H_{La} H_{Sr}, H_{Lr}

the environmental parameters of absolute humidity (W) was converted into SI unity by the following:

$$W(\text{nm water/cm}^3 \text{ air}) = W(\text{lb water/lb air}) \times \left(\frac{8.918 \times 10^5}{v} \right) \quad \dots(18)$$

the calculation and conversion of energy exchange is covered in the following section:

2.6 Energy Exchange Calculations

The difference obtained between the reference and analytical properties of the air are a measure of the actual exchange due to the presence of the plant in the analytical box. The observed Exchange values for sensible heat (ΔH_{S_0}), water vapour enthalpy (ΔH_{L_0}) and total heat (ΔH_{T_0}) were then calculated:

$$\Delta H_{S_0} = H_{Sa} - H_{Sr} \quad (\text{Btu/lb dry air}) \quad \dots(19)$$

$$\Delta H_{L_0} = H_{La} - H_{Lr} \quad (\text{Btu/lb dry air}) \quad \dots(20)$$

$$\Delta H_{T_0} = H_{Ta} - H_{Tr} \quad (\text{Btu/lb dry air}) \quad \dots(21)$$

where the variables have been then usual meanings (refer Table 5 on page 40). These calculations are mathematically correct but they do not account for heat losses through the walls and cover of the boxes and for the fact that the psychrometers do not give a matched response. Two corrections have therefore to be applied to the exchange results so as to compensate for the heat loss and psychrometer offset. The corrected values are then converted into SI units and finally expressed in rates per unit canopy area.

2.6.1 Sensible Heat Exchange

The amount of heat loss through the boxes was obtained by recording the temperature differential between the inlet (t_i) and outlet (t_o) of an empty box at different outside temperature (t_g) and for the same rates of airflow as those used during a normal experiment, as shown in figure 10. The drop in temperature between the inlet (t_i) and outlet (t_o) represented the amount of heat loss (HLOSS) through the box material and was calculated according to:

$$\text{HLOSS} = 0.24 \times 1.8 \times (t_i - t_o) \quad \dots (22)$$

the heat loss having a positive value when going outwards. In this situation, the heat lost could be linearly correlated on a log-log scale with the temperature gradient existing between the inside of the box (assumed to be at t_o) and the outside (t_g) thus:

$$\text{HLOSS} = K(t_o - t_g)^n \quad (\text{btu/lb dry air}) \quad \dots (23)$$

where the constants K and n had the experimental values shown: (Table 6)

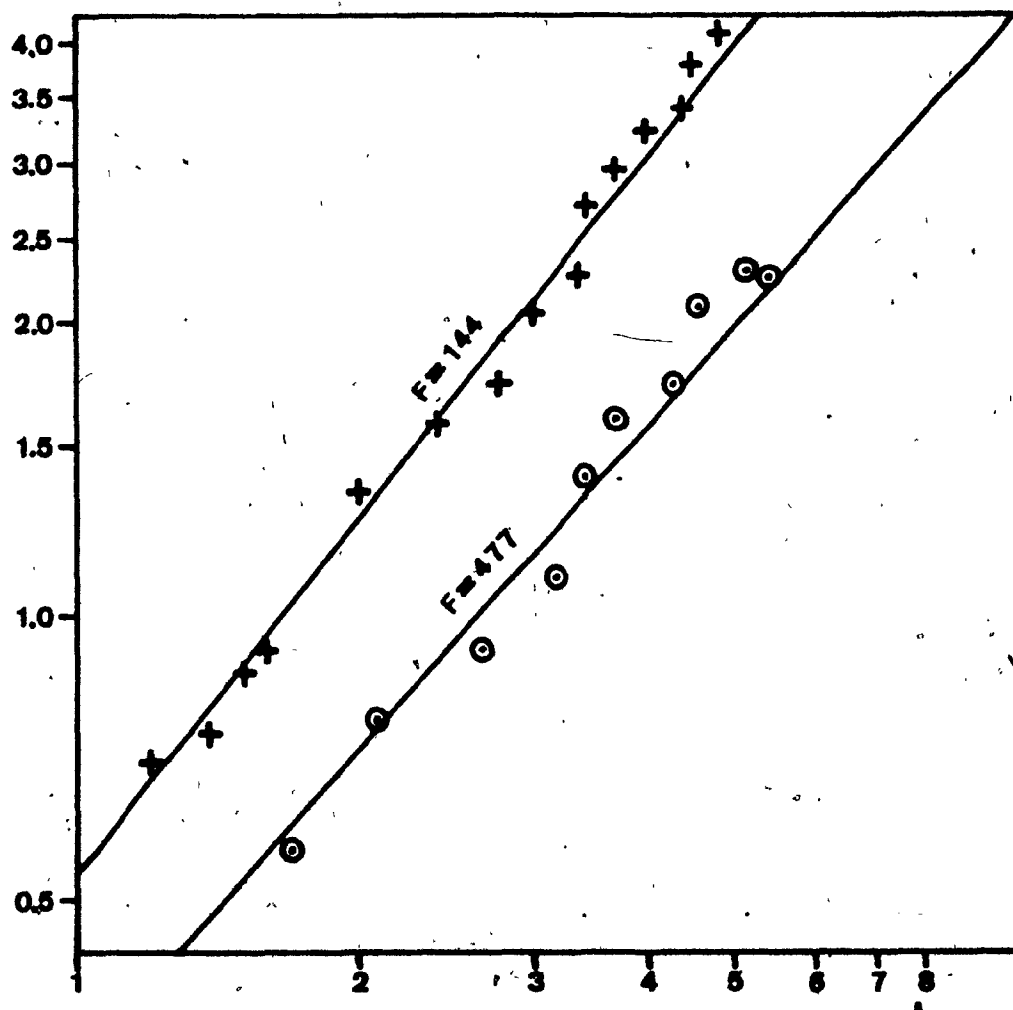
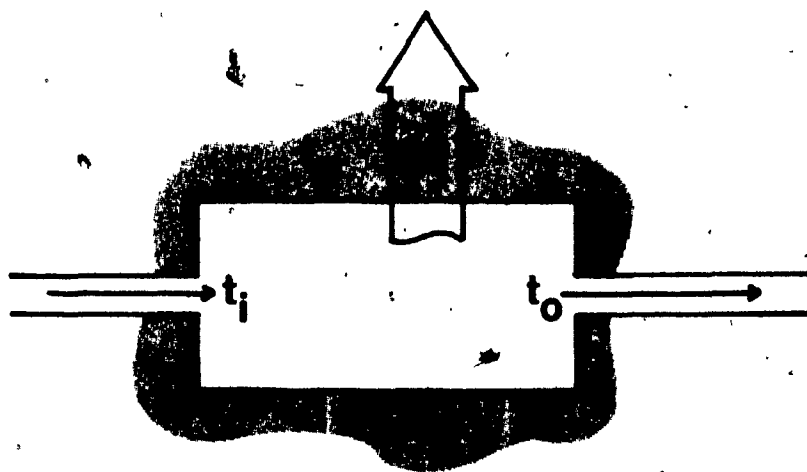


Fig. 10 Heat Losses in the Boxes

The calculations were made for the two flow rates used in the experiment. F , Flowrate (cm³/sec).

Table 6
Sensible Heat Loss Calculation

Flowrate	K	N	Regression Coefficient
cm ³ /sec			
477	0.2959	1.235	0.992
144	0.5236	1.2864	0.992

In the enclosure, the inlet temperature (t_i) of the boxes was always very close or equal to the enclosure temperature because the tubing carrying the air to the inlet was left uninsulated. In this situation, the temperature gradient across the walls of the boxes could be expressed as ($t_A - t_i$) for the analytical box and ($t_r - t_i$) for the reference box, the true Exchange value for the true dry air enthalpy (ΔH_S) was written:

$$\Delta H_S = \Delta H_{S_0} + K(t_A - t_i)^n - K(t_r - t_i)^n \quad (\text{btu/lb dry air}) \quad \dots(24)$$

Converting to SI units:

$$\Delta H_S (\text{j/cm}^3) = \Delta H_S (\text{btu/lba}) \times \left[\frac{2.723 \times 10^{-3}}{v} \right] \quad \dots(25)$$

where v = volume density (ft^3/lba)

The rate of sensible heat produced by the plant was finally computed as:

$$S = \Delta H_S \frac{F}{A} \quad (\text{j/cm}^2/\text{sec}) \quad \dots(26)$$

where

S = Sensible heat rate $(\text{j/cm}^2/\text{sec})$

F = Flowrate of air (cm^3/sec)

A = Canopy area (cm^2)

2.6.2 Latent Heat Exchange

Although the two psychrometers were constructed in a similar way, their absolute response to the same air condition was not the same. This difference was due to two factors. A first discrepancy was caused by a different offset for each psychrometer and corresponded to a similar bias observed in the original paper (Slatyer and Bierhuizen, 1964). This offset value could be eliminated from the readings by temporarily connecting both psychrometers to the same box outlet and recording the offset value, later to be subtracted from the readings. However, another type of bias was also present and corresponded to the equilibration period when the system was switched from the open to the closed circuit configuration. During that period, the psychrometer had to adjust to a new and instantaneous air condition. It was found experimentally that the new condition achieved by the psychrometer, after the beginning of an experiment, required a period of time of no more than three readings corresponding to about three minutes and depended upon the initial air conditions at the beginning of the experiment. Consequently, the calculations of the latent heat from the observed readings (H_{L_o}) were a biased estimate of the true latent heat (H_L) according to the above factors, thus:

$$\text{Reference} \quad H_{Lr} = H_{L_o r} + O_r + \psi_r \quad \dots(27)$$

$$\text{Analytical} \quad H_{La} = H_{L_o a} + O_a + \psi_a \quad \dots(28)$$

where

O = offset value for each psychrometer

H_L = true latent heat for each psychrometer

H_{Lo} = observed latent heat for each psychrometer

ψ = transition bias between open to closed circuit configuration
for each psychrometer

Consequently, the calculation of the latent heat exchange was also biased

$$\Delta H_L = \Delta H_{Lo} + (O_a - O_r) + \psi_a - \psi_r \quad \dots(29)$$

where

ΔH_{Lo} = observed latent heat exchange

ΔH_L = true latent heat exchange

Because of the presence of the transition bias (ψ), it was not possible to derive a practical correction equation that would have yielded a true value. For all the experiments performed the individual error of each psychrometer was found to be about 10% of the reading at the beginning and no more than 5% after the third reading when the transition bias became negligible. Since the calculated value of the latent heat exchange (ΔH_L) was obtained by the difference between each psychrometers, the error on this difference became so large that meaningful results could not be achieved. This inadequate situation did not reflect a poor performance of the differential psychrometer apparatus of Slayter and Bierhuizen (1964) per se, but showed that it could not be adequately used in this set up due to the transition changes between open and closed system, which should be avoided in the future.

It is therefore for the above reasons that an alternate method

for calculating latent heat exchange (ΔH_L) was used and is as follows: the conservation of energy requires that the total energy released by the canopy equals the total incoming radiation absorbed (R_v). Since the total released energy equals $S + LE$ we have:

$$R_v = S + LE \quad \text{and} \quad LE = R_v - S \quad \dots(30)$$

An experimental verification of this relation was done by comparing the rate of change of ΔH_{L_0} with respect to S and comparing with its theoretical value which is obtained by combining equations (29) and (30)

$$\Delta H_{L_0} = R_v - S - (O_a - O_r) - \psi_a + \psi_r \quad \dots(31)$$

If the first three readings from the experiment are not considered, the transition functions (ψ) become negligible.

$$\Delta H_{L_0} = R_v - S - (O_a - O_r) \quad \dots(32)$$

thus, if R_v is kept constant, the theoretical regression of ΔH_{L_0} on S should be equal to -1, since the offset values are themselves constant within each experiment. Table 7 shows that the experimental value of ΔH_{L_0} on S agreed closely with this theoretical value of -1.

Table 7

Experimental Verification of Energy Conservation

Regression of ΔH_{L_0} on S and R_v . The first three readings were eliminated from each experiment in order to eliminate the effect of the transition function.			
Variable S	Coefficient -1.06	STD error 0.108	Multiple Regression $r = 0.7958$ $r^2 = 0.6333$ # of cases = 328
R_v	3.07	0.237	
constant	7.82×10^{-3}	6.05×10^{-4}	

95% confidence interval for $d(\Delta H_{L_0})/dS$

$$d(\Delta H_{L_0})/dS = 1.06 \pm 0.213$$

Consequently, the latent energy (LE) was estimated as:

$$LE = R_v - S \quad \dots(33)$$

where

L = latent heat of vaporization

$$(j/nM \text{ water}) = 4.5 \times 10^{-5}$$

R_v = total visible radiation absorbed by the canopy

$$(j/cm^2/sec)$$

S = Sensible heat rate $(j/cm^2/sec)$

2.6.3 Error in the Estimation of Individual Terms

The error involved in this estimation lies in calculating the true energy exchanges of the plant which includes a term for reradiation (RAD). From the plant's point of view, part of the reradiation term is absorbed by the walls and cover of the analytical box and expressed as sensible heat. The remaining reradiated energy is reabsorbed by the plant. The greenhouse effect of the glass cover presents the escape of reradiated energy such that:

$$R_v + \alpha = RAD + S - \beta + LE \quad \dots(34)$$

where α = Reabsorbed Radiation by plant

β = radiation absorbed by analytical box

in estimating the latent heat (LE) the sensible heat (S) was subtracted from the Visible Radiation absorbed (R_v) then :

$$R_v - S = RAD - \alpha - \beta + LE \quad \dots(35)$$

by which an error of $\gamma = RAD - \alpha - \beta$ was introduced in the estimation of the latent heat (LE). Thus, the true convection (c), and latent heat (LE) for the plant are as shown:

$$R_v + \alpha = RAD + (S - \beta) + (LE - \gamma) \quad \dots(36)$$

$$Q_{ABS} = RAD + C + LE \quad \dots(37)$$

Since the value of RAD is usually small, the corresponding values of α , β and γ will bias the estimations of individual terms by even smaller amounts since $\alpha + \gamma + \beta = RAD$. The bias on individual terms of Q_{ABS} , C and LE was therefore assumed to be negligible on the overall value of each term.

2.7 Data Processing

All the calculations presented this far were programmed (Fig. 11). The experimental readings were first typed on computer cards and properly identified in three categories: readings obtained from the chart recorder (t_{wr} , t_r , t_a , t_p), readings obtained manually (t_i , t_n , t_g), and the calibration readings produced by the multiplexor/transducer unit; this card input was treated in order to calculate the actual temperature values from a regression of the calibration data. The readings from the chart recorder and those obtained manually were merged taking into account that the manual readings were taken less frequently than the recorded ones; such that missing values had to be generated by linear

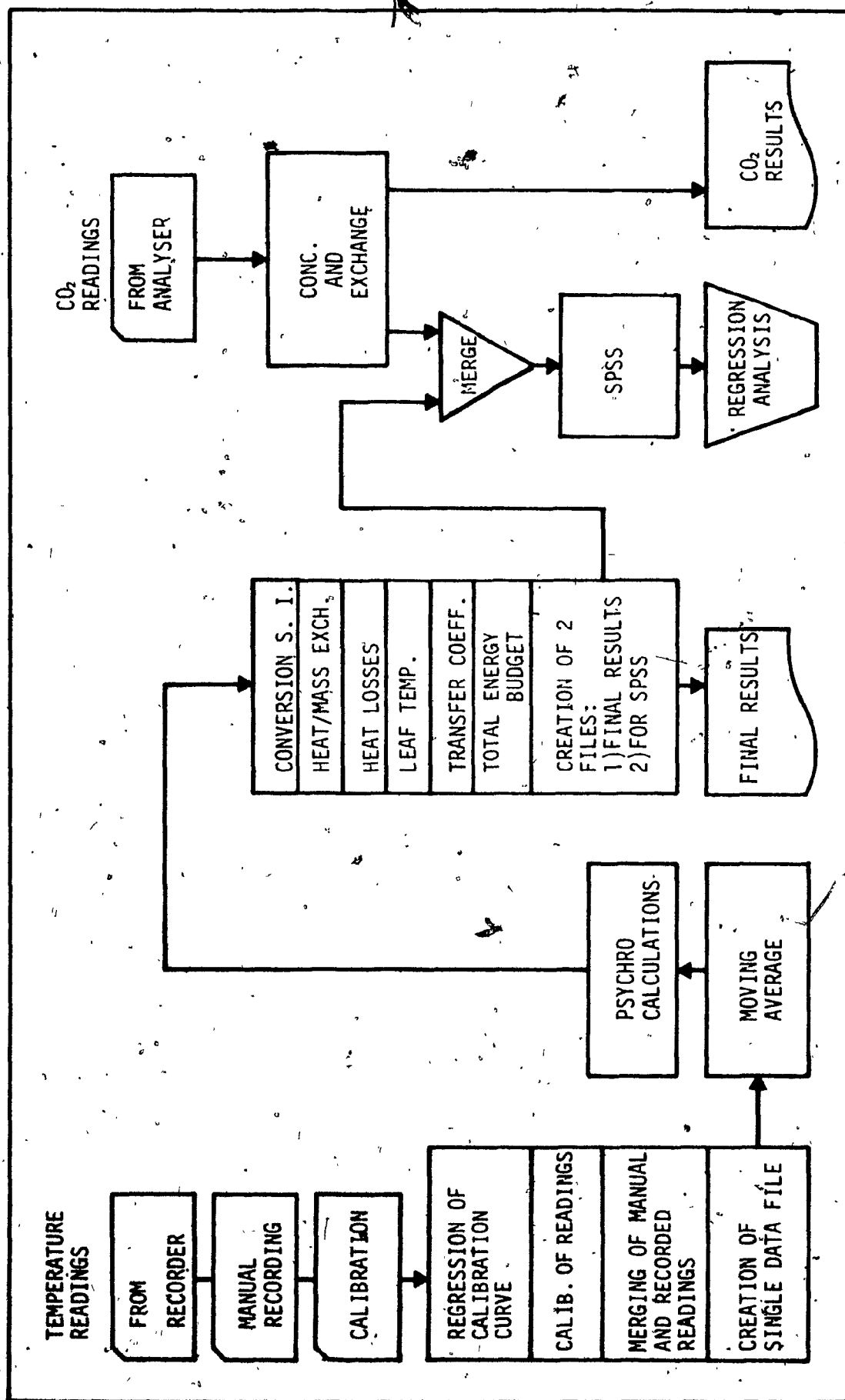


Fig. 11 Data Processing

interpolation between known values. The merged data was then put into a single working file and a three point moving average was done in order to eliminate random noise peaks from the instrumentation. The psychrometric calculations were performed and the convected sensible and latent heat rates were then calculated.

The energy budget calculations that followed were printed out as the *final results* and included all the pertinent temperature and humidity values of the surrounding air along with the calculated exchanges and transfer coefficient. These last calculations are covered in *results and discussion*. This same output was also merged with the CO₂ exchange readings. A multiple regression analysis of these results could then be executed by the SPSS (U. of Minnesota) system. The graphic displays of the experimental results used in this paper were produced according to this regression analysis. The program listings for all the above can be found in the appendix.

Chapter 13

RESULTS AND DISCUSSION

3.1. Transpiration, Humidity and Light Intensity

The transpiration performances for tobacco, tomato and dwarf bean were closely linear with light intensity and absolute H (Figs. 12, 13, 14) and the results show that an increased humidity resulted in a decreased transpiration when the outside air was brought nearer to the saturation point. A regression analysis of latent energy exchange (LE) versus visible absorbed radiation (R_v) and absolute humidity (W_a) is shown in the following table.

Table 8

Correlation of Transpiration Energy (LE) on Visible Absorbed Light Intensity (R_v) and Absolute Humidity (W_a). Cste. stands for the Regression Constant

Variable		B Coefficient	Error	N Normalized Coefficient	Simple Regress.	Multiple Regress.
Tobacco	R_v	4.04	1.22×10^{-1}	0.988	0.934	0.980
	W_a	-7.88×10^{-3}	7.57×10^{-1}	-0.310	-0.130	
	Cste	-8.55	7.45×10^{-1}			
Tomato	R_v	3.27	1.05×10^{-1}	0.998	0.910	0.966
	W_a	-6.17×10^{-3}	5.86×10^{-1}	-0.338	-0.077	
	Cste	9.18	7.02×10^{-1}			
D. Bean	R_v	1.32	3.23×10^{-2}	0.832	0.575	0.992
	W_a	-1.07×10^{-2}	2.68×10^{-1}	-0.848	-0.597	
	Cste	18.16	3.23×10^{-1}			

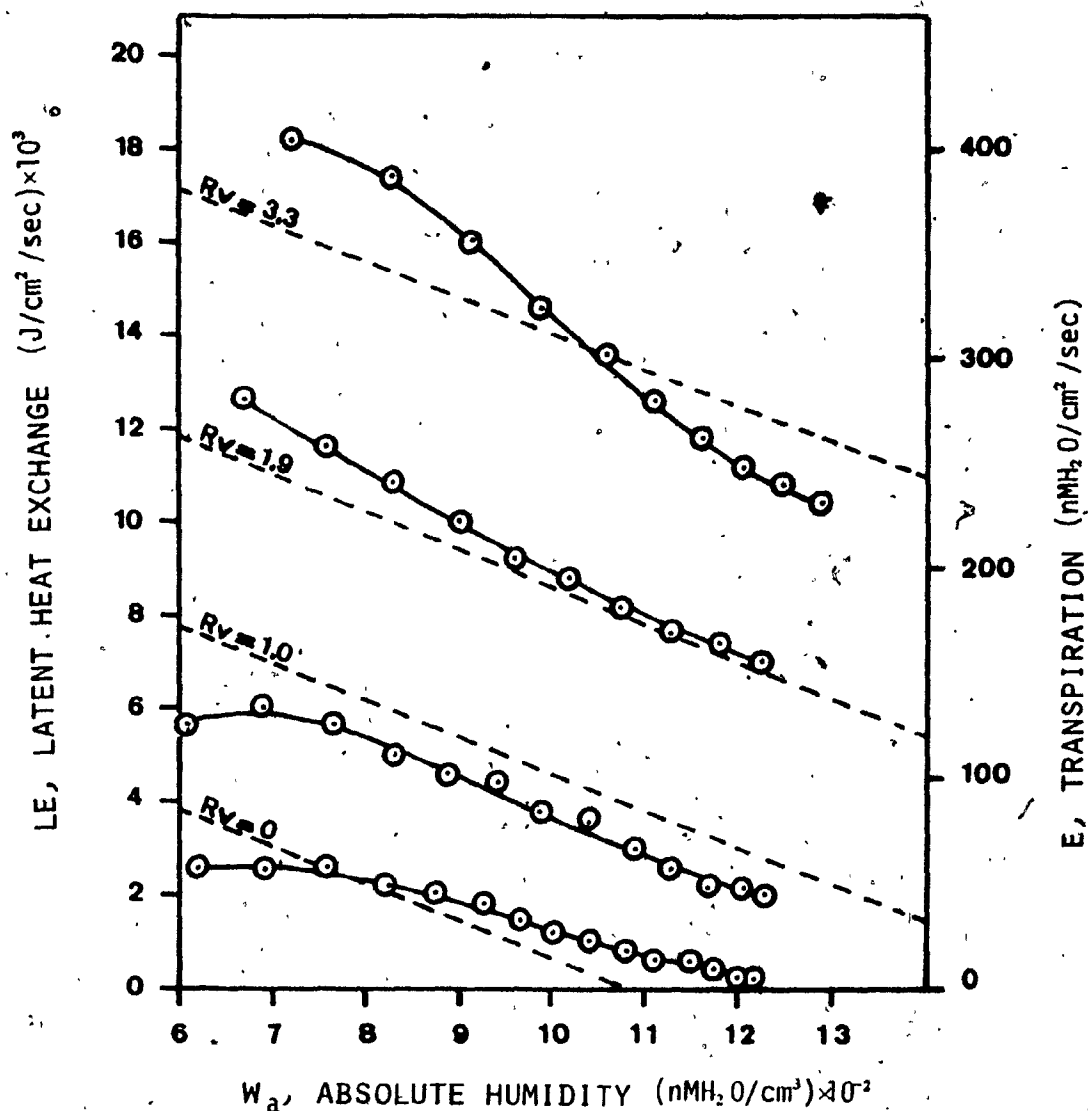


Fig. 12 Effect of Light and Humidity on Transpiration in Tobacco

The multiple regression analysis was calculated for the values of light (R_v) shown, and according to table 8. R_v , Visible absorbed radiation $(\text{j}/\text{cm}^2/\text{sec}) \times 10^3$. Air temperature, $t_a = 29.2^\circ\text{C}$ ± 0.14 . CO_2 concentration, $C_a = 340 \text{ ppm} \pm 8.0$.

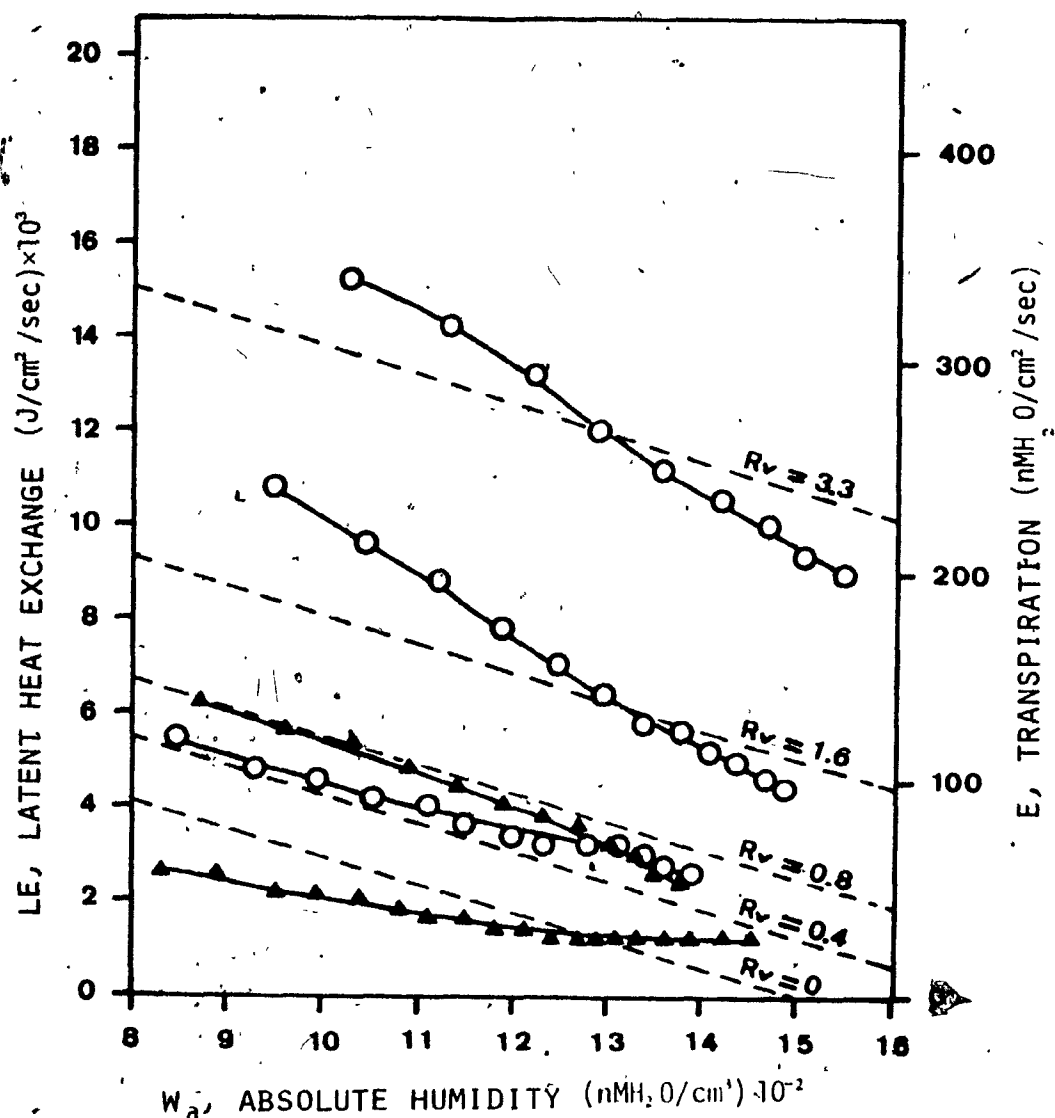


Fig. 13 Effect of Light and Humidity on Transpiration in Tomato.

The multiple regression analysis (dotted lines) was calculated for the values of light (R_v) shown, and according to table 8. The experimental points shown as triangles curve obtained 1 day later (exp #37 and 38); see table 2. R_v , Visible absorbed radiation ($\text{j/cm}^2/\text{sec}) \times 10^3$. Air temperature, $t_a = 29.0^\circ\text{C} \pm 0.1$. CO_2 concentration, $C_a = 378.1 \text{ ppm} \pm 2.2$.

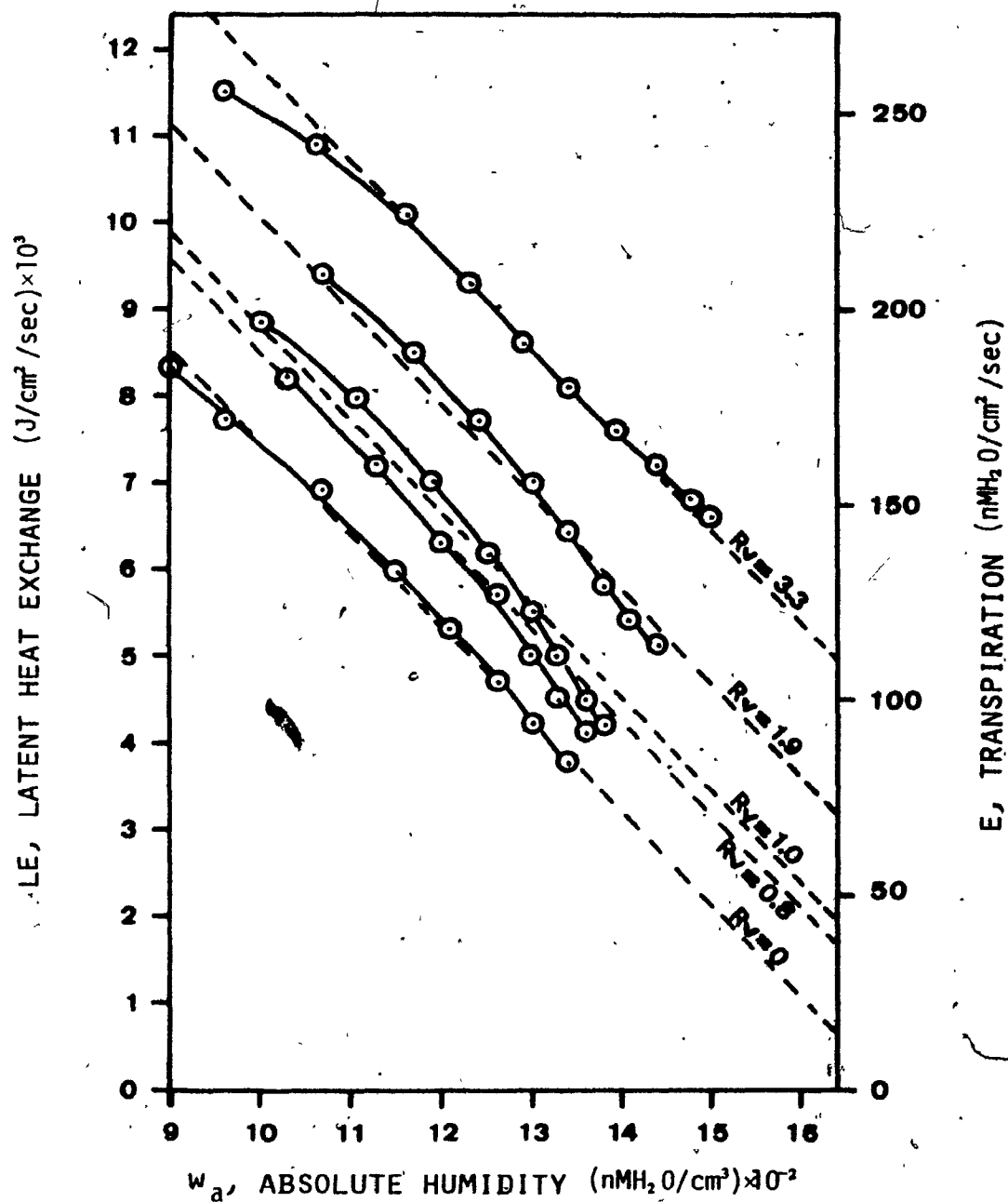


Fig. 14 Effect of Light and Humidity on Transpiration in Bean

The multiple regression analysis was calculated for the values of light (R_v) shown, and according to table 8. R_v , Visible absorbed radiation ($\text{j}/\text{cm}^2/\text{sec}$). Air temperature, $t_a = 27.1^\circ\text{C} \pm 0.34$. CO_2 concentration, $C_a = 374 \text{ vpm} \pm 5.0$.

Inspection of the normalized coefficients reveals that an equal contribution to transpiration was provided by humidity and light intensity in the case of D. Bean while transpiration was mostly explained by the light intensity in the other cases. Since transpiration is controlled by the concentration gradient existing between leaf and environment, and by the diffusive resistance, it follows that for an increased dependance on absolute humidity, the control of transpiration shifts from the leaf to the environment. It is expected that the leaf diffusion resistance will tend towards a constant value when control is entirely left to the environment. A variability index (I_v) can be defined as the ratio of the normalized coefficients for light intensity (N_{rv}) to that for humidity (N_{wa}) such that:

$$I_v = \frac{N_{rv}}{N_{wa}} \quad \dots(38)$$

and is indication of the diffusive resistance variability under changing light and humidity conditions. When equal to zero, the diffusive resistance tends to remain constant and transpiration is solely controlled by the humidity variations, Table 9 shows these numbers.

Table 9
Variability of Diffusion
Resistance

Tobacco	Tomato	Bean
-3.19	-2.95	-.96

Thus it can be expected that the calculated values for diffusion resistance will tend to be more constant in the Bean experiment than in Tobacco, the results of Tomato being of intermediate variation.

Table 10

Net Photosynthesis, Light Intensity and Transpiration

Tobacco Leaf Area = 124.5 cm²
Avg. Concentration CO₂ = 340 ppm s.d. = 28.0

	CO ₂ Exchange			Transpiration			
Experiment	Mean	#Cases	Error	Mean	#Cases	Error	Light Intensity
	nM/cm ² /sec						j/sec/cm ²
50	+1.008	10	0	302.8	10	19.80	-3.306×10^{-3}
51	+0.574	10	0	207.2	10	13.25	1.945×10^{-3}
52	+0.296	13	0	86.0	13	8.85	0.972×10^{-3}
53	-0.370	16	0	32.8	16	5.13	0.0×10^{-3}

Tomato Leaf Area = 279.7 cm²
Avg. Concentration CO₂ = 378.1 s.d. = 9.4 ppm

	CO ₂ Exchange			Transpiration			
Experiment	Mean	#Cases	Error	Mean	#Cases	Error	Light Intensity
34	+1.080	9	.030	259.1	9	16.10	3.306
35	+0.585	12	.038	149.7	12	14.83	1.556
36	+0.196	13	.014	81.9	13	5.05	0.778
37	+0.202	13	.014	94.4	13	9.05	0.389
38	-0.029	25	.008	34.9	25	2.35	0.0

Dwarf Bean Leaf Area = 258.8 cm²
 Avg. Concentration CO₂ = 374.0 ppm s.d. = 15.9 ppm

	CO ₂ Exchange			Transpiration			
Experiment	Mean	#Cases	Error	Mean	#Cases	Error	Light Intensity
20	+0.713	10	.041	192.8	10	12.1	3.306
21	+0.355	8	.028	153.5	8	12.1	1.945
22	-0.01	8	.028	136.8	8	13.1	0.972
23	-0.00	7	.034	129.7	7	12.5	0.778
24	-0.182	8	.000	130.1	8	13.0	0.0

3.2 Net Photosynthesis and Transpiration

Plots of Net photosynthesis (as CO₂ exchange) response to light intensity in tobacco, tomato and bean gave the performance shown in figure 15 and Table 10 with respect to visible light. The slope of net photosynthesis (Gaastra 1963) and light variations in the linear portions of the curves gave the Net Photosynthetic yield, being the ability of the plant to capture CO₂ for a given amount of light. This yield is:

$$I_p = \frac{\Delta P_n}{\Delta R_v} \quad \dots (39)$$

Table 11

Net Photosynthesis Yield (I_p)

Tobacco	Tomato	D. Bean	
305.9	319.2	295.9	Efficiency nM/j. × 10 ³
0.064	0.067	0.062	Quantum yield nM CO ₂ /nE

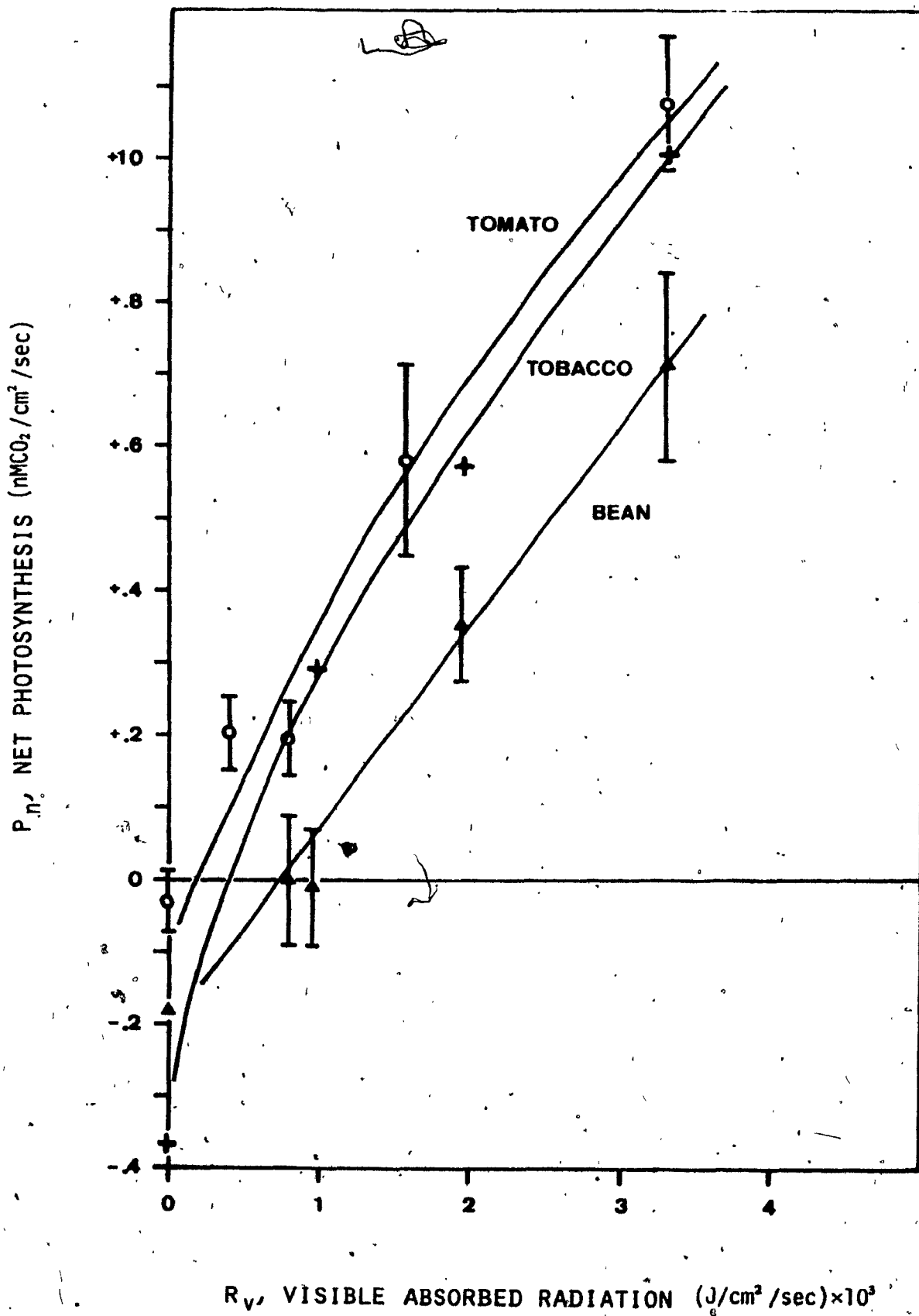


Fig. 15 Net Photosynthesis and Visible Absorbed Radiation for Tomato, Tobacco and Bean: the linear portion of the curve was used to calculate the quantum yield.

Assuming a photon to energy flux ratio of $1.2 \times 10^9 \pm 10\%$ (photons cal^{-1}) occurring in the band 400-700 nm, (Anderson, 1967) it is possible to convert these values into quantum yield (Ehleringer, 1977) expressed in Mol CO_2 per absorbed Einstein. These results compare favorably with those of *Plantago*, 0.066 (Björkman, 1966) and species of *Atriplex*, *Encelia* and *Plantago*, 0.054 (Ehleringer, 1977) all of them being C_3 plants. However, the transpiration values can be expressed as a function of the CO_2 exchange. Figure 16 shows the relationship existing between these results for the three plants. Regression was performed with the means of transpiration and CO_2 exchange (Table 10) the regressed line was plotted against a background showing the deviations around each point. Although the results were obtained from three different plants under a wide range of light and humidity treatments, a linear response was observed (Table 12).

Table 12

Trend for Transpiration and Assimilation:
Light Variations

(I_L) slope = 165.21	$\text{MH}_2\text{O}/\text{MCO}_2$	$r = 0.8970$
constant = 78.5	$\text{nMH}_2\text{O}/\text{cm}^2/\text{sec.}$	$r^2 = 0.8046$

Thus, in a general sense, a change in transpiration is correlated linearly with a change in net photosynthesis. The high positive correlation of transpiration and light intensity shown earlier

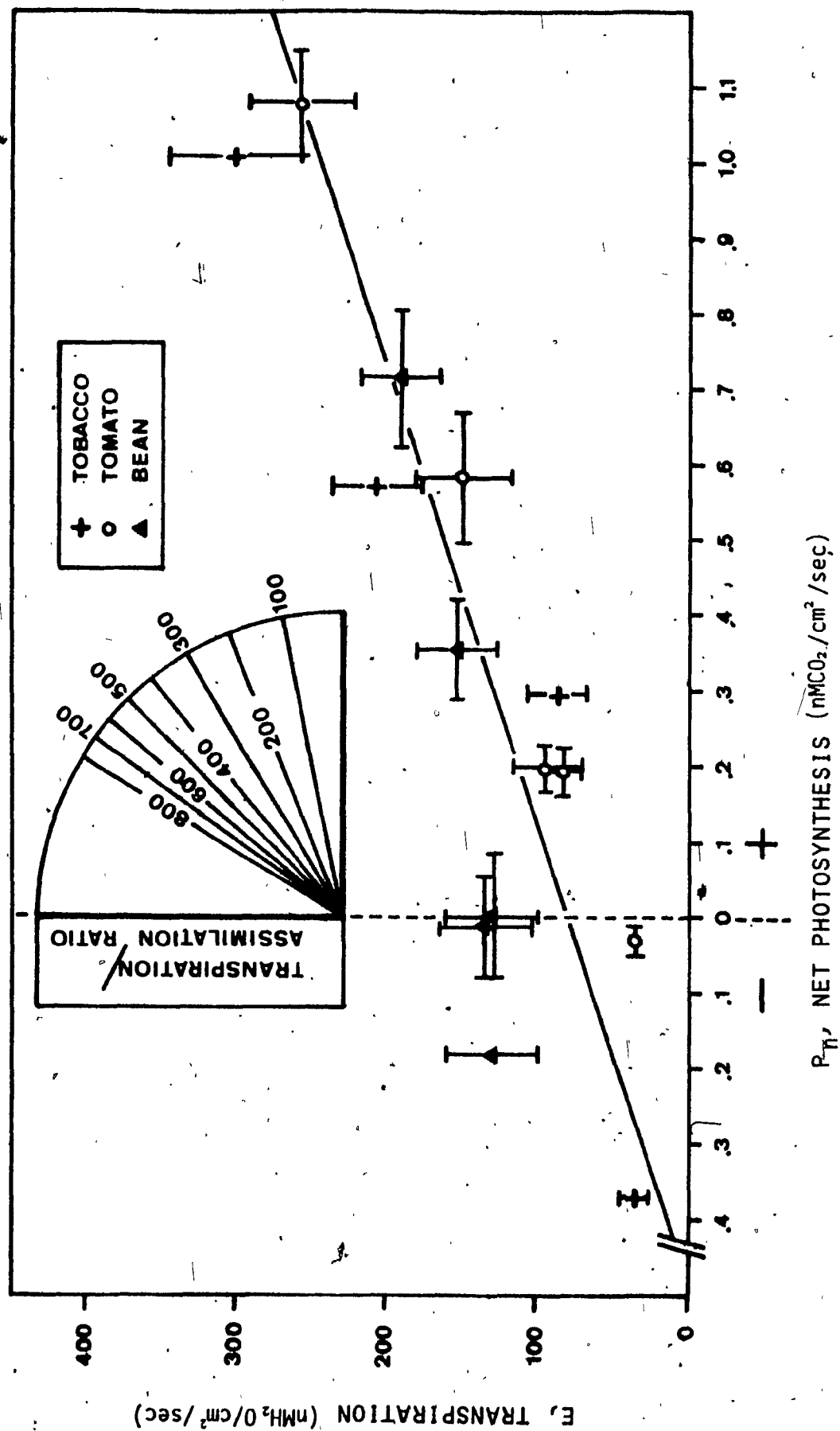


Fig. 16 Trend for Transpiration and Assimilation: Light Variations.

This figure shows the linear trend under a wide range of light and humidity variations. The value of the transpiration/Assimilation ratio is obtained by the slope of the line linking the desired location on the graph to the point $(P_n, E) = (0, 0)$

(see Table 10) along with a nearly constant quantum yield (Ehleringer, 1977) support the validity of this linear relation. The point at which net photosynthesis equals zero represents therefore the transpiration equivalent of the light compensation point averaged for the three plants. The implications of this equivalent value with respect to C_3 and C_4 plants will be discussed later. Another index has already been used in the literature; the transpiration/assimilation ratio. (Lommen 1971) relates the CO_2 assimilated to transpiration; see figure 16. At compensation this ratio achieves an infinite value and is very sensitive to variations in treatments. The sometimes large deviations that occurred in the results made the estimation of this ratio impractical. The transpiration to net photosynthesis ratio used in this paper has the advantage of being a constant since it describes the slope of the linear relationship in figure 16.

$$I_L = \frac{\Delta E}{\Delta P_n} \bigg|_{CO_2} = 165.21 (MH_2O/MCO_2) \quad \dots (40)$$

3.3 Effect of CO_2 Concentration on Transpiration and Assimilation

When the external CO_2 concentration was allowed to decrease, the transpiration in tobacco lost its linear relationship with humidity (Fig. 17). The results show that in a general sense, transpiration increased with a decreasing value of CO_2 concentration and reached an upper limit beyond which no further transpiration increase occurred. However, the overall transpiration, averaged over

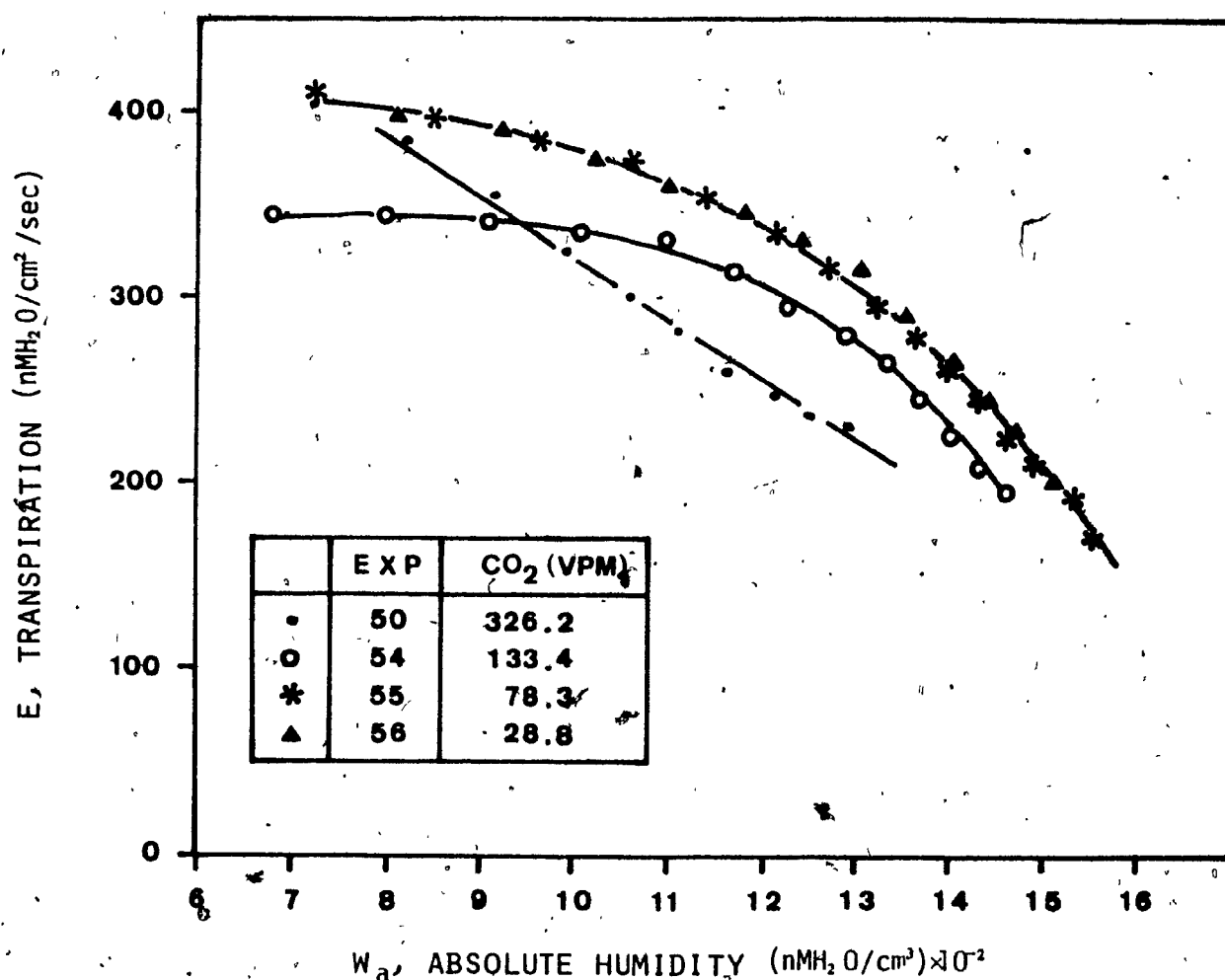


Fig. 17 Transpiration and Humidity for Tobacco at Decreasing CO₂ Treatments

Relation between Transpiration and Humidity on Tobacco at the various CO₂ concentrations shown. The visible absorbed radiation (R_v) was kept constant at 3.306×10^{-3} (j/cm²/sec) and air temperature (t_a) at 30.0°C ± 0.12 at 95%.

a range of absolute humidity common to all experiment shown in figure 17, was found to retain its linearity with net photosynthesis, (see Table 13 and Fig. 18). Furthermore, the dependence on absolute humidity variations did not influence this linearity by a great amount as shown in figure 18.

Table 13

Effect of CO_2 Concentration on Net Photosynthesis and Transpiration in Tobacco

Values for transpiration were averaged from values between 800 and 1300 $\text{nMH}_2\text{O}/\text{cm}^2$

Exp #	#of Cases	CO ₂ Concentration		Transpiration		Net Photosynthesis	
		vpm	nM/cm ³	nMH ₂ O/cm ² /sec		nMCO ₂ /cm ² /sec	
		Mean	STD Err.	Mean	STD Err.	Mean	STD Err.
50	9	326.2	13.11	291.48	18.13	1.01	0
54	7	133.4	5.36	320.27	9.24	0.35	0.03
55	6	78.3	2.15	360.22	12.86	-0.14	0.05
56	7	28.8	1.16	359.56	11.8	-0.66	0.04

Visible light intensity was kept at 3.306 mW/cm^2 , $T_a = 30^\circ\text{C}$

Two constants were derived from these results. The transpiration to net photosynthesis ratio for CO_2 (I_{CO_2}) was obtained in the same manner as before (see Table 12), but yielded a different value corresponding to the change in production of water per mole of CO_2 resulting from a decrease of the CO_2 concentration, while keeping light intensity constant, thus:

$$I_{CO_2} = \frac{\Delta E}{\Delta P_n} \bigg|_L \quad \dots(41)$$

is equal to the regression slope of net photosynthesis versus transpiration, and E_T is the transpiration rate at compensation, (Fig. 18)

Table 14

Trend for Transpiration and Net Assimilation:
CO₂ Variations

slope (I_{CO_2}) = -44.422	MH ₂ O/MCO ₂	$r = 0.8623$
constant (E_T) = 339.1	nMH ₂ O/cm ² /sec	$r^2 = 0.7436$

It can be seen that, in the case of tobacco, the plant was handicapped by 339.1 nMH₂O/cm²/sec transpiration at the CO₂ compensation point near 90 vpmCO₂ (Fig. 19). The plant was a very inefficient producer. A similar remark applies for transpiration at the light compensation points (see Fig. 16). C₃ plants are generally known to grow in cool and temperate climates where water stresses are not severe (Black, 1973). Ku et al (1977) showed similar trends in *Solanum* species. The low compensation point of C₄ plants along with their rate of net photosynthesis being independent of air CO₂ concentration (Bjorkman, 1966) would flatten the slope of figure 22 to zero. Transpiration is likely to be decreased also since full stomatal openings occurred at higher light intensities in C₄ than in C₃ plants (Downes 1970, Ku et al 1977, Das 1977). Thus the C₄

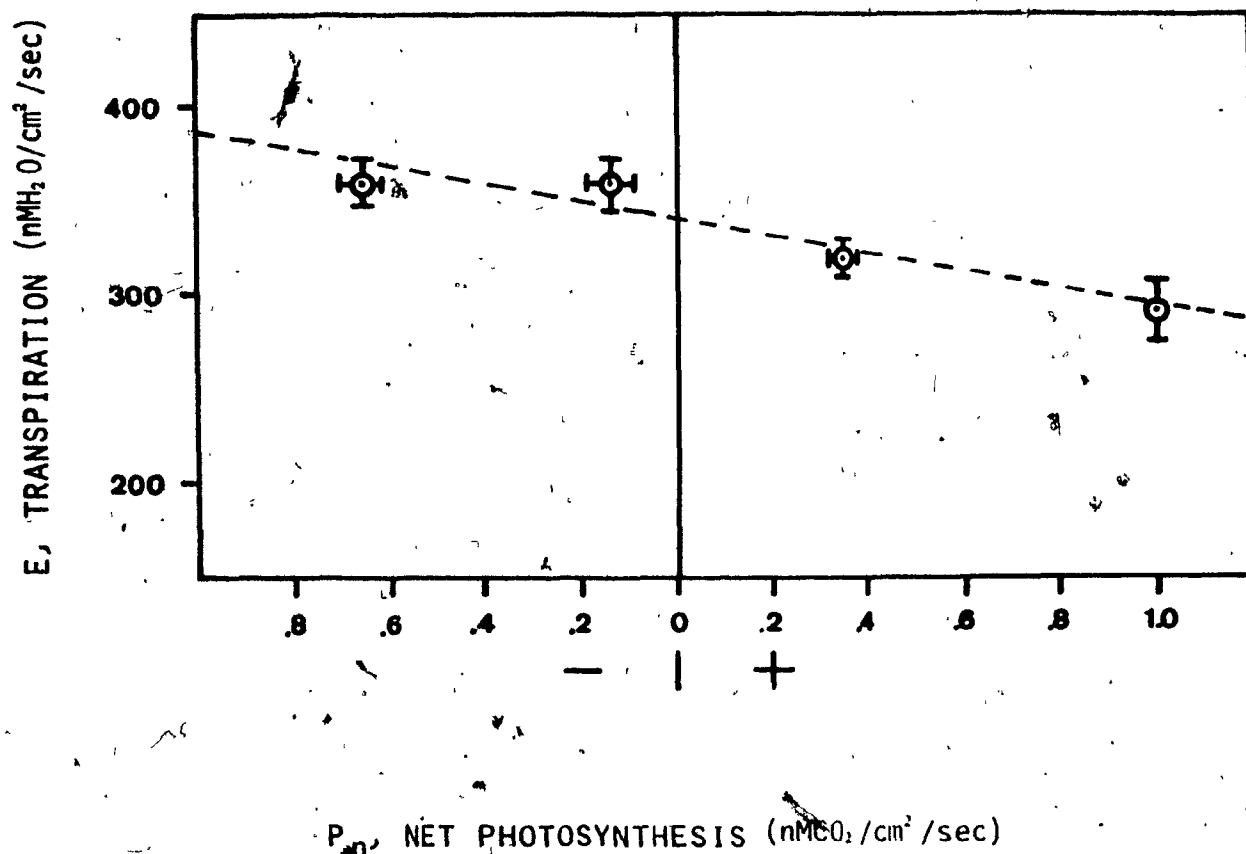


Fig. 18 Trend for Net Assimilation and Transpiration in Tobacco:
CO₂ Variations

All values of transpiration were averaged between 800 and 1300 nMH₂O/cm² absolute humidity, the plot shows the error of the mean at the 95% confidence level. Visible absorbed radiation (R_{va}) = 3.306×10^{-3} j/cm²/sec. Air temperature (t_a) = 30.0 °C ± 0.12 at 95%. Data was taken from Table 14.

plant produces more at a lesser water loss. The results for CO₂ concentrations versus net photosynthesis were regressed on a semilog scale to yield the curve of figure 19; the equation is:

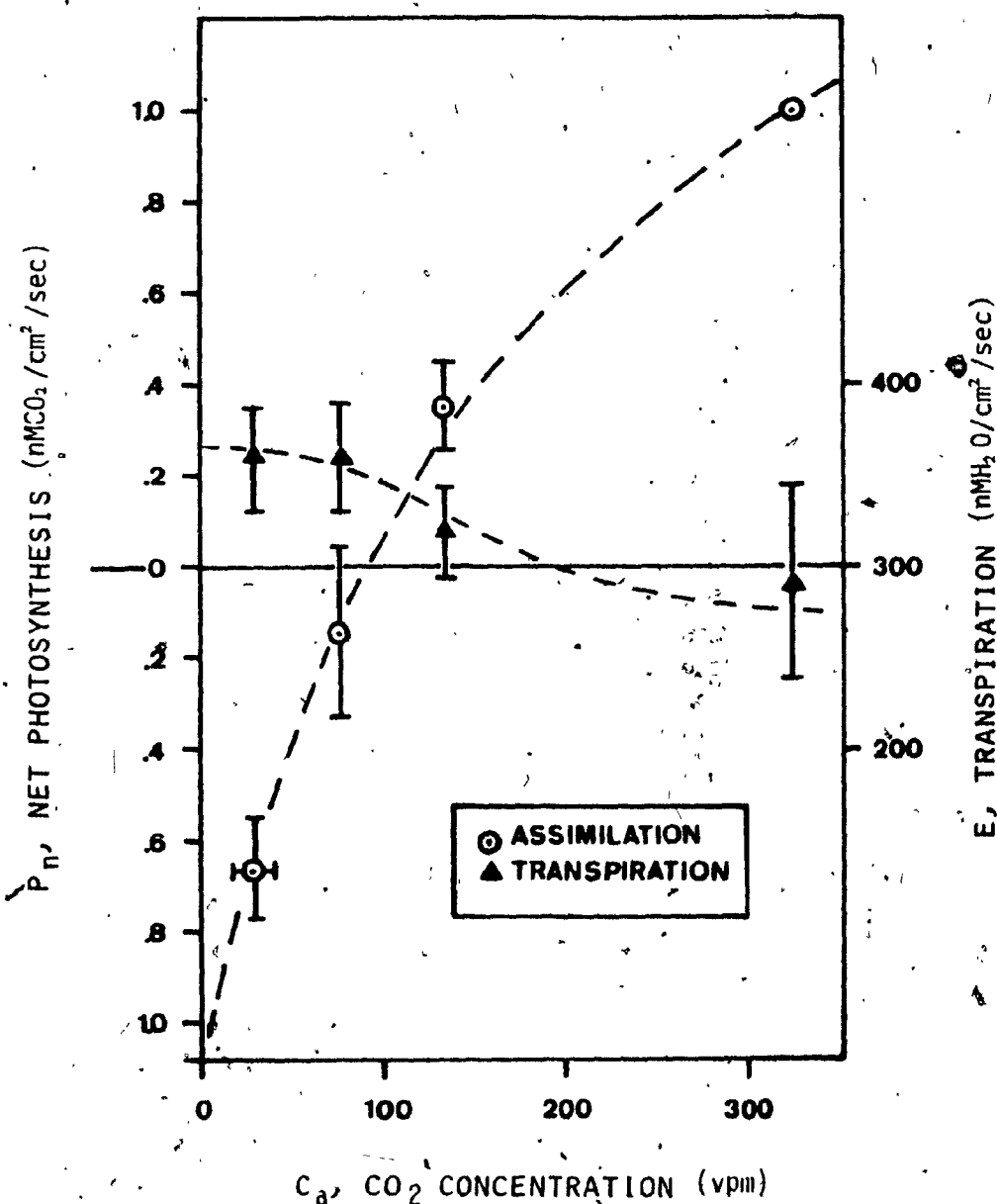


Fig. 19 Effect of CO_2 Concentration on Net Photosynthesis and Transpiration in Tobacco

All the values shown represent the mean values of readings taken between 800 and 1300 nMH_2O/cm^3 absolute humidity (W_a), the error of the mean is shown at the 95% level of confidence. Data taken from Table 14. Visible absorbed Radiation, $R_{va} = 3.306 \times 10^{-3} j/cm^2/sec$. Air temperature, $t_a = 30.0^\circ C \pm 0.12$ at 95%.

$$P_n = \ln(7.449 \times 10^3 C_a + 0.3314) \quad r = 0.9951 \quad \dots(42)$$

$$r^2 = 0.9903$$

with $P = 89.9$ vpm (CO_2 compensation point)

Some care should be exercised in extrapolating the above relation above 350 vpm CO_2 since the range of concentration did not allow for an upper limit in net photosynthesis. Such a limit cannot be adequately represented by a log function. The extensive model of Lommen *et al* (1971) involves a quadratic equation which takes limiting factors into account.

Thus the results for CO_2 variations have shown that the net photosynthesis cannot be simply related to changes in absolute humidity or changes in CO_2 concentration (Figs. 18 and 19). But, on the other hand, net photosynthesis showed a linear trend with transpiration when the source of variation was either light or CO_2 concentration, in which case the influence of humidity was small (Figs. 16 and 19), although the values of the slopes and intercepts for the above situations differed from one another (Table 12 and 14). It follows from this that the linearity between net photosynthesis and transpiration results in the sharing by these two processes of the same pathway such that the variations of one has an immediate and linear relation with the other, and that the pathway must have a predominant and limiting effect upon both these processes. The relationship between net photosynthesis and diffusion resistance is considered in the following section.

3.4 Diffusion Resistance and CO_2 Exchange

Lake (1967a) has proposed a model of CO_2 and transpiration flow

through the leaf allowing for mitochondrial respiration, photorespiration and photosynthesis to occur along with transpiration.

Figure 20 shows this model. It can be seen that the pathway common to both fluxes lies through the intercellular spaces, the stomatal and the boundary layer, the sum of which form the total diffusive resistance r_t assumed to be of the same value for water as for CO_2 . The mesophyll resistance r_m is formed by the triangle of resistances shown, and represents the total contributions of individual respiratory and assimilating components. Several indirect methods were used in the literature to evaluate this mesophyll resistance r_m . The rate in the

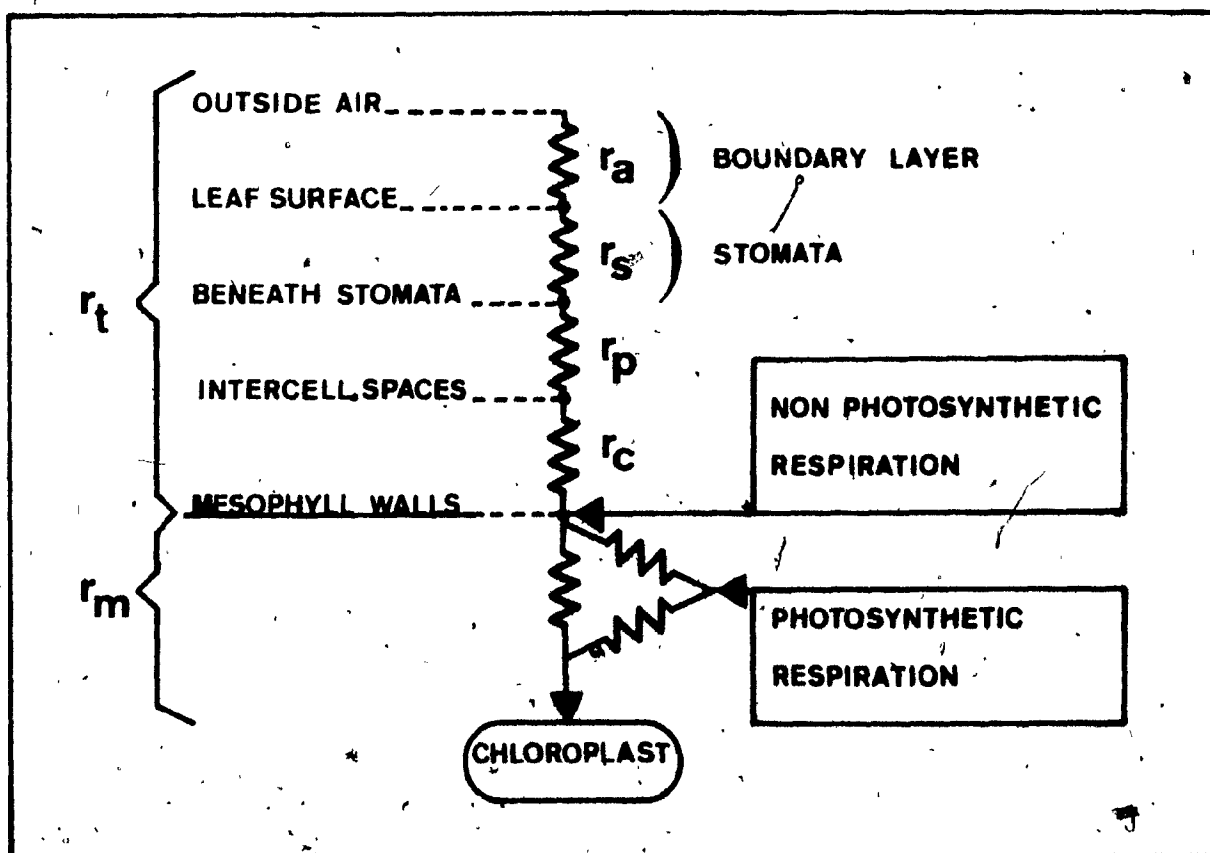


Fig. 20 - Resistance Network for Photosynthesis, Respiration and Transpiration from Lake (1967a)

linear portion of the net photosynthesis curve (Fig. 19) with respect to CO_2 concentration has been already used in the literature as a means of estimating the CO_2 diffusion across the mesophyll. Tregunna (1966) for instance defined it as the *carboxylation efficiency* while Lake (1967b) proposed to use it as the best estimate for the mesophyll resistance in an attempt to improve on Gaasstra's method. The whole point lay in estimating, by indirect means, the CO_2 concentration at the chloroplast, assumed to be zero by Gaasstra and at compensation by Lake and others. The resulting estimate of this resistance differed widely depending on the method used. O'Toole (1976) considered that these estimations were not reliable and proposed an enzyme assay method while the model of Lommen *et al* (1971) provided for an exact description of net photosynthesis as controlled by light and CO_2 concentration using diffusion and enzyme kinetics. The model accounted for respiration and photorespiration but, the parameters of the equation are difficult to obtain experimentally. An alternate way was to correlate the net photosynthesis with transpiration per unit vapour pressure difference between the leaf and the air, the latter being simply a measure of total water conductance through the leaf in cm sec^{-1} . the vapour density gradient was correlated with transpiration in *Malus* and the total change in the results at two different CO_2 concentrations was assigned to the total diffusion resistance (r_{t_w}). Full stomatal control of transpiration was likely to occur only at the higher absolute humidities ($\approx 1000 \text{ nM/cm}^3$) (West and Gaff, 1976). However, stomatal pore width variations from 2 to 7.5μ did not change the rate of CO_2 evolution

in tobacco (Poskuka et al, 1967).

When the external relative humidity was changed by 10%, leaves of tobacco showed resistance changes that were attributed to the internal pathway being stretched under the forces of the increased water vapour gradient (Slavik, 1975), but, the author assumed that a constant value of CO_2 exchanges warranted a constant stomatal opening to water diffusion, and thus disagreed with Paskuka et al. However the objection is a minor one since stomatal control seems to play a small role in CO_2 exchanges and, at the lower humidities, in transpiration. Thus the net photosynthesis and transpiration seem to be linked mainly through the internal diffusion pathways, with stomatal control serving as a limiting adjustment.

Accordingly, the relation between net photosynthesis and transpiration could be described by the total diffusive resistance such that if the total diffusive resistance to CO_2 is proportional to that for water, then:

$$P_n = K_n \frac{1}{r_{tw}} + P_o \quad \dots (43)$$

where

r_{tw} = total diffusive resistance to water diffusion
(the sum of boundary, stomatal, and internal
(r_a , r_s , r_i) resistances) (sec/cm)

P_n = net photosynthesis ($\text{nMCO}_2/\text{cm}^2/\text{sec}$)

K_n = rate of net photosynthesis to conductance ($\text{nMCO}_2/\text{cm}^2$)

P_o = net photosynthesis when r_{tw} is great.

Hesketh (1968) found that the expression is linear for both C_s and C_a

plants. The linearity of equation (43) was also found to hold well under conditions of water stresses in sugar beet crops when the slope of the relation did not significantly change between the leaves of young and mature plants, although wilted mature leaves afforded smaller photosynthetic rates and lowered the value of the slope, as a result of the excessive water stress, (Lawlor and Milford, 1975).

Since the value of K_n in the above equation embodies both a rate of change along with the ratio of water to CO_2 diffusion resistance, it would be expected to vary with the species and ecotype encountered as its value depends upon the leaf's anatomy and its specific range of photosynthesis and transpiration in a given environment. Based on this point of view, the constant K_n could be viewed as an indication of plant environment relationships such that for any green type of communities the individual differences between plant members would even out if the community is considered as a whole entity and, in that case, the value of K_n would depend mostly upon the environmental parameters alone.

The practical advantage of describing net photosynthesis as a function of environmental parameters alone is dependent on the ability to also evaluate the total diffusive resistance to water vapour r_{tw} as a function of environmental parameters. The total energy budget of Rashke (1960) and Gates (1965b) already presented in this report has required an experimental procedure that afforded a solution for which it was necessary to measure the temperature of the leaf and control the amount of radiation that it absorbed. These conditions render a field

application most impractical especially when the performance of a population is considered as a whole entity. A solution of the energy budget using environmental parameters alone is proposed in the following section.

3.5 Solving the Energy Budget

The energy balance of a plant results in the release of absorbed radiation energy through convection, transpiration and reradiation. The control of leaf temperature and leaf total diffusion resistance (r_{tw}) results in equilibrating the above parameters. The total diffusive resistance (r_{tw}) is separated into a boundary layer (r_a) and a leaf resistance (r_l) such that $r_{tw} = r_a + r_l$. The boundary layer resistance (r_a) is dependent upon both wind speed and the shape of the leaf as in Gates (1965b), Vogel (1970). The leaf resistance (r_l) includes the total diffusion pathway for transpiration through the leaf and is therefore dependent upon both leaf anatomy and stomatal opening. This resistance also includes the cuticular resistance (r_c) which is in parallel with r_s . Figure 21 shows this arrangement for water diffusion and convection transfers.

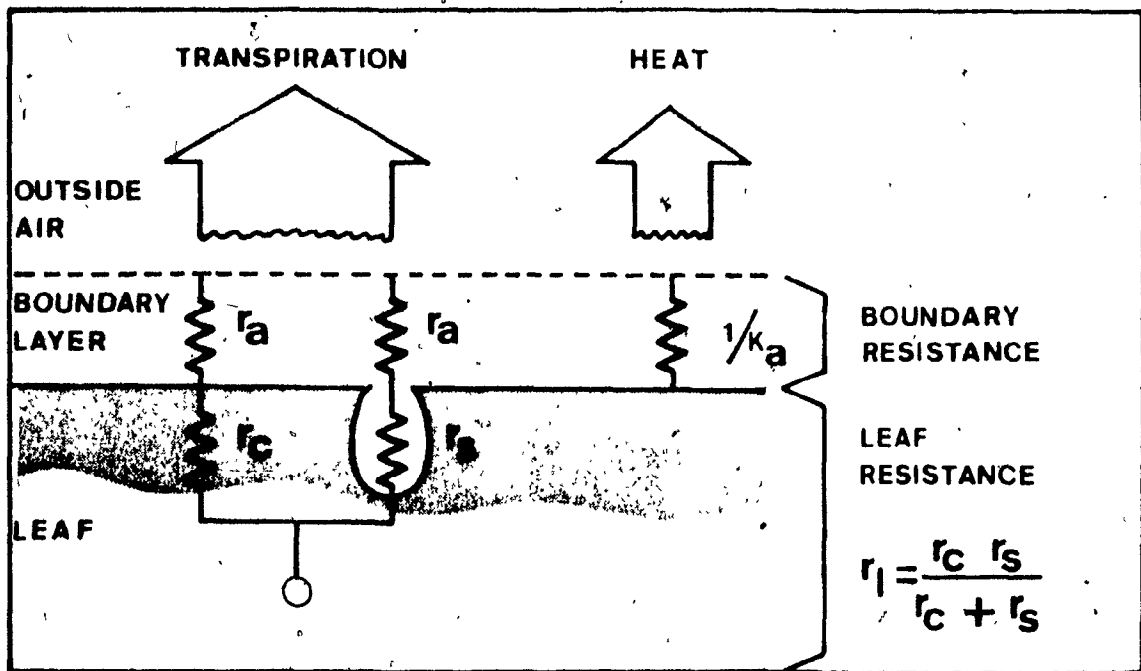


Fig. 21 Resistance Network for Diffusion and Convection

The convective resistance ($1/k_a$) is the equivalent boundary layer resistance for heat flux and is proportional to r_a as in Rashke (1960).

The total energy budget equation as of Gates (1968) is this:

$$Q_{ABS} = \epsilon \sigma (T_l)^4 + K_a (T_l - T_a) + \frac{L}{r_l + r_a} (W_{sl} - W_a) \quad \dots (44)$$

if we define $\Theta = T_l - T_a$ and note that the radiation term can be approximated by a linear function (Gates 1965b)

$$\epsilon \sigma (T_l)^4 \approx \epsilon \sigma (T_a)^4 + \epsilon \sigma 4 T_a^3 \Theta \quad \dots (45)$$

for given air temperature (T_a) equation (44) then becomes:

$$Q_{ABS} = \epsilon \sigma T_a^4 + \epsilon \sigma 4 T_a^3 \Theta + K_a \Theta + \frac{L}{r_l + r_a} (W_{sl} - W_a) \quad \dots (46)$$

and, putting K_r as a transfer coefficient for reradiation equal to

$4\epsilon\sigma T_a^3$ we can write:

$$Q_{ABS} = \epsilon\sigma T_a^4 + K_r\theta + K_a\theta + \frac{L}{(r_l + r_a)} (W_{sl} - W_a) \quad \dots(47)$$

The term Q_{ABS} includes both thermal radiation and visible radiation:

$Q_{ABS} = R_T + R_V$. If we define the net absorbed radiation (Q_N) as the sum of all the radiation terms independent of the leaf temperature then

$$Q_N = R_T + R_V - \epsilon\sigma T_a^4 \quad \text{and}$$

$$Q_N = K_r\theta + K_a\theta + LE \quad \dots(48)$$

where

$$E = \frac{1}{(r_l + r_a)} (W_{sl} - W_a)$$

the term $K_r\theta$ represents net leaf reradiation and is equal to amount of thermal reradiation produced by the leaf between leaf and air temperature. The remaining reradiation lost to the environment between air temperature (T_a) and absolute zero is included in the absorbed radiation term (Q_N) as defined above. This manipulation of the original equation is made with the purpose of presenting the energy budget with respect to a black body transmitter at the air temperature, which has a radiation value of $\epsilon\sigma T_a^4$, while the original equation (44) was referenced to a black body at absolute zero temperature, which has a radiation value of zero. Two exact conditions can be derived from equation (48). If the net absorbed radiation (Q_N) is released through transpiration alone then: (Case 1)

$$Q_N = LE; \quad LE = K_r\theta + K_a\theta + LE \rightarrow K_r\theta + K_a\theta = 0$$

CASE 1

it then follows that $\Theta = 0$, and leaf temperature equals environment temperature. If on the other hand the net absorbed radiation (Q_N) is released solely through net reradiation ($K_r\Theta$), the transpiration energy (LE) will match convection ($K_a\Theta$): (Case 2)

$$Q_N = K_r \Theta \quad K_r \Theta = K_r \Theta + K_a \Theta + LE$$

then $-K_a \Theta = LE$

CASE 2

Case 2 describes the properties of a psychrometer. In such a case, the temperature of the leaf acting as a psychrometer will achieve the thermodynamic wet bulb which can be closely, approximated by the wet bulb of the surrounding air (ASHRAE, 1972) hence, $t_l = t_a^*$. If we define Θ^* as the difference between the environment wet bulb (t_a^*) and dry bulb (t_a) we have, for case 2:

$$\text{CASE 2} \quad -K_a \Theta^* = LE \quad \text{when} \quad Q_N = K_r \Theta^*$$

which corresponds to the wet paper analogue of Gaastra (1963). In order to solve the model represented by equation (48), there remains to ascertain the relationship existing between total net radiation and leaf temperature so that a solution be found by extrapolation of cases 1 and 2. Hari et al (1975) have found that the time integration of daily differences between the wet and dry bulb and daily radiation readings correlated well with total daily transpiration of birch seedlings. A similar relationship was found in this report. The regression in Table 15 for tobacco, tomato and bean shows a high

correlation between sensible heat (S), radiation (R_v) and wet bulb difference (θ^*). Thus:

$$S = aR_v + b\theta^* + c \quad \dots(49)$$

where a , b , c are the regression coefficients in Table 15. Since S is proportional to θ ,

$$f\theta = aR_v + b\theta^* + c \quad \dots(50)$$

Assuming that at a specific humidity and temperature of the environment (and hence at a specific θ^*) the convection coefficient is constant:

$$\theta = \frac{a}{f} R_v + \frac{b}{f} \theta^* + \frac{c}{f} \quad \dots(51)$$

Table 15.

Regression of Sensible Heat with Visible Absorbed Radiation and Wet Bulb Depression

Tomato		
Coefficients	STD Error	Regression
a -2.303	0.121	r = 0.9175 r ² = 0.8418
b 0.650	0.077	
c 0.698×10 ⁻³	0.350×10 ⁻³	

Tobacco		
Coefficients	STD Error	Regression
a -2.898	0.128	r = 0.9625 r ² = 0.9263
b 0.769	0.081	
c 3.742×10 ⁻³	0.561×10 ⁻³	

D. Bean		
Coefficients	STD Error	Regression
a 0.1758	0.0587	$r = 0.9611$ $r^2 = 0.9237$
b 1.672	0.0781	
c -2.227×10^{-3}	0.1869×10^{-3}	

where a = regression factor for Visible absorbed radiation (Rv_a)
b = regression factor for wet bulb depression (Θ)
c = regression constant

Cases 1 require that:

$$0 = \frac{a}{f} LE + \frac{b}{f} \Theta^* + \frac{c}{f} \quad \dots (52)$$

Case 2:

$$\Theta^* = \frac{a}{f} K_r \Theta^* + \frac{b}{f} \Theta^* + \frac{c}{f} \quad \dots (53)$$

Solving for $\frac{a}{f}$ yields

$$\frac{a}{f} = \frac{\Theta^*}{K_r \Theta^* - LE} \quad \dots (54)$$

Since Θ^* is constant, $\frac{b}{f} \Theta^* + \frac{c}{f}$ is also constant and yields:

$$\frac{b}{f} \Theta^* + \frac{c}{f} = - \frac{\Theta^* LE}{K_r \Theta^* - LE} \quad \dots (55)$$

Replacing in equation (51) yields:

$$\Theta = \left[\frac{\Theta^*}{K_r \Theta^* - LE} \right] Rv_a - \frac{\Theta^* LE}{K_r \Theta^* - LE} \quad \dots (56)$$

Which reduces to:

$$\theta = \theta^* \left[\frac{Rv - LE}{K_r \theta^* - LE} \right] \quad \text{and } t_l = t_a + \theta \quad (^\circ\text{C}) \quad \dots(57)$$

The transfer coefficients can now be calculated

Convection coefficient:

$$K_a = \frac{S}{\theta^*} \left[\frac{K_r \theta^* - LE}{Rv - LE} \right] \quad (\text{j cm}^{-2} \text{ sec}^{-1} \text{ } ^\circ\text{C}^{-1}) \quad \dots(58)$$

The total diffusive resistance to water vapour can be found by:

$$r_{wt} = r_a + r_l = (W_{sl} - W_a)/E \quad (\text{sec/cm}) \quad \dots(59)$$

where W_{sl} is the saturation water vapour concentration and is a function of t_l . For leaf temperatures within the range $20^\circ\text{C} \leq t_l \leq 35^\circ\text{C}$ the values of W_{sl} can be closely approximated by the relation:

$$W_{sl} = e^{(0.06201 t_l - 5.4596)} \quad (\text{lbw/lba}) \quad \dots(60)$$

where

$$t_l = \text{leaf temperature } (^\circ\text{C})$$

The conversion from (lbw/lba) into (nm/cm^3) was described earlier.

Then, the leaf resistance is:

$$r_l = r_{tw} - r_a \quad (\text{sec/cm}) \quad \dots(61)$$

$$\text{and } r_a = \frac{1}{K_a} \frac{G}{v} \quad (\text{sec/cm}) \quad \dots(62)$$

the term G representing the specific heat of air ($\text{j grain}^{-1} \text{ } ^\circ\text{C}^{-1}$)

and (v) the volume density of dry air (cm^3/grain) are used to convert the convection coefficient of the boundary layer (k_a) into an equivalent resistance for water vapour diffusion (r_a) as in Rashke (1960) and ASHRAE (1972).

The calculations of equations (57) to (62) were programmed and executed according to the main flowchart presented in the material and method section (Fig. 11). The following graphs and tables were derived from these calculations. Figure 22 shows the regression of the calculated parameters as a function of transpiration and humidity in tobacco.

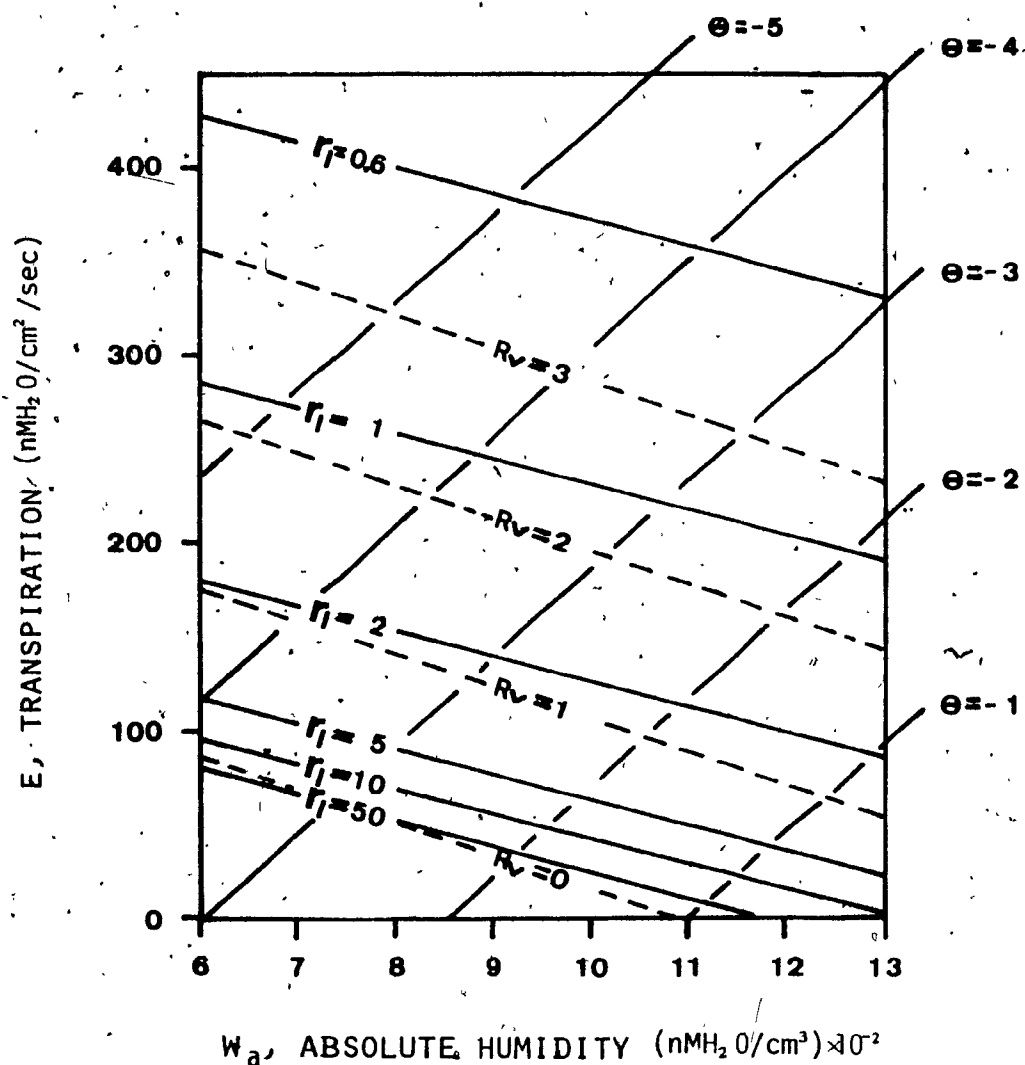


Fig. 22 Parameter Grid for the Tobacco Experiments

The values were obtained by the regression of the calculated parameters. Θ , leaf temperature minus air temperature. W_a absolute humidity r_i = stomatal resistance, R_v visible absorbed radiation. E , transpiration, the regression analysis of this grid are shown in Table 12. The graph shows clearly the increase in stomatal resistance caused by the simultaneous reduction in light intensity (as R_v) and Absolute humidity (W_a). Air temperature, $t_a = 29.2 \pm 0.14^\circ\text{C}$.

3.6 Values of Diffusive Resistance

The relation between leaf resistance (r_l), stomatal resistance (r_s) and cuticular resistance (r_c) has already been presented in Figure 21. The values can be expressed as

$$\frac{1}{r_l} = \frac{1}{r_s} + \frac{1}{r_c} \quad \dots(63)$$

where r_s represents the total stomatal resistance pathway from the mesophyll wall to the guard cell of the stomata. In most cases the cuticular resistance is very high compared to the stomatal resistance. The variations in leaf resistance will therefore be due in the greater part to the stomatal resistance variation. The value of r_l will equal the cuticular resistance only when the stomata are closed in which case:

$$\frac{1}{r_l} \approx \frac{1}{r_c} \quad \dots(64)$$

the measurement of r_l on leaves when their surface was allowed to dry was used as an estimate of r_c since the stomata were then presumably closed. Slayter (1967), citing the work of Kuiper gives an estimate of 20 sec cm^{-1} for tomato and bean. Estimates from the tobacco and tomato experiment in this report give an average resistance at zero light intensity of 16.7 and 8.4 sec cm^{-1} respectively. The estimate is however imprecise since it represents the limiting value of the above equation. The variation of leaf resistance with light intensity of both tobacco and tomato agree well with the literature. The boundary layer resistance (r_a) was nearly constant as in (Kramer 1969) while the leaf resistance varied between 0.5 to a high value. The

corresponding stomatal resistance was cited as being $<4 \text{ sec cm}^{-1}$ by Slayter (1967). These relationships are shown in figures 23 and 24.

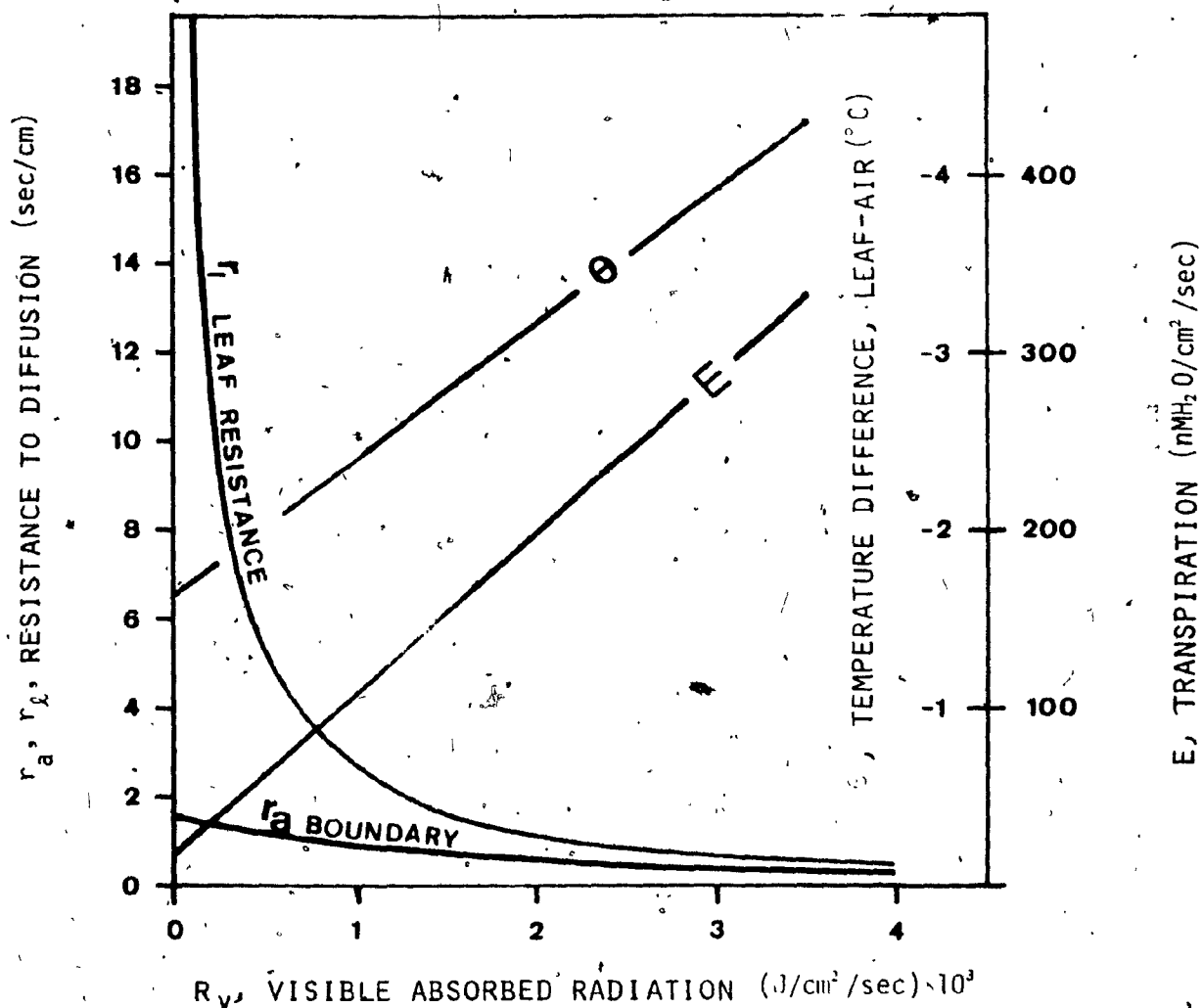


Fig. 23 Effect of Visible Absorbed Radiation on Plant Parameters at Constant Humidity and Temperature: TOBACCO

The calculations were made at the mean value of the experimental humidity range according to the regression analysis shown in Table 16. Air temperature; $t_a = 29.2 \pm 0.14^\circ\text{C}$; Absolute humidity, $W_a = 980 (\text{nMH}_2\text{O}/\text{cm}^3)$; Relative humidity, $\phi = 60\%$.

Table 16

Regression of Plant Parameters with Absolute Humidity (W_a) and Visible Absorbed Radiation (Rv_a): Tobacco

Dependent Independent	E	θ	$1/r_l$	$1/r_a$
W_a	-0.175	5.50×10^{-3}	-1.83×10^{-4}	1.75×10^{-4}
Rv	89.797	-0.766	0.426	0.583
constant	190.1	-7.0	0.2	0.5
Multiple Regression	0.98011	0.97963	0.97811	0.98016
r^2	0.96061	0.95968	0.95669	0.96071
STD deviation	22.7	0.3	0.1	0.2
units	(nM/cm ² /sec)	(°C)	(cm/sec)	(cm/sec)

E, Transpiration; θ , temperature difference between leaf and air;
 $1/r_l$, leaf diffusion conductance; $1/r_a$, boundary diffusion conductance

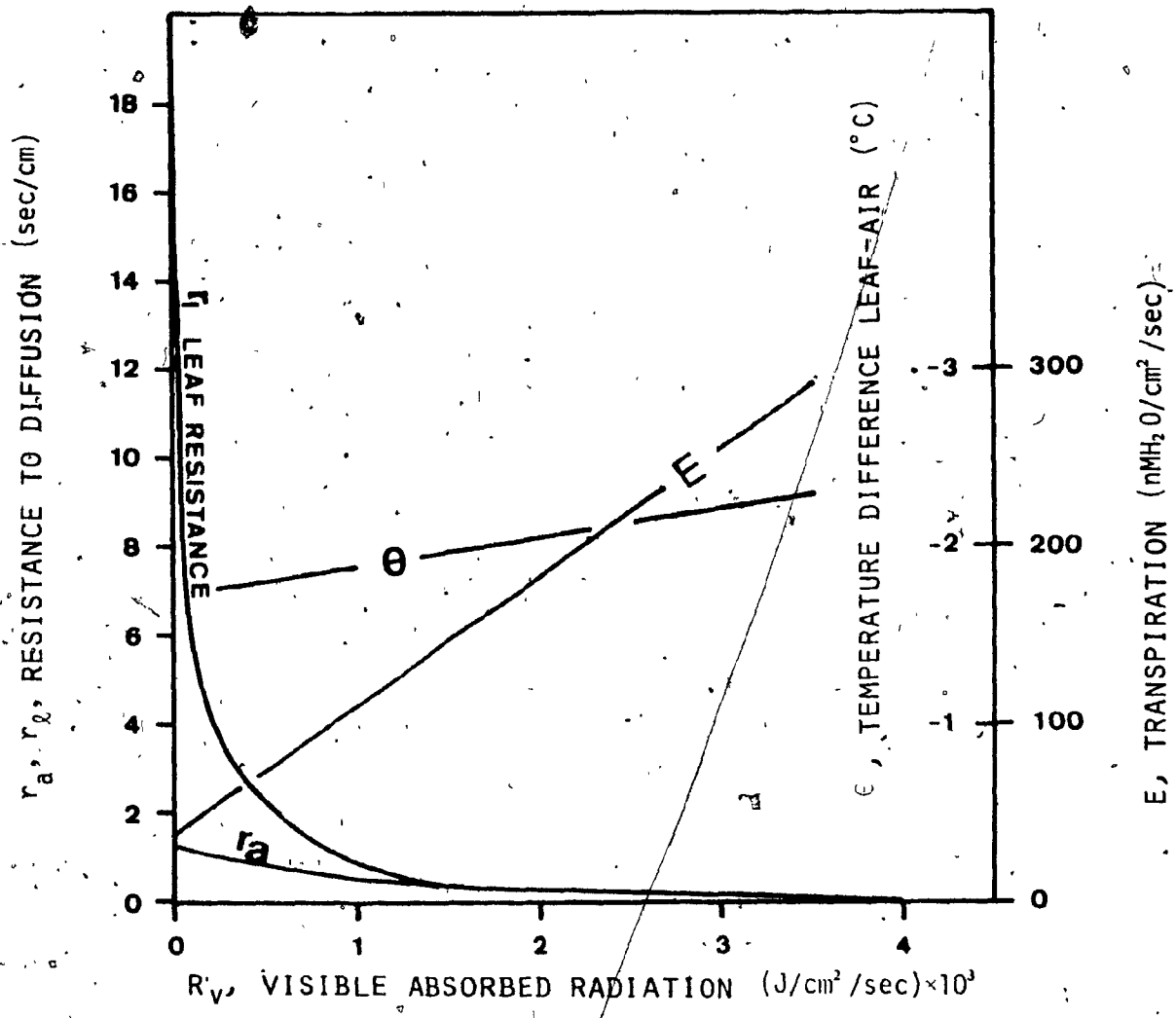


Fig. 24 Effect of Visible Absorbed Radiation on Plant Parameters at Constant Humidity and Temperature: TOMATO

The calculations were made at the mean value of the experimental humidity range, according to the gression analysis shown in Table 17. Air temperature, $t_a = 29.0 \pm 0.1^{\circ}C$; Absolute humidity, $W_a = 1200$ (nMH₂O/cm³); Relative humidity, $\phi = 76\%$.

Table 17.

Regression of Plant Parameters with Absolute Humidity (W_a) and Visible Absorbed Radiation (RV_a): Tomato

	E	θ	$1/r_l$	$1/r_a$
W	-0.137	4.227×10^{-3}	5.812×10^{-4}	1.560×10^{-3}
RV_a	72.624	-0.160	0.961	1.245
constant	203.9	-6.8	-0.6	-1.1
Multiple R.	0.96629	0.95053	0.95443	0.93164
r^2	0.93372	0.90351	0.91094	0.86795
STD Dev.	20.3	0.3	0.3	0.6
units	($\text{nM}/\text{cm}^2/\text{sec}$)	($^{\circ}\text{C}$)	(cm/sec)	(sm/sec)

E, transpiration; θ , temperature difference between leaf and air; $1/r_l$, leaf diffusion conductance; $1/r_a$, boundary diffusion conductance

The case of the Bean experiment showed a different response where the stomata apparently remained open for all values of light intensities as shown in figure 25. This may be due to an indirect effect of the near saturation of air in keeping a high level of turgor in the guard cells of the stomata. This condition could prevail over the normally

observed closure when light intensity is decreased. Furthermore, the calculated value of leaf resistance represents the pathway of diffusion from the vaporisation interface to the surface of the leaf and in this case, the vaporisation interface is assumed to be at the mesophyll walls. For a high outside humidity, however, the interface may very well locate nearer the stomatal pore so that the effective pathway is reduced in length and consequently, in resistance. The value of the leaf resistance is thus dependent upon its definition (Slatyer 1967).

The calculation method used in this report generated a value for r_l between the leaf surface and the saturation interface, irrespective of its location inside the leaf. The low variability index already presented in section 3.1 (Table 5) supports a constant value for diffusion resistance, while the linear relationship between net photosynthesis and light intensity for that plant (Fig. 15) supports a low value, thus agreeing with the curve shown in figure 25.

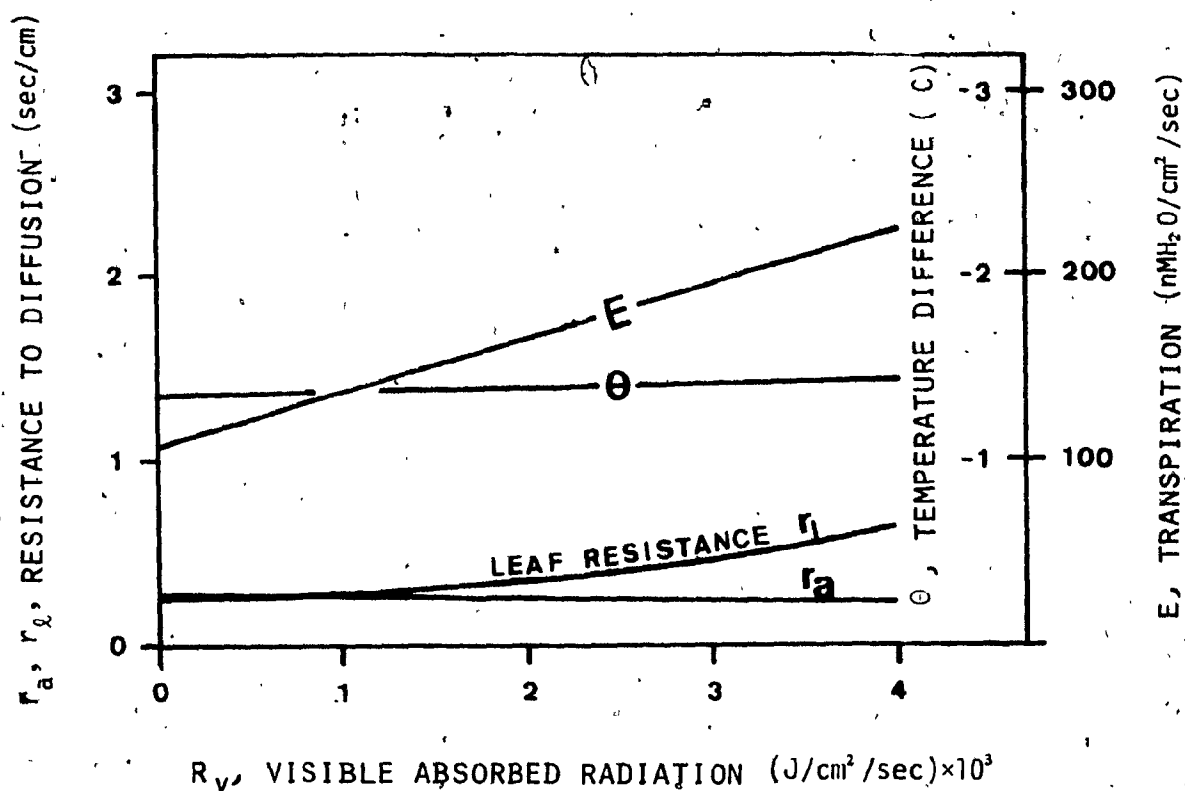


Fig. 25 Effect of Visible Absorbed Radiation on Plant Parameters at Constant Temperature and Humidity: Bean

The calculations were made at the mean value of the experimental humidity range, according to the regression analysis shown in Table 18. Air temperature, $t_a = 27.1 \pm 0.34^\circ\text{C}$; Absolute humidity, $W_a = 1240$ (nMh₂O/cm³); Relative humidity, $\phi = 86\%$.

Table 18

Regression of Plant Parameters with Absolute Humidity (W_a) and Visible Absorbed Radiation (R_v): Bean

	E	θ	$1/r_l$	$1/r_a$
W	-0.239	4.38×10^{-3}	2.345×10^{-3}	4.289×10^{-3}
R_v	29.447	-2.496×10^{-2}	-0.610	0.243
constant	403.6	-6.8	1.1	-2.0
Multiple R.	0.99226	0.98574	0.84403	0.93538
r^2	0.98458	0.97168	0.71239	0.87494
STD Dev.	5.4	0.1	0.5	0.3
units	(nM/cm ² /sec)	(°C)	(cm/sec)	(cm/sec)

E , transpiration; θ , temperature difference between leaf and air; $1/r_l$, leaf diffusion conductance; $1/r_a$, boundary diffusion conductance

3.7 Effects of Chemicals on Resistance to Diffusion

Some preliminary experiments were run in order to evaluate the ability of the proposed calculation method to measure changes in stomatal resistance due to external contaminations. The contaminants were selected and administered to the plant at doses producing unmistakable

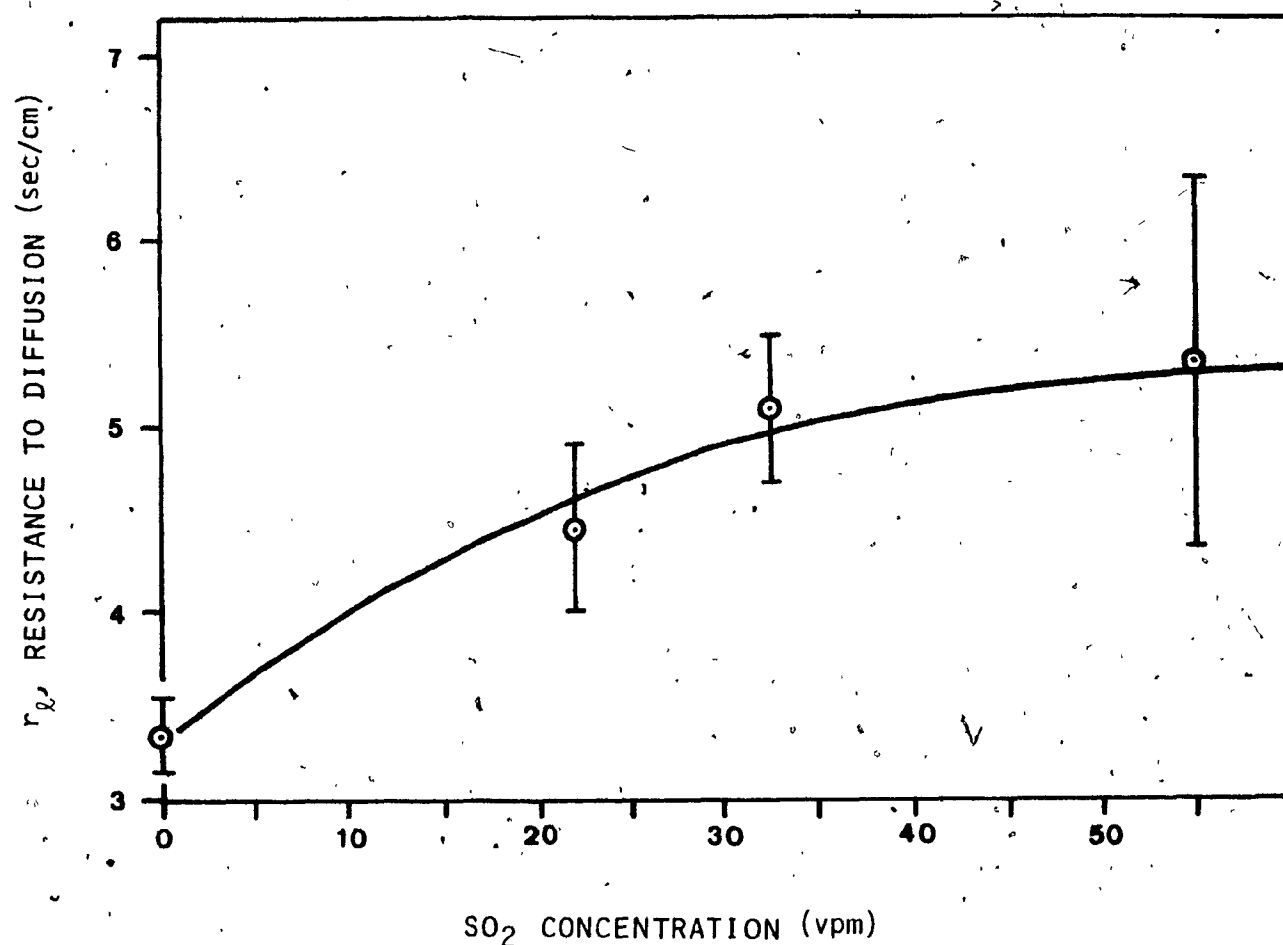


Fig. 26 Leaf Resistance and SO_2 Doses in Bean, for an average Humidity of $42\% \pm 17\%$ and an Exposure of 11 minutes ± 1 at 95% confidence

Exp	r_l	STD Error	95% C.I.	Exposure (minute)	SO_2 Treatment (ppm)
84	3.146	.065	.143	11	0
85	3.528	.112	.253	9	0
86	4.468	.213	.469	11	22
87	5.059	.175	.385	11	33
88	5.342	.475	1.036	12	55

visual long term effects on the leaf anatomy. The plant reaction to SO_2 gas produced the usual intervenal chlorosis 3 days after the experimental treatment on a bean plant. 3-Amino 1-2-4 triazole, diluted at 10^{-3} Molar in the nutrient medium produced the characteristic bleaching in the new leaves of a growing tobacco plant.

In the case of SO_2 the stomatal resistance increased immediately upon contact with the gas. Further addition of doses did not produce a linear increase as shown in figure 26. Majernik and Mansfield (1972) found that the stomata either opens or closes in presence of SO_2 depending on whether the outside air is humid ($>80\%$) or not ($<80\%$). The results (in Fig. 26) support their findings for low humidities. Mudd and Kozlowski (1975) have reviewed the effects of SO_2 on plants.

The effect of 3-amino 1-2-4 triazole did produce a cyclic variation in the calculated leaf resistance (Fig. 27). Since the effect of this herbicide was found to impede the formation of chlorophyll in newly forming leaves only (Hall, 1953), the performance of the older already grown leaves should remain unaffected by the treatment. However, the lower curve of figure 27 shows the variation in total effective leaf area for that plant. This measurement, based on green leaves, did not read a white leaf such as the one resulting from the herbicide treatment. When the new white leaves grew and expanded, the total photosynthetically active area of the plant was reduced as the new white leaves overshadowed the older green ones. This resulted in a drop of total effective leaf area as measured by

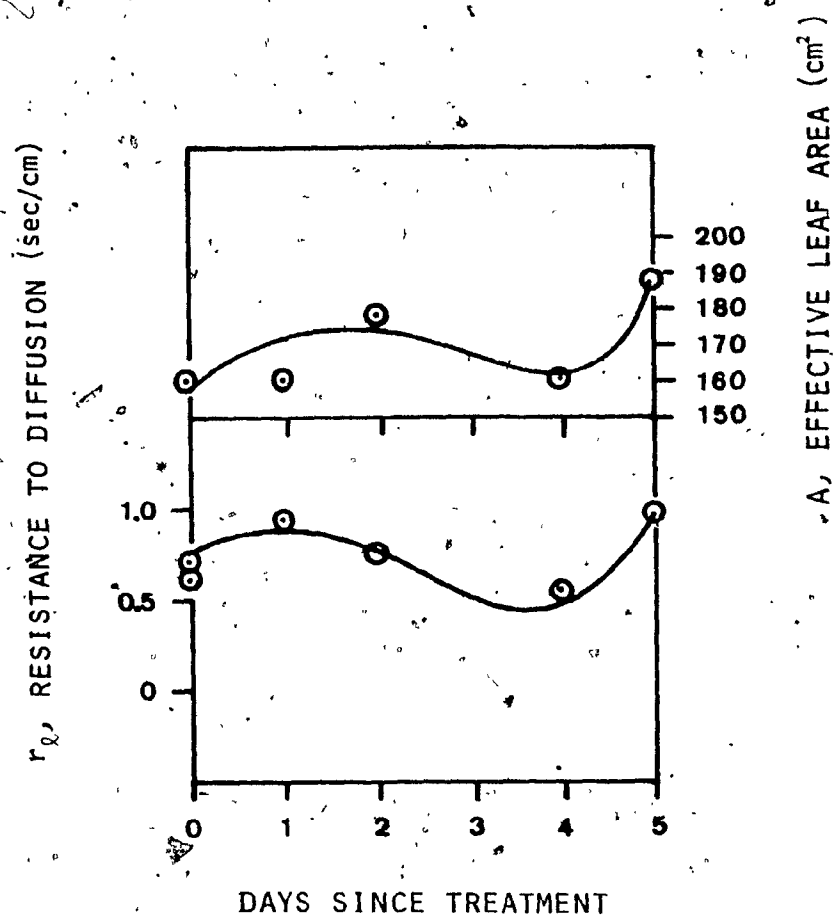


Fig. 27 Leaf Resistance and 10^{-3} AMITROLE in Tobacco

Exp	Average Resistance	Error	95% C.I.	Days since Treatment
57	0.596	.012	.026	0
58	0.707	.010	.021	0
59	0.936	.020	.051	1
60	0.754	.013	.027	2
61	0.545	.011	.023	4
62	0.978	.016	.034	5

the optical device described earlier (section 2.4.3) the observed cyclic variation needs to be cautiously interpreted because in that case, the diffusive resistances were calculated for the plant taken as a whole entity and with respect to the effective green (photosynthesising) leaf area exposed. The calculated resistances are thus an indication of the canopy being altered according to physiological reactions to the herbicide and not of stomatal movements in single leaves.

3.8 Diffusion Resistance, Net Photosynthesis and Photosynthetic Yield

The relationship between net photosynthesis and total diffusive resistance presented in section 3.4 was verified by plotting net photosynthesis with total diffusive conductance (the inverse of total diffusive resistance). A linear relationship was observed in all cases at the 95% level as shown in figure 28 and Table 16. However the light intensity used were not saturating for the species used in these experiments such that the diffusion process was the sole limiter of photosynthesis.

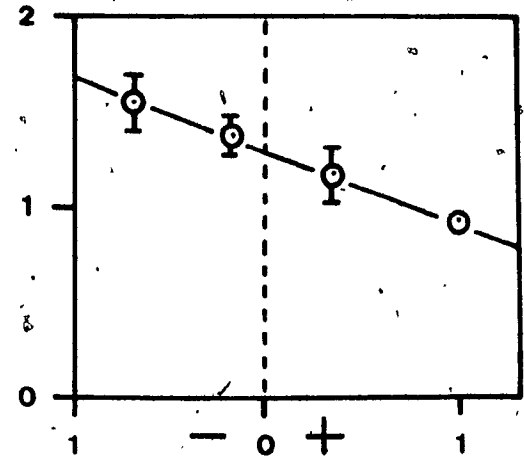
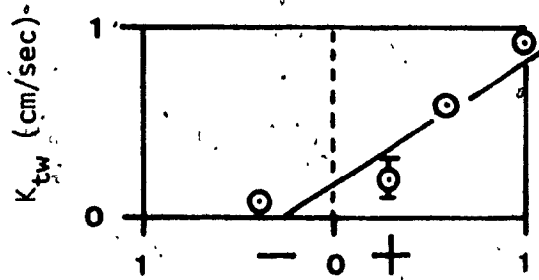
In order to be able to extrapolate the above relationship into the field, the effect of light saturation on photosynthesis must be taken into account. Strong evidence exists that the rate of photosynthesis is limited by enzymatic activity in the CO_2 fixing cycle of *P. vulgaris* (Neales et al 1971), a C_3 plant. However Bull (1971) attributed the net photosynthesis mostly to changes in diffusion resistance for both C_3 and C_4 plants. The linear relation of net

photosynthesis to diffusive resistance was obtained by Gifford (1971) in *Zea mays*, the author then estimated the value of photosynthesis at light saturation by compensating the curves to eliminate the effect of stomatal resistance. The resulting light saturation values for photosynthesis were at the same level as those of C_3 plants. It was concluded that the high light saturation of C_4 plants was mainly due to the lower stomatal resistance and not to the different carbon fixing mechanism. Thus the relation of net photosynthesis to the diffusion resistance should remain linear as long as diffusion resistance is the limiting factor. Figure 18 shows this relation when the source of net photosynthesis variation is a decrease in CO_2 concentration while Downes (1971) has also shown this linearity with stomatal changes induced by a decreasing temperature of the roots.

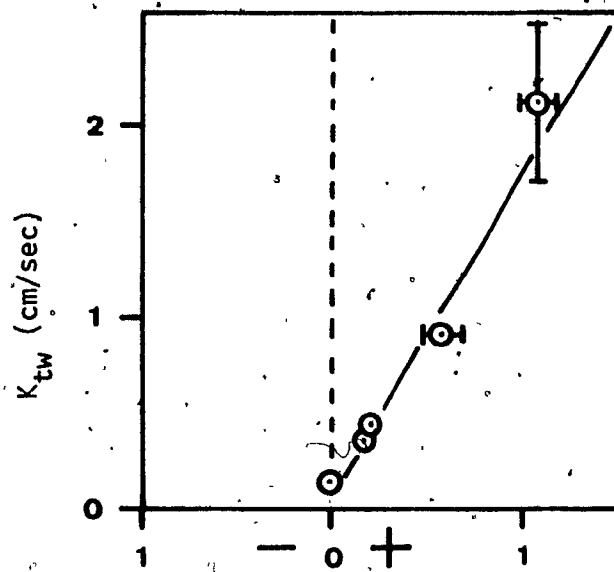
Measurements made with single leaves differ from those taken from whole fields or crops. Gaastra (1963) has shown that although photosynthesis may be limited by saturating light intensities in single leaves, the saturating light intensity for closed canopies can be as high as 4 times that of single leaves because the mutual shadowing of leaves prevents them from achieving saturation at the same time. In this case, the canopy will always be limited by light and the variation of photosynthesis will depend mostly upon the canopy diffusive resistance and equation (43) (section 3.4) thus, for a constant and limiting amount of light.

$$P_n = K_n \frac{1}{r_{tw}} + P_0 \quad \dots (65)$$

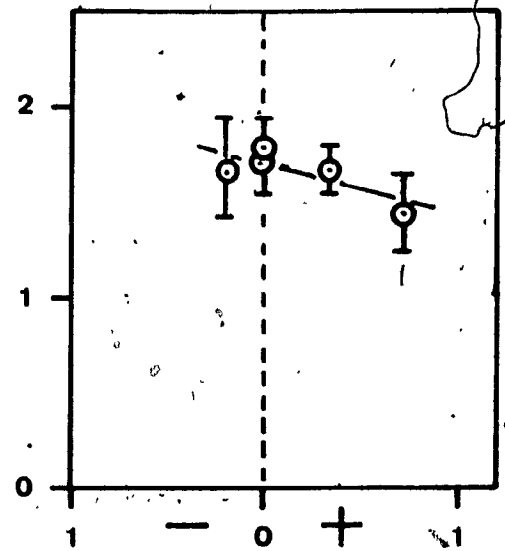
TOBACCO, LIGHT VARIATIONS



TOMATO, LIGHT VARIATIONS



BEAN, LIGHT VARIATIONS



P_n , (nMCO₂/cm²/sec)

P_n , (nMCO₂/cm²/sec)

Fig. 28 Relation between Net Photosynthesis (P_n) and Total Diffusive Conductance (K_{tw}), for the Plants and the Conditions shown. The Graphs were obtained from the Data of Table 16.

Table 19

Diffusion Resistance and Photosynthesis

TOBACCO. LIGHT VARIATION

Exp	K_{tw}			P_n		
	Average	Error	95% C.I.	Average	Error	95% C.I.
50	0.91	0.01	0.02	1.008	0	0
51	0.59	0.01	0.02	0.574	0	0
52	0.19	0.01	0.02	0.296	0	0
53	0.06	0.01	0.02	-0.37	0	0

TOBACCO. CO₂ Variations

Exp	K_{tw}			P_n		
	Average	Error	95% C.I.	Average	Error	95% C.I.
50	0.91	0.01	0.02	1.008	0	0
54	1.17	0.07	0.15	0.352	.029	.06
55	1.39	0.05	0.11	-0.143	.047	.09
56	1.52	0.07	0.15	-0.661	.036	.08

TOMATO. LIGHT VARIATION

Exp	K_{tw}			P_n		
	Average	Error	95% C.I.	Average	Error	95% C.I.
34	2.12	0.18	0.41	1.08	.03	.06
35	0.91	0.01	0.02	0.585	.04	.08
36	0.32	0.01	0.02	0.196	.01	.02
37	0.43	0.01	0.02	0.202	.01	.02
38	0.14	0.01	0.02	-0.029	.01	.02

Table 19 (Cont'd)

BEAN. LIGHT INTENSITY VARIATIONS

Exp	K_{tw}			P_n		
	Average	Error	95% C.I.	Average	Error	95% C.I.
20	1.45	0.09	0.20	0.713	.041	.08
21	1.68	0.05	0.12	0.355	.028	.06
22	1.77	0.06	0.14	-0.01	.028	.06
23	1.70	0.05	0.12	0	.034	.06
24	1.66	0.12	0.28	-0.182	0	0

where

K_n = proportionality constant ($\text{nMCO}_2/\text{cm}^3$)

P_n = net photosynthesis ($\text{nMCO}_2/\text{cm}^2/\text{sec}$)

R_{tw} = total diffusion resistance (sec/cm)

P_o = value of net photosynthesis at closure of stomates
(respiration)

In the bean case (Fig. 25) the effect of diffusion resistance was negligible and net photosynthesis was almost perfectly linear with R_v (Fig. 14). Most of net photosynthesis was therefore explained by a change in R_v thus:

$$P_n = Q_p R_v + P_o \quad \dots (66)$$

where

Q_p = Net Photosynthesis yield (nMCO_2/j)

R_v = Total absorbed visible radiation ($\text{j}/\text{cm}^2/\text{sec}$)

So, depending upon environmental conditions and limitations, the net photosynthesis could be described by a linear combination of the

above equations

$$P_n = a K_n \left(\frac{1}{R_{tw}} \right) + b Q_p R_v + P_0 \quad \dots(67)$$

where a and b are regression constants corresponding to the weight attributed to diffusion control (Eq. 65) and visible radiation control (Eq. 66). The values of aK_n , bQ_p and P_0 have to be determined experimentally upon the plants being tested. The values obtained would reflect the interactions between the plant and environment. Although a change of temperature has produced a reduction in net photosynthesis, a similar reduction in transpiration and an increase in diffusion resistance was found to occur (West and Gaff, 1976) so that the linearity of equation (67) would still hold for changes in photosynthesis produced by increasing the leaf temperature. It is thus expected that for canopies under light limited conditions, the variations in net photosynthesis can adequately be correlated by the measures of diffusion resistance and light intensity. This relation does not imply that the factors of temperature, CO_2 concentration or turgor pressure have no effects, but rather that similar effects are observed on diffusion conductance such that a practical correlation can be derived between diffusion conductance and net photosynthesis. When considering large systems, the use of this correlation in conjunction with the proposed mathematical method for solving the energy budget (section 3.5) could simplify the work of ecologists in establishing the productivity of such systems as a function of measurable parameters.

Chapter 4

CONCLUSION

Although leaf temperature is not a controlling factor in the energy budget, but rather the resultant of an equilibrium between the three forms of energy released by the leaf, the solution to the exact balance between reradiation, convection and transpiration required that leaf temperature be known since leaf temperature is involved in all the energy budget terms. Consequently the complete solution to the budget was obtained by the simultaneous measurement of transpiration and leaf temperature and also by estimating the boundary layer resistance value. With these three variables known, the other variables of the energy budget could be calculated, namely stomatal resistance, reradiation, convection and latent heat. For this purpose, leaf temperature was obtained by the direct method of inserting a fine temperature sensor into the leaf blade; the elevation of water vapour concentration in closed chambers was used to evaluate transpiration; while the boundary layer resistance was estimated by analogy with the heat transfer studies of flat planes or by placing in the transpiration chamber a dummy leaf made out of white wet paper, cut and positioned in the same manner as the real leaf (Gaastra 1963).

The underlying assumption made by the use of this method is that

the performance of the leaf lies at an intermediate position between the performance of a wet bulb psychrometer (the wet paper analogue) in which case the stomatal resistance is assumed to be zero (completely open), and a dry surface where the transpiration is negligible, in which case the stomatal resistance achieves a very high value (cuticular resistance).

This study investigated the possibility that the leaf temperature could be obtained as the result of a mathematical solution between two known cases derived directly from the energy budget equation and the assumptions just mentioned. The first case required that when convection and transpiration exactly match one another, the leaf temperature be that of a wet bulb psychrometer at the environment temperature and humidity (the wet paper analogue). The second case required that the leaf temperature be the same as the environment temperature in which case all the energy was released solely in the form of transpiration. The resulting solution yielded the leaf temperature as a function of absorbed radiation (Q_N), difference between wet bulb and dry bulb of the environment (θ^*) and transpiration (LE).

$$\theta = \theta^* \frac{(Q_N - LE)}{(K\theta^* - LE)} \quad \dots(68)$$

where

θ = leaf temperature minus air temperature

The calculated values for boundary layer resistance (r_a) and leaf resistance (r_l) were then obtained. These were found to be in

close agreement with values reported in the literature. The main advantage of this method over the previous one is that the plant parameters can be derived by the sole measurement of the air and radiation properties, and that the calculated values reflect the performance of the whole plant. In this respect, the method is more suitable to field conditions.

During these experiments the value of net photosynthesis was always linearly correlated with a change in water diffusion resistance and of light intensity irrespective of the source of variation. In this study the net photosynthesis variations were produced by light intensity and CO_2 variations, while other studies in the literature found a similar relationship to hold for C_3 and C_4 plants, for plants under water stress and for changing root and leaf temperatures. The only serious limitation to the above statement is when the leaf achieves maximal photosynthesis under saturation light intensities, but this case is rarely occurring in the field due to the mutual shadowing of leaves in closed canopies.

It is by combining the proposed mathematical solution to leaf temperature and the net photosynthesis relation that the possibility of being able to evaluate the performance of whole systems by the virtues of remote sensing technology arises. The recent advances of thermographic mapping are nowadays used to detect insulation faults in houses by precisely monitoring the actual temperature of their walls. The aerial thermographic mapping of a whole natural area could thus reveal the leaf temperature of the canopy. This mapping when correlated

with the field measurements of temperature, humidity, net photosynthesis and radiation would provide the necessary data to relate the performance of the system with respect to photographic and thermographic data obtained from planes or satellites and thus allow a rapid interpretation.

In summary, the results support the following points:

- 1) That a complete solution to the energy budget can be derived from the use of environmental parameters and by the properties of moist air, without the need to measure the leaf temperature.
- 2) Generally, for field conditions, net photosynthesis is linearly correlated with the total water diffusion resistance and light intensity, irrespective of the source of variation, as long as light intensity limits photosynthesis.
- 3) The combination of the above two would result in a more simple and practical approach to the remote sensing of the productivity of large plant systems.

BIBLIOGRAPHY

Anderson, M. 1967. Photon flux, chlorophyll content, and Photosynthesis under natural conditions. *Ecology*, 46 (6): 1050-1053.

ASHRAE, 1972. American Society of Heating, Refrigerating and Air Conditioning Engineers, Handbook of fundamentals. New York.

Bassaz, F. A., Boyer J. S. 1972. A compensating method for measuring carbon dioxide exchange, transpiration, and diffusive resistance of plants under controlled environmental conditions. *Ecology*, 53: 343-349.

Björkman, O. 1966. The effect of Oxygen concentration on photosynthesis in higher plants. *Phys. Plant.* 19: 618-633.

Black, C.C. Jr., 1973. Photosynthetic carbon fixation in relation to net CO₂ uptake. *Ann. Rev. Plant. Physiol.* 24: 253-286.

Brogardh, T., Johnson, A. 1975. Regulation of transpiration in *Avena Sativa* responses to white light steps. *Physiol. Plant.* 35(2): 115-125.

Brown, H. T., Escombe, F., 1905. Research on some of the physiological processes of green leaves, with special reference to the interchange of energy between the leaf and its surrounding. *Proc. Roy. Soc. (London) B*, 76: 29-111.

Bull, T. A. 1971. The C₄ Pathway related to growth rates in Sugarcane. (Hatch et al. Photosynthesis and Photorespiration. Wiley-Interscience, 1971, p. 82.).

Catsky, J., Ticha, I. 1975. A closed system for the measurement of photosynthesis, photorespiration and transpiration Rates. *Biologia. Plant.* 17(6): 405-410.

Curtis O. F. 1936a. Leaf temperature and the cooling of leaves by radiation. *Plant. Physiol.* 11(2): 343-364.

_____ 1936b. Transpiration and the cooling of leaves. *Amer. Jour. Bot.* 23 (1): 7-10.

Das, V. S. R., Santakumari, M. 1977. Stomatal characteristics of some dicotyledonous plants in relation to the 4 carbon and 3 carbon pathways of photosynthesis. *Plant and Cell Physiol.* 18 (4): 935-938.

Decker, W. L. 1965. Atmospheric Humidity and the energy budget of plant canopies. (Humidity and Moisture, Vol. 2, p. 95-102. Reinhold, N. Y.).

Downes, R. W. 1970. Effect of light intensity and leaf temperature on photosynthesis and transpiration in wheat and sorghum. Aust. J. Biol. Sci. 23: 775-782.

_____. 1971. Adaptation of Sorghum plants to light intensity: its effect on gas exchange in response to changes in light, temperature, and CO_2 . (Hatch et al. Photosynthesis and Photorespiration, Wiley Interscience, 1971, p. 57.).

Ehleringer, J., Björkman, O. 1977. Quantum yield for CO_2 uptake in C_3 plants. Plant. Physiol. 59: 86-90.

Forrester, M. L., Krotkov, G., Nelson, C. D., 1966. Effect of Oxygen on photosynthesis, photorespiration and respiration in detached leaves: Soybean. Plant. Physiol. 41: 422-427.

Gasstra, P. 1959. Photosynthesis of crop plants as influenced by light, carbon dioxide, temperature, and stomatal diffusion resistance. Landbouwhogeschool, Wageningen. 59: 1-68.

_____. 1963. Environmental control of plant growth (Evans LT editor, Academic Press N. Y.) p. 113.

Gaffney, J. J. 1978. Relative humidity - Physical realities and horticultural implications. Hort Science. 13 (5), October.

Gates, D. N. 1963a. The energy Environment in which we live. Am. Scientist. 51-327-348.

_____. 1963b. Convection phenomena from plants in still air. Am. J. Bot. 50: 563-573.

_____. 1965a. The measurement of water vapour boundary layers in biological systems with a radio refractometer. (Humidity and moisture. 2. chapter 5: 33-38, Reinhold, N. Y.).

_____. 1965b. Energy, plants, and Ecology. Ecology. 46 (1): 1-13.

_____. 1968. Transpiration and leaf temperature. Ann. Rev. Plant. Physiol. 19: 211-238.

_____, Papian, L. E. 1971. Atlas of energy budgets of plant leaves. Academic Press, N. Y.

Gifford R. M. 1971. The light response of CO_2 exchange: On the source of difference between C_3 and C_4 species. (Hatch et al. Photosynthesis and Photorespiration. Wiley-Interscience, p. 51).

Hall, W. C., Pruchelut, G. B., Lane, H. C. 1953. Chemical defoliation and regrowth inhibition in cotton. Texas. Agri. Exp. Sta. Bull. 759: 3-25.

Hammarshand, K. 1976. Exponential dilution flask. Varian Instruemnts Applications, 10, #2: 14-15.

Hari, P., Smolander, H., Luukkanen, O. 1975: A field method for the estimation of the potential evapotranspiration rate. Jour. Exp. Bot. 26 (94), 675-678.

Hesketh, 1968. Effect of light and temperature during plant growth on subsequent leaf CO₂ assimilation rates under standard conditions. Aust. J. Biol. Sci. 21: 235-241.

Kramer, 1969. Plant and soil water relationships: a modern synthesis. McGraw-Hill Co.

Ku, S. B., Edwards G. E., Tanner, C. B. 1977. Effects of light, carbon dioxide and temperature on photosynthesis: Oxygen inhibition of photosynthesis and transpiration in Solanum Tuberosum. Plant Physiology, 59 (5): 868-872.

Lake, J. V. 1967a. Respiration of leaves during Photosynthesis. I, Estimates from an electrical analogue. Aust. J. Biol. Sci. 20: 487-493.

1967b. Respiration of leaves during photosynthesis. II. Effects on the estimation of leaf resistance. Aust. J. Biol. Sci. 20: 495-499.

Lawlor, D. W., Milford, G. F. J. 1975. The control of water and carbon dioxide flux in water stressed sugar beet. Jour. Exp. Bot. 26 (94): 657-665.

Lommen, P. W. 1971. A model describing photosynthesis in terms of gas diffusion and enzyme kinetics. Planta 98 (3): 195-220.

Ludwig, L. J., Calvin, D. T. 1971. An open gas exchange system for the simultaneous measurement of the CO₂ and ¹⁴CO₂ fluxes from leaves. Can. J. Bot. 49: 1299-1313.

Majernik, O., Mansfield, T. A., 1970. Direct effect of SO₂ pollution on the degree of opening of stomates. Nature (London) 227: 337-378.

1971. Effect of SO₂ pollution on stomatal movements in Vicia Faba. Phytopathol. Z. 71: 123-218.

Meidner, H., Mansfield, T. A. 1968. Physiology of stomata. McGraw-Hill ed.

Mudd, J. B., Kozlowski, T. T. 1975. Response of plants to air pollution. Academic Press (London):

Nilsen, S., Kristiansen, E., Halldal, Per. 1975. A system for continuous measurement of photosynthetic rate and dark respiration at constant CO₂ level. *Physiol. Plant.* 35: 59-61.

Neales, T. F., Treharne, K. J., Wareing, P. F. 1971. A relationship between net photosynthesis, diffusive resistance, and carboxylating enzyme activity in bean leaves. (Hatch et al. *Photosynthesis and Respiration*. Wiley-Interscience inc.): 89.

O'Toole, J. C., Crookston, R. K., Treharne, K. J., Ozbun, J. L. 1976. Mesophyll resistance and carboxylase activity. A comparison under water stress conditions. *Plant. Physiol.* 57 (4): 465-468.

Poskukä, C. D., Nelson, C. D., Krotkov, G. 1967. Effects of metabolic inhibitors on the rates of CO₂ evolution in light and in darkness by detached Spruce twigs, Wheat and Soybean leaves. *Plant. Physiol.* 42: 1187-1190.

Rabideau, G. S., French, C. S., Holt A. S. The absorption and reflection spectra of leaves, chloroplast suspensions, and chloroplast fragments as measured in an Ulbrich sphere. *Amer. J. Bot.* 33: 769-777.

Rashke, K., 1960. Heat transfer between the plant and environment. *Amer. Rev. Plant Physiol.* 11: 111.

Slavík, B. 1975. Transpiration rate and intercellular diffusive resistance in the tobacco leaf. *Biol. Plantarum.* 17 (6): 400-404.

Slatyer, R. O., Bierhuizen, J. F. 1964. A differential Psychrometer for continuous measurement of transpiration. *Aust. J. Biol. Sci.* 17: 348.

Slatyer, R. O. 1967. Plant water relationship. Academic Press, N. Y.

Tregunna, E. B., Krotkov, G., Nelson, C. D. 1966. Effect of O₂ on the rate of photorespiration in detached Tobacco leaves. *Phy. Plantarum.* 19: 723-733.

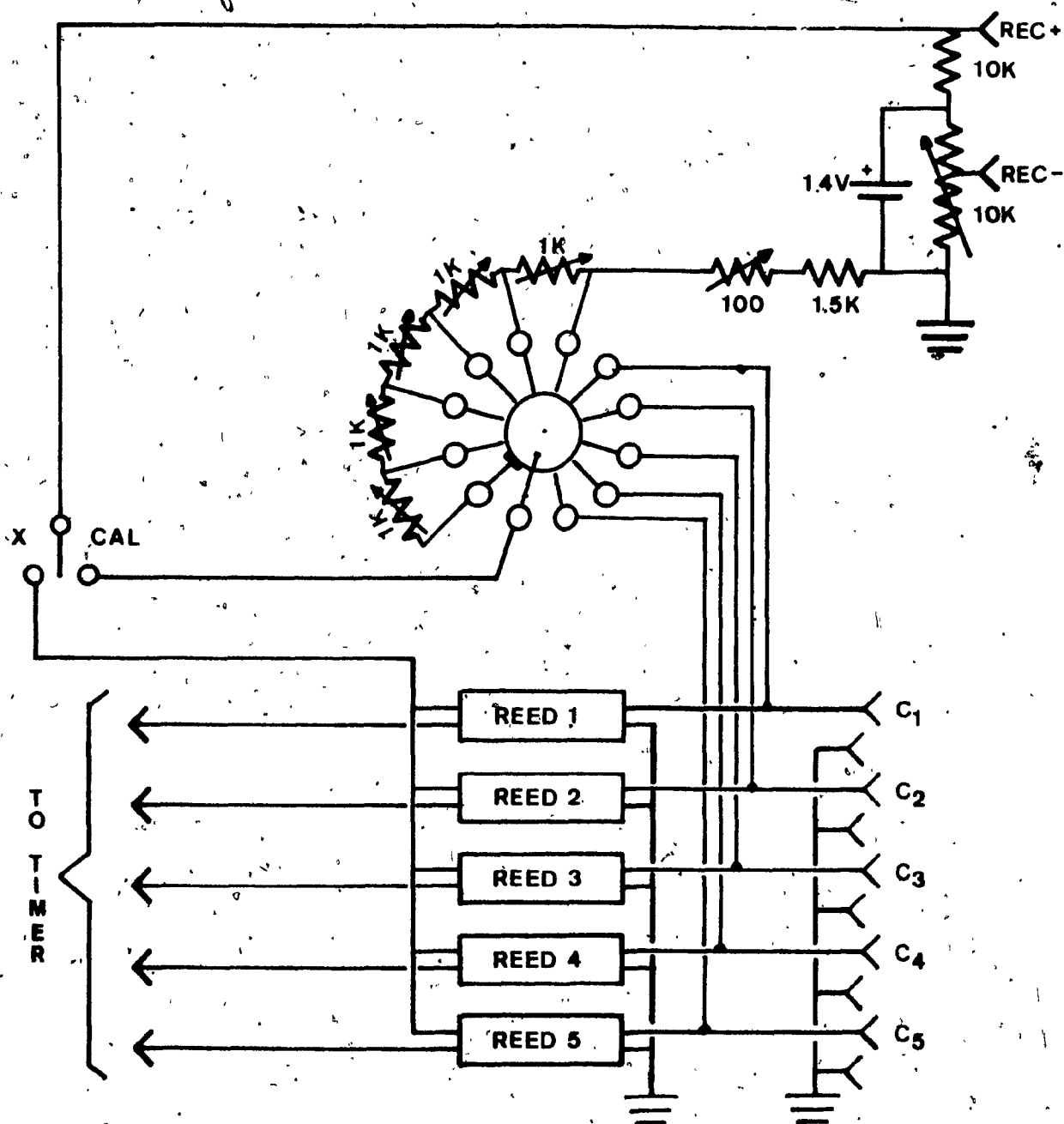
Vogel, S. 1970. Convective cooling at low airspeed and the shapes of broad leaves. *J. Exp. Bot.* 21 (66): 91-101.

West, D. W., Gaff, D. F. 1976. The effect of leaf water potential, leaf temperature, and transpiration of leaves of Malus Sylvestris. Physiologia Plant. 38 (2): 98-104.

Wilks, 1976. Operation and Maintenance manual. Wilks corp., Norwalk.

APPENDIX I

DIAGRAMS



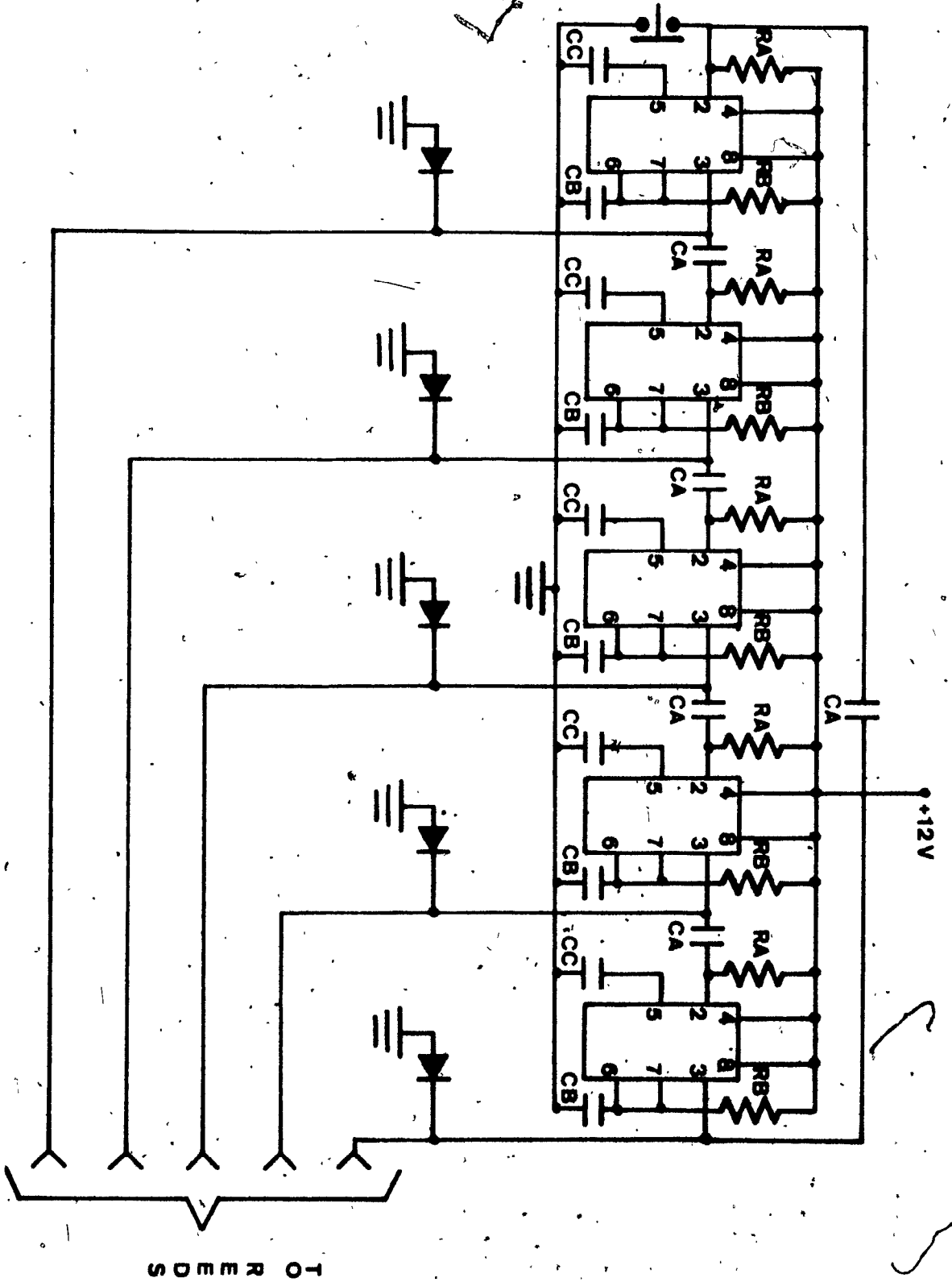
Multiplexer: Transducer and switching

C₁ to C₅: thermistor probe connections

CAL : Calibration mode

X : Multiplex mode

Reed 1 to 5 : Reed relays



Multiplexer: Timing Circuit

Five integrated timers (LM555) are used to sequentially fire the reed relays.
 $R_A = 33 \text{ k}\Omega$; $R_B = 1 \text{ M}\Omega$; $C_A = 0.001 \text{ }\mu\text{F}$; $C_B = 20 \text{ }\mu\text{F}$; $C_C = 0.01 \text{ }\mu\text{F}$.

APPENDIX II

PROGRAMS

```

PROGRAM MOD1(INPUT,OUTPUT,TAPE1,TAPE2)
DIMENSION DATA(40),MAIN(100,20),LABEL(100),HF(10),HI(10)
REAL MAIN
INTEGER CODE
COMMON MAIN,L
666 CONTINUE
READ 97,IN
97 FORMAT(A7)
IF(IN.EQ.3HFND) GO TO 101
CALL GET(5HTAPE2,IN,0,0)
72 CONTINUE
TI=0
CELLV=5.6
I=0
CT=0.024167
50 READ 1,EXP,CT
IF(CT.EQ.-0.0) CT=0.024167
IF(EXP.LT.0.0) GO TO 666
PRINT 1,EXP,CT
60 READ(2,2) CODE,(DATA(J),J=1,20)
IF(CODE.EQ.1H*) GO TO 100
IF(DATA(1).NE.FXP) GO TO 60
I=I+1
LABEL(I)=CODE
DO 77 J=1,40
MAIN(I,J)=DATA(J)
77 CONTINUE
MAIN(I,4)=MAIN(I,3)+MAIN(I,4)/60.
GO TO 60
100 DO 88 K=1,I
IF(LABEL(K).EQ.1HC) GO TO 89
88 CONTINUE
89 NO=K
LIM=NO+1
TIME=MAIN(NO,4)
DO 99 K=NO,I
MAIN(K,4)=TIME+CT*(K-NO)
MAIN(K,3)=0.0
99 CONTINUE
LIM=NO-1
DO 303 L=1,LIM
IF(LABEL(L).NE.1HD) GO TO 395
TF=MAIN(L,4)
DO 43 JJ=5,7
HF(JJ)=MAIN(L,JJ)
IF(TI.EQ.0.0) GO TO 380
DO 396 JJ=5,7
IF(HF(JJ).EQ.-0.0) GO TO 396
SLOP=(MAIN(L,JJ)-HI(JJ))/(TF-TI)
DO 397 J=NO,I
IF(MAIN(J,4).LT.TI) GO TO 397
IF(MAIN(J,4).GT.TF) GO TO 397
MAIN(J,JJ+6)=SLOP*(MAIN(J,4)-TI)+HI(JJ)
DO 49 II=8,12
MAIN(J,II+8)=MAIN(L,II)
49

```



```

MAIN(J;10)=MAIN(L,13)
397 CONTINUE
396 CONTINUE
380 TI=TF
DO 44 JJ=5,7
44 HI(JJ)=HF(JJ)
395 CONTINUE
IF(LABEL(L).NE.1HE) GO TO 350
DO 140 J=NO,I
DO 140 JJ=5,9
IF(MAIN(J,JJ).EQ.-0.0) GO TO 140
MAIN(J,JJ)=MAIN(J,JJ)+MAIN(L,JJ)
140 CONTINUE
350 IF(LABEL(L).NE.1HW) GO TO 355
CALL CALIB
DO 356 J=NO,I
IF(MAIN(J,4).LT.MAIN(L,4)) GO TO 356
DO 357 JJ=5,6
IF(MAIN(J,JJ).EQ.-0.0) GO TO 357
357 CONTINUE
MAIN(J,5)=MAIN(J,5)*MAIN(L,16)+MAIN(L,17)
356 CONTINUE
355 CONTINUE
IF(LABEL(L).NE.1HT) GO TO 400
CALL CALIB
DO 45 J=NO,I
IF(MAIN(J,4).LT.MAIN(L,4)) GO TO 45
DO 46 JJ=5,9
IF(MAIN(J,JJ).EQ.-0.0) GO TO 46
MAIN(J,JJ)=MAIN(J,JJ)*MAIN(L,16)+MAIN(L,17)
46 CONTINUE
45 CONTINUE
400 IF(LABEL(L).NE.1HP) GO TO 401
CALL CALIB
DO 61 J=NO,I
IF(MAIN(J,16).EQ.-0.0) GO TO 61
MAIN(J,16)=MAIN(J,16)*MAIN(L,16)+MAIN(L,17)
61 CONTINUE
401 IF(LABEL(L).NE.1HL) GO TO 404
CALL CALIB
DO 62 J=NO,I
IF(MAIN(J,4).LT.MAIN(L,4)) GO TO 62
IF(MAIN(J,17).EQ.-0.0) GO TO 62
MAIN(J,17)=MAIN(J,17)*MAIN(L,16)+MAIN(L,17)
62 CONTINUE
404 CONTINUE
303 CONTINUE
DO 32 L=NO,I
32 WRITE(1,3) LABEL(L), (MAIN(L,J), J=1,20)
REWIND 2
GO TO 72
101 CONTINUE
LL=1H*
WRITE(1,3) LL
REWIND 1
STOP

```

```

1  FORMAT(F4.0,F10.7)
2  FORMAT(A1,2F4.0,2F2.0,10F5.1,15X,F2.0,5F5.1)
3  FORMAT(A1,2F4.0,18F6.2)
   END

```

```

SUBROUTINE CALIB
  DIMENSION MAIN(100,20)
  REAL MAIN
  COMMON MAIN,L
  N=0
  SUMX=0.0
  SUMX2=0.0
  SUMXY=0.0
  SUMY=0.0
  SUMXS=0.0
  DO 50 J=5,13,2
    X=MAIN(L,J+1)
    Y=MAIN(L,J)
    IF(X.EQ.-0.0.OR.Y.EQ.-0.0) GO TO 50
    N=N+1
    SUMX2=SUMX2+X*X
    SUMXY=SUMXY+X*Y
    SUMX=SUMX+X
    SUMY=SUMY+Y
50  CONTINUE
    SUMXS=SUMX*SUMX
    MAIN(L,16)=(N*SUMXY-SUMX*SUMY)/(N*SUMX2-SUMXS)
    MAIN(L,17)=(SUMY*SUMX2-SUMX*SUMXY)/(N*SUMX2-SUMXS)
  RETURN
  END

```

```

PROGRAM MAVERAG(TAPE1,TAPE2,OUTPUT)
DIMENSION AVG(20),AL(20),AC(20),AH(20),DATA(20)
READ(1,3) ICODE,(DATA(J),J=1,20)
200 ISFN=DATA(1)
DO 99 I=4,13
99  AL(I)=DATA(I)
    READ(1,3) ICODE,(AC(J),J=1,20)
    READ(1,3) ICONF,(AH(J),J=1,20)
    DO 100 I=4,13
100  AVG(I)=(AL(I)+AC(I)+AH(I))/3.0
    GO TO 260
300  READ(1,3) ICODE,(DATA(J),J=1,20)
    IF(ICODE.EQ.14) GO TO 250
    IF(DATA(1).NE.7SEN) GO TO 200
    DO 105 J=4,13
    AL(J)=AC(J)
    AC(J)=AH(J)
    AH(J)=DATA(J)
    IF(J.NE.4) GO TO 7
7    CONTINUE
    AVG(J)=(AL(J)+AC(J)+AH(J))/3.0
105  CONTINUE
260  CONTINUE
    WRITE(2,3) ICODE,(DATA(J),J=1,3),(AVG(J),J=4,13),(DATA(J),J=14,20)
250  GO TO 300
    WRITE(2,3) ICONF
3    FORMAT(A1,2F4.0,18F6.2)
    STOP
    END

```

```

PROGRAM ENERGY(INPUT,OUTPUT,TAPE1,TAPF2)
DIMENSION DEG(20),RES(20),V(20)
COMMON WETP,DRYP,DRYI,DRYO,W,RHI,RHO,HI,HO,HWI,HWO
IL=1H1
WRITE(2,1) IL
60 READ (1,1) CODE,(DEG(J),J=1,20)
IF(CODE.EQ.1H*) GO TO 100
IF(DEG(13).EQ.-0.0) GO TO 60
IF(DEG(9).EQ.-0.0.OR.DEG(11).EQ.-0.0) GO TO 60
RA=53.352
DO 5 J=7,9
S CONTINUE
WETP=DEG(5)
DRYP=DEG(9)
DRYI=DEG(13)
DRYO=DEG(7)
CALL PSY
X=(1.0+1.6078*W)
V=V*X
FC=DEG(10)/(V*60.0*28.317)
AMC=454.55
AMOL=18.0
EC=1054.35
V=RA*(491.4+DEG(7)*1.8)/2116.1986
VR=V
V=V*(1.0+1.6078*W)
WCONCR=AMC*10.0**((6.0)/(V*28.317*AMOL))
WR=W
HIS=HI
HWIS=HWI
HRS=HO
HWS=HWO
WR1=W*WCONC
HIR=HI*FC*EC
HOR=HO*FC*EC
HWIR=HWI*FC*EC
HWOR=HWO*FC*EC
RH=RHO
HGI=HWI
WETP=DEG(6)
DRYO=DEG(8)
CALL PSY
V=RA*(491.4+DEG(8)*1.8)/2116.1986
VA=V
V=V*(1.0+1.6078*W)
WCONCA=AMC*10.0**((6.0)/(V*28.317*AMOL))
WA=W
HAS=HO
HWAS=HWO
HOA=HO*FC*EC
HWOA=HWO*FC*EC
RHA=RHO
DELHR=(HOR-HIR)
DELHWR=(HWOR-HWIR)

```

```
DELHA=(HOA-HIR)
DELHWA=(HWOA-HWIR)
WSI=FC*AMC*100000000.0/AMOL
WETP=DRYP=DFG(R)
CALL PSY
WAS=W
WRITE (2,2) (DFG(I),I=1,4),DEG(13),DEG(7),DFG(8),RH,
+RHA,DEG(16),DEG(17),FC,WCONCR,WCONCA
WRITE(2,3) HIS,HRS,HAS,HWIS,HWRS,HWAS,
+WR,WA,VR,VA
1  FORMAT(A1,2F4.0,18F6.2)
2  FORMAT(2(1XF4.0),1XF2.0,1XF5.2,10(1XE10.3))
3  FORMAT(19X,10(1XF10.3))
GO TO 60
100 IL=1H*
WRITE(2,1) IL
REWIND 2
STOP
END
```

```

SUBROUTINE PSY
DIMENSION F(10),H(5),HW(5),R(5),PW(5)
COMMON WETP,DRYP,DRYI,DRYO,W,RHI,RHO,HI,HO,HWI,HWO
F(1)=-741.9242
F(2)=-29.741
F(3)=-11.55286
F(4)=-0.8685635
F(5)=-0.1094098
F(6)=-0.439993
F(7)=-0.2540658
F(8)=-0.05418684
B(1)=DRYP
B(2)=WETP
B(3)=DRYI
B(4)=DRYO
DO 15 J=1,4
DO 20 K=1,8
SUM=SUM+F(K)*(0.65-0.01*B(J))**(K-1)
20 CONTINUE
E=0.01*(374.136-R(J))*SUM/(273.15+B(J))
PW(J)=217.99*EXP(E)
SUM=0.0
15 CONTINUE
WSW=0.62198*PW(2)/(1.0-PW(2))
WS=0.62198*PW(1)/(1.0-PW(1))
W=(1093-0.556*(B(2)*1.8+32.0))*WSW-0.24*1.8*(B(1)-B(2))
B(1)=B(1)*1.8+32.0
B(2)=B(2)*1.8+32.0
B(3)=B(3)*1.8+32.0
B(4)=B(4)*1.8+32.0
W=W/(1093+0.444*R(1)-B(2))
DO 26 N=3,4
WS=0.62198*PW(N)/(1.0-PW(N))
X=W/WS
R(N)=X/(1.0-PW(N))*(1.0-X)
IF (R(N).LT.0.0) R(N)=-0.0
H(N)=0.24*B(N)
HW(N)=W*(1061.0+0.444*B(N))
26 CONTINUE
HI=H(3)
HO=H(4)
HWI=HW(3)
HWO=HW(4)
RHI=R(3)
RHO=R(4)
RETURN
END

```

```

PROGRAM C400SEF(INPUT,OUTPUT,TAPE1,TAPE2,TAPE4)
REAL MAX,MIN,IA,IN
INTEGER SENT, SORT, COD.
DIMENSION A(24), DATA(2,5), MAX(2,5), MIN(2,5)
RAD(T,E)=(273.0+T)**(4.0)*SIG*E
-----INITIAL VALUES
SENT=0
SORT=0
COD=0
COMP=0.0
JJ=5
CA=1.0032
CVIS=0.0389
CSEN=1.8*0.24
CENE=1054.35/28317.0
SIG=8.132*10.0**(-11.0)*4.18/60.0
FLOW=6.936/1000.0
FHIGH=2.0972/1000.0
WRITE(2,9)
9  FORMAT(1H1)
5  FORMAT(10(1XE10.3))
  READ(1,1)
  -----READ AND OUTPUT MIN AND MAX
70 READ(1,1) ICODE,(A(J),J=1,14)
  IF(ICODE.NE.1H*) GO TO 11
1  FORMAT(A1,F4.0,1XF4.0,1XF2.0,1XF5.2,10(1XE10.3))
  FORMAT(19X,10(1XE10.3))
  SENT=SENT+1
  WRITE(2,2) ((MAX(I,J),I=1,2),J=1,JJ)
  WRITE(2,2) ((MIN(I,J),I=1,2),J=1,JJ)
  FORMAT(2X,10E10.3)
  REWIND 1
  READ(1,1)
  GO TO 70
11 SORT=SORT+1
  READ(1,3) (A(J),J=15,24)
  -----DATA DEFINITION
  HA=A(9)
  IA=A(22)-A(21)
  IF(IA.EQ.0.0) GO TO 70
  IF(A(11).LE.0.0) GO TO 70
  RHR=A(23)*(1.0+1.6078*A(21))
  RHA=A(24)*(1.0+1.6078*A(22))
  HSIR=CENE/RHR
  HSIA=CENE/RHA
  WCONCR=A(13)
  WCONCA=A(14)
  SK=0.684983
  IF(A(1).LE.24.0) SK=1.2121
  SN=1.23449
  IF(A(1).LE.24.0) SN=1.2864
  F=FHIGH
  IF(A(1).LE.24.0) F=FLOW
  FL=1.0/F
  DELTR=A(6)-A(5)

```

```

DELTA=A(7)-A(5)
IF(DELTR.LT.0.0) GO TO 60
HLOSSR=SK*DELTR**(SN)
GO TO 61
60 HLOSSR=SK*(0.0-DELTR)**(SN)
HLOSSR=-HLOSSR
61 IF(DELTA.LT.0.0) GO TO 62
HLOSSA=SK*DELTA**(SN)
GO TO 63
62 HLOSSA=SK*(0.0-DELTA)**(SN)
HLOSSA=-HLOSSA
63 CONTINUE
IF(A(11).EQ.0.0) A(11)=1.0
HSA=(A(17)-A(15))+CSEN*HLOSSA
HSR=(A(16)-A(15))+CSEN*HLOSSR
DELHS=(HSA*HSIA-HSR*HSIR)/F
DELHL=(A(20)*HSIA-A(19)*HSIR)/F
DELHT=DELHS+DELHL
AREA=A(11)
HR=A(17)+A(20)
TW=(ALOG(HR)-1.787)/0.02487
TW=(TW-32.0)/1.8
TA=A(7)
TP=A(6)
DELHS=DELHS/A(11)
DELHT=DELHT/A(11)
RADV=A(10)*CVIS*0.5
DELHL=RADV-DELHS
QABS=RAD(TA,0.95)+RADV
RAD3=4.0*SIG*0.95*((273.0+TA)**(3.0))
THET=(RADV-DELHL)*TW-TA/(RAD3*(TW-TA)-DELHL)
TL=THET+TA
RG=THET/DELHS
WSTL=EXP(TL*0.06201-5.4596)
WSTL=WCONCA*WSTL
EA=WCONCA*A(22)
V=RHA*28317.0/454.5
RA=RG*CA/V
TRANS=DELHL*400.0/1.8E-02
RS=(WSTL-EA)/TRANS-RA
DATA(1,1)=EA
DATA(2,1)=HA
DATA(1,2)=TA
DATA(2,2)=TL
DATA(1,3)=TRANS
DATA(2,3)=RG
DATA(1,4)=RA
DATA(2,4)=RS
DATA(1,5)=RA)*1000.0
DATA(2,5)=A(11)
-----DECISION
500 CONTINUE
IF(SENT-1) 20,21,22
-----INITIAL SORT VALUES
20 IF(SORT.NE.1) GO TO 50
DO 7 J=1,JJ

```



```

DO 7 I=1,2
7  MAX(I,J)=MIN(I,J)=DATA(I,J)
C  ----- S O R T ROUTINE
50 CONTINUE
DO 8 J=1,JJ
DO 8 I=1,2
IF(DATA(I,J).GT.MAX(I,J)) MAX(I,J)=DATA(I,J)
IF(DATA(I,J).LT.MIN(I,J)) MIN(I,J)=DATA(I,J)
A  CONTINUE
GO TO 70
C  -----OUTPUT DATA
21 IF (COMP.NE.A(1)) COD=0
IF (COMP.NE.A(1)) WRITE(4,9)
RADV=RADV*1000.0
IF (COMP.NE.A(1)) WRITE(4,26) A(1),A(2),RADV,A(11),FL
26 FORMAT(//,* EXPERIMENT NUMBER *,F4.0,10X,*DATE*,2X,F4.0,//
*,* VIS.ABS.RAD.*,F6.2,//,* LEAF AREA *,F7.2,//,* FLOW RA
*TE *,F7.2,//
*,5X,1H*,4X2HEA,4X1H*,4X2HHA,4X1H*,4X2HTA,4X1H*,4X2HTL,4X1H*,
*,3X5HTRANS,2X1H*,4X2HRS,4X1H*,4X2HRA,4X1H*,
*,3X5HDELHL,2X1H*,3X5HDELHS,2X1H*,//)
COMP=A(1)
COD=COD+1
WRITE(2,4) COD,((DATA(I,J),I=1,2),J=1,JJ),A(1),A(2)
4  FORMAT(1X12,10F10.3,5X,2(1XF4.0))
DELHL=DELHL*1000.0
DELHS=DELHS*1000.0
WRITE(4,25) EA,HA,TA,TL,TRANS,RS,RA,DELHL,DELHS
25 FORMAT(5X,1H*,11(F9.3,1X,1H*))
GO TO 70
37 WRITE(4,29) EA,HA,TA,TRANS,DELHL
29 FORMAT(5X,1H*,3(E10.3,1H*),11(1H*),E10.3,1H*,33(1H*),1(E10.3
*,1H*),22(1H*))
GO TO 70
C  -----END FILE OUTPUT.
22 CONTINUE
LD=1H)
WRITE(2,6) LD
WRITE(4,9)
6  FORMAT(1XA1)
REWIND 2
STOP
END

```

```

PROGRAM CARB(INPUT,TAPE1)
REAL MOYT,MOYC
CONC(Z)=AM*Z+AB
READ 1,C02
AM=23.198
AB=-1044.0
PPM=44642.857
SENT=0.0
L=50
75  IF(L.NE.50) GO TO 80
    WRITE(1,30)
    L=0
80  READ 1,EXP,DATE,TIME,START,STOP,RSTART,RSTOP,Z0,X,DR
    IF(EXP.EQ.0.0) GO TO 100
    IF(SENT.EQ.EXP) GO TO 50
    WRITE(1,40)
    WRITE(1,40)
    L=L+1
    SENT=EXP
50  DELT=(STOP-START)*60.0
    DELR=(RSTOP-RSTART)*PPM/C02
    IF(DR.LE.0.0) GO TO 70
    DR=-DR
    DELT=STOP
    DELR=DR*PPM/C02
    STOP=START+STOP/60.0
70  CONTINUE
    DELR=DELR/DELT
    Z=Z0+RSTART/X
    STARTC=CONC(Z)
    Z=Z0+RSTOP/X
    STOPC=CONC(Z)
    MOYC=(STARTC+STOPC)/2.0
    MOYT=(START+STOP)/2.0
    WRITE(1,2) EXP,DATE,TIME,START,STOP,STARTC,STOPC,MOYT,MOYC,D
    *ELR
    WRITE(1,40)
    L=L+1
    GO TO 75
100 STOP
30  FORMAT(1H1)
40  FORMAT(1H )
1   FORMAT(10F5.0)
2   FORMAT(5X,3(3H * ,F5.0),7(3H * ,E10.3),3H * )
END

```